LBL-32361
UC-400

Lawrence Berkeley Laboratory
UNIVERSITY OF CALIFORNIA

CHEMICAL BIODYNAMICS DIVISION

Study of the Mn-Binding Sites in Photosystem II Using Anibodies Raised Against Lumenal Regions of the D1 and D2 Reaction Center Proteins

E.A. Dalmasso
(Ph.D. Thesis)

April 1992

For Reference

Not to be taken from this room

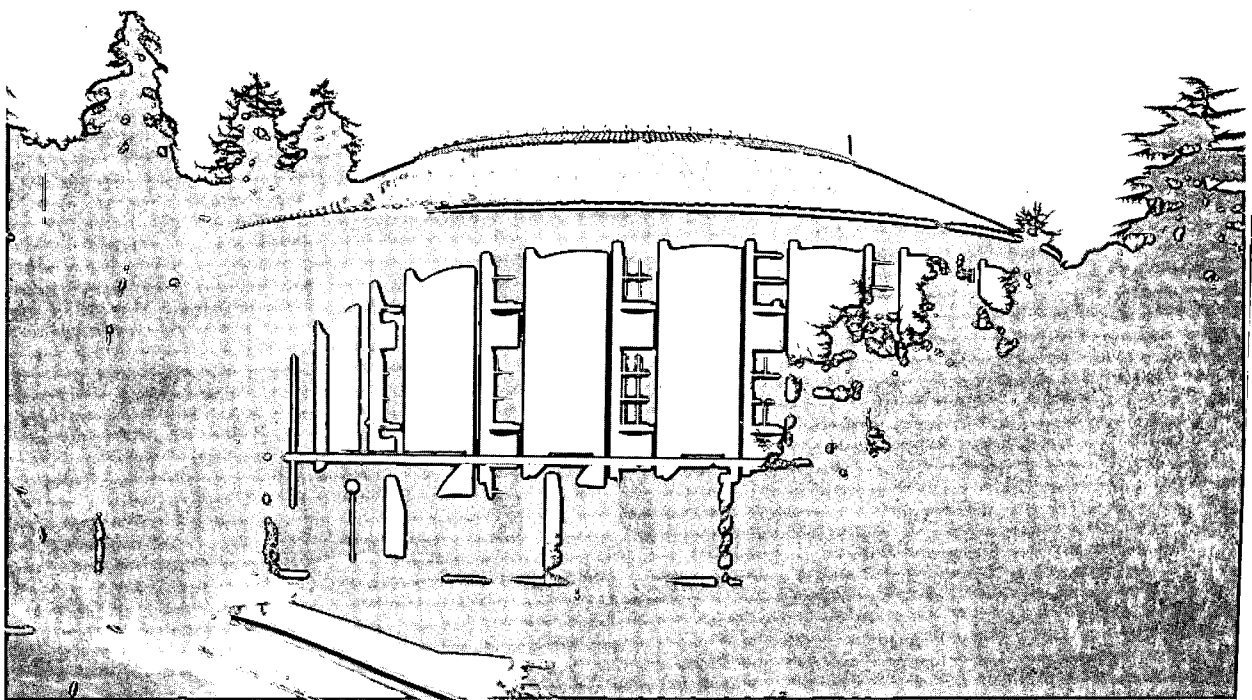

LBL-32361
Copy 1
Bldg. 50 Library.

Prepared for the U.S. Department of Energy under Contract Number DE-AC03-76SF00098

DISCLAIMER

This document was prepared as an account of work sponsored by the United States Government. Neither the United States Government nor any agency thereof, nor The Regents of the University of California, nor any of their employees, makes any warranty, express or implied, or assumes any legal liability or responsibility for the accuracy, completeness, or usefulness of any information, apparatus, product, or process disclosed, or represents that its use would not infringe privately owned rights. Reference herein to any specific commercial products process, or service by its trade name, trademark, manufacturer, or otherwise, does not necessarily constitute or imply its endorsement, recommendation, or favoring by the United States Government or any agency thereof, or The Regents of the University of California. The views and opinions of authors expressed herein do not necessarily state or reflect those of the United States Government or any agency thereof or The Regents of the University of California and shall not be used for advertising or product endorsement purposes.

Lawrence Berkeley Laboratory is an equal opportunity employer.

DISCLAIMER

This document was prepared as an account of work sponsored by the United States Government. While this document is believed to contain correct information, neither the United States Government nor any agency thereof, nor the Regents of the University of California, nor any of their employees, makes any warranty, express or implied, or assumes any legal responsibility for the accuracy, completeness, or usefulness of any information, apparatus, product, or process disclosed, or represents that its use would not infringe privately owned rights. Reference herein to any specific commercial product, process, or service by its trade name, trademark, manufacturer, or otherwise, does not necessarily constitute or imply its endorsement, recommendation, or favoring by the United States Government or any agency thereof, or the Regents of the University of California. The views and opinions of authors expressed herein do not necessarily state or reflect those of the United States Government or any agency thereof or the Regents of the University of California.

LBL-32361

Study of the Mn-Binding Sites in Photosystem II Using Antibodies Raised Against Lumenal Regions of the D1 and D2 Reaction Center Proteins

Enrique Agustin Dalmasso

(Ph.D. Thesis)

Department of Chemistry
University of California
and
Chemical Biodynamics Division
Lawrence Berkeley Laboratory
University of California
Berkeley, California 94720

April, 1992

This work was supported by the Director, Division of Energy Biosciences, Office of Basic Energy Sciences, U. S. Department of Energy under contract DE-AC03-76SF00098

Study of the Mn-Binding Sites in Photosystem II Using Antibodies Raised Against Lumenal Regions of the D1 and D2 Reaction Center Proteins

by

Enrique Agustin Dalmasso

Abstract

The experiments discussed in this thesis focus on identifying the protein segments or specific amino acids which provide ligands to the Mn cluster of photosystem II (PS II). This Mn cluster plays a central role in the oxygen-evolving complex (OEC) of PS II. The Mn cluster is thought to be bound by lumenal regions of the PS II reaction center proteins known as D1 and D2. First, several peptides were synthesized which correspond to specific lumenal segments of the D1 and D2 proteins. Next, polyclonal antibodies were successfully elicited using three of these peptides. The peptides recognized by these antibodies correspond to protein segments of the spinach reaction center proteins: Ile-321 to Ala-344 of D1 (D1-a), Asp-319 to Arg-334 of D1 (D1-b), and Val-300 to Asn-319 of D2 (D2-a). These antibodies were then used in assays which were developed to structurally or functionally probe the potential Mn-binding regions of the D1 and D2 proteins.

The two assays yielding structural information were western blotting and solution binding experiments. Western blotting identified the denatured proteins of spinach PS II membrane preparations to which the antibodies bound. The solution antibody binding assay was used to confirm antibody binding to native PS II membranes. Three assays which examined functional aspects of PS II were measurement of oxygen evolution, yield of photoactivation, and $MnCl_2$ inhibition of diphenylcarbazide (DPC) to 2,6-

dichlorophenol indophenol (DCIP) photoreduction. Assays of oxygen evolution tested the ability of antibodies to affect the naturally bound Mn of PS II. The yield of photoactivation assays investigated the ability of antibody to block the binding and subsequent photoligation of Mn to PS II membranes lacking the endogenous Mn cluster. Finally, experiments which assayed the $MnCl_2$ inhibition of DPC to DCIP photoreduction addressed whether bound antibody could block any of the four components of the high-affinity Mn-binding site that become available in the presence of DPC.

The results of these experiments include the following: All three antibodies reacted with their corresponding denatured protein (D1 or D2) on western blots. In solution binding assays, the binding of the three antibodies to several PS II preparations was demonstrated and characterized. The first antibodies available, those against D1-a, were used in initial experiments to examine effects on oxygen evolution. Using PS II membrane preparations of varying extrinsic protein composition, no adverse effects of these antibodies were observed on oxygen evolution. All three antibodies were then used to test for possible effects on the ability to photoactivate the Mn cluster of the OEC. These assays showed no effect for the antibodies recognizing the D1-b or D2-a peptide and some decrease in yield for the antibodies recognizing the D1-a peptide. Finally, incubation of Tris-treated PS II membrane preparations with antibodies to the D1-a peptide resulted in an inhibition of one component of the high-affinity Mn-binding site as measured by the $MnCl_2$ inhibition of DPC to DCIP photoreduction. This did not occur with antibodies raised against the D1-b or the D2-a peptides. This suggests that the carboxyl end of the D1 protein may provide a ligand for the high-affinity binding of Mn in PS II. Additionally, the inability of the other two antibodies to block any of the high-affinity, Mn-binding sites is an indication that their epitopes are in regions of D1 and D2 which do not contain Mn-binding residues detectable by the Mn^{2+}/DPC assay.

To those who face challenges, struggle against adversity and surmount seemingly impossible obstacles.

They are the ones who survive the difficult times and truly appreciate the good.

TABLE OF CONTENTS

	Abstract	1
	Table of contents	iii
	Acknowledgements	iv
Chapter 1:	Introduction	1
Chapter 2:	Peptides	32
Chapter 3:	Antibodies	63
Chapter 4:	Western blotting assays	68
Chapter 5:	Oxygen evolution assays	96
Chapter 6:	Solution binding assays	111
Chapter 7:	Photoactivation assays	121
Chapter 8:	Assay of high-affinity Mn-binding sites	149
Appendix 1:	List of Abbreviations	176
Appendix 2:	List of Amino Acid 3 and 1 Letter Codes	179
Appendix 3:	List of Figures	180
	References	182

Acknowledgements

Finally, the "acknowledgements." This seems to be the section of a thesis that the author saves for last, but most readers look at first. It is the place where one is allowed to be formal or friendly, and to express gratitude to those people that have enriched one's graduate years. I greatly appreciate the opportunity to do so on paper. But, whether specifically named here or not, I hope that my appreciation is not silent and that I have personally demonstrated my gratitude to everyone involved.

Educationally, I would like to especially thank J. Michel and J. Jaglo at RHS, who sparked and fanned my early interests in science; Profs. Carlin, Mohrig, Rammette and Buffington at Carleton, who gave me the foundations of Chemistry within the "confines" of a liberal arts education; John Hearst, my advisor at Berkeley, whose patience, understanding and encouragement have gotten me to where I am today; and Ken Sauer, an outstanding teacher and educator, who served as an advisor and provided the motivation behind my interest in teaching.

During my years in graduate school, several individuals have directly affected and encouraged my progress. Peter Sandusky, Jeff Gingrich and Jean-Luc Zimmermann taught me the basics of research in photosynthesis. Gary Smith and Phil Eggers maintained the computers and electronics at LCB in excellent fashion. Anita Hong (formerly at Applied Biosystems), Joe Pease and David Koh were extremely helpful with the synthesis and purification of peptides. Joe and David were also involved in numerous lunch and cappuccino runs. And, the technicians and veterinarians at the UCB Office of Laboratory Animal Care were invaluable during antibody production.

Michael Seibert and Chris Preston at the Solar Energy Research Institute in Golden, Colorado were important collaborators in the experiments involving the assay of high-affinity Mn-binding sites in photosystem II. John Hearst, Nacho Tinoco and Taso Melis had the unenviable opportunity to officially read and critique this thesis. Of more importance to the accuracy of the thesis were Ken Sauer, Yvonne Gindt, Vittal Yachandra

and Mike Seibert, who provided very useful and thorough comments and insights during its preparation.

The entire Hearst group at Hildebrand, to which I am now known as the "Last of the Hildebrand's," has been a special "extended family." I shared many important occasions with this group, which has included Sam, Yun-Bo, Suzanne, Pete and Susie, Jason and Effie, Joe and Tracy, John Hubbard and John Tessman. I have benefitted from the variety of scientific and personal interests of the Hearst group at LCB, namely Greg A., Dave, David O', Don, Marie, Zack and Bhupinder. In addition to Ken and Mel, the members of the Sauer-Klein group at LCB, especially Yvonne, Martin, Wen, Matthew, Ishita, Dave, Warren, Vickie and Vittal, have provided a fruitful learning environment.

Several other friends deserve special mention. David and Martin were challenging skiing partners. The instructors and students of the UCB Underwater Scientific Research Program, especially Jen, Shivaun, Ken, Chris, Skip, Bob, Tiff, Jenni, Johnny, Kyler, Dorothy, Lisa, Katie, Jon, Jim, Bruce, Jack, Paul, Scott, Charles, Lloyd and Doris are reliable buddies and good friends. My friends in Davis, especially Ashley, Pat, Thom and Joy have treated me as part of the family. And, the Husky Siberian scholar, Nanook Poochinski, has been constantly at my side during the past two years.

Finally, the end of this section was reserved for the most special people in my life. Ken and Susan, who encouraged the yearly pilgrimage to Seattle, are genuinely good friends. My brothers, Luis and Horacio, continue to become better friends as time progresses. The unending love, support and encouragement from my parents, Maria and Agustin, have shown me that they often understand me better than I do myself. Most importantly, Jen Koeber and I have grown as individuals and learned so much together in the past five years that I simply cannot thank her enough.

This work was supported by the Director, Division of Energy Biosciences, Office of Basic Energy Sciences, U. S. Department of Energy under contract DE-AC03-76SF00098.

1. INTRODUCTION

The general theme of the topics discussed in this thesis focuses on the identification of the location of the Mn cluster of the oxygen-evolving complex (OEC) of photosystem II (PS II). Specifically, the development and use of several assays using antibodies raised against synthetic peptides corresponding to specific lumenal segments of the D1 and D2 proteins are discussed. The D1 and D2 proteins are thought to constitute the reaction center of PS II and to be the location of the OEC. The assays were used to identify protein segments or specific amino acids which may provide ligands to the OEC Mn (Chapters 4-8). The choice of peptides, their synthesis and the production of antibodies are also discussed (Chapters 2 and 3). This chapter (Chapter 1) is divided into several sections which provide the basic conceptual framework and background necessary to understand the relevance of the assays which are discussed in the chapters that follow. The first two sections present a brief general discussion of photosynthesis and PS II. The next section addresses the relevance of the D1 and D2 proteins. For further details on these topics, refer to publications referenced in the corresponding section. The characteristics of the oxygen-evolving complex are dealt with in greater detail in the next section, with emphasis on current chemical and structural proposals for the Mn cluster of the OEC. The identification of the D1 and D2 proteins as the proteins which provide the most likely sites for binding of the OEC Mn is discussed in the next two sections. The initial genetic and biochemical evidence for this proposal is presented first. The second of these two sections concentrates on the more recent, chemical and spectroscopic, evidence supporting the same proposal. After that, a selection of recent publications where antibody effects on enzymatic functions were used to investigate the structure and function of several other enzyme systems are reviewed. Finally, the specific goals of the work presented in this thesis are outlined.

Photosynthesis

Photosynthetic organisms that have evolved on earth can be classified as either oxygenic or anoxygenic. Anoxygenic photosynthetic organisms include both sulfur and non-sulfur green and purple bacteria. These bacteria are thought to be the evolutionary precursors to chloroplasts and mitochondria. Photosynthetic organisms which evolve oxygen are called oxygenic and include the prokaryotic cyanobacteria, algae and higher plants. The organisms of this group use solar energy to drive the fixation of CO_2 to carbohydrates. Water is used as the terminal electron donor for these reactions and its oxidation produces oxygen as a by-product. All of the respiring organisms are indebted to the oxygenic photosynthetic organisms because they provide the reduced carbon compounds and oxygen necessary to sustain non-photosynthetic life.

The conversion of light energy to chemical energy takes place on internal membranes of the photosynthetic organisms. For oxygenic organisms, these processes take place on the thylakoid membranes. Higher plants contain these thylakoid membranes within organelles known as chloroplasts. Imbedded within the thylakoid membranes are several protein complexes which function to capture light energy, create proton and charge gradients, and convert the potential energy of these gradients into chemical energy. Two of these protein complexes function in the trapping of light energy and are schematically shown in the Z-scheme (Blankenship and Prince, 1985) presented in Figure 1-1. This Z-scheme positions the chromophores and electron transfer components of Photosystem II (PS II) and photosystem I (PS I) on a vertical axis of increasing reduction potential. The light energy is used in the pumping of electrons across the thylakoid membrane from the lumenal to the stromal side. PS II uses photon energy to oxidize two molecules of water producing molecular oxygen on the oxidizing (lumenal) side of the membrane. On the reducing (stromal) side of the membrane, PS II reduces plastoquinone to form a

Figure 1-1: Photosynthetic Z-scheme

Z-scheme representing non-cyclic electron flow in oxygenic photosynthesis (adapted from Blankenship and Prince, 1985). Redox active chromophores and electron transfer components of PS II and PS I are positioned on a vertical axis of increasing reduction potential. Dark dashed arrows indicate the absorption of a photon by a primary donor, small solid arrows indicate electron transfer steps, light dashed arrows indicate the direction of proton flow and solid lines represent the thylakoid membrane boundaries.

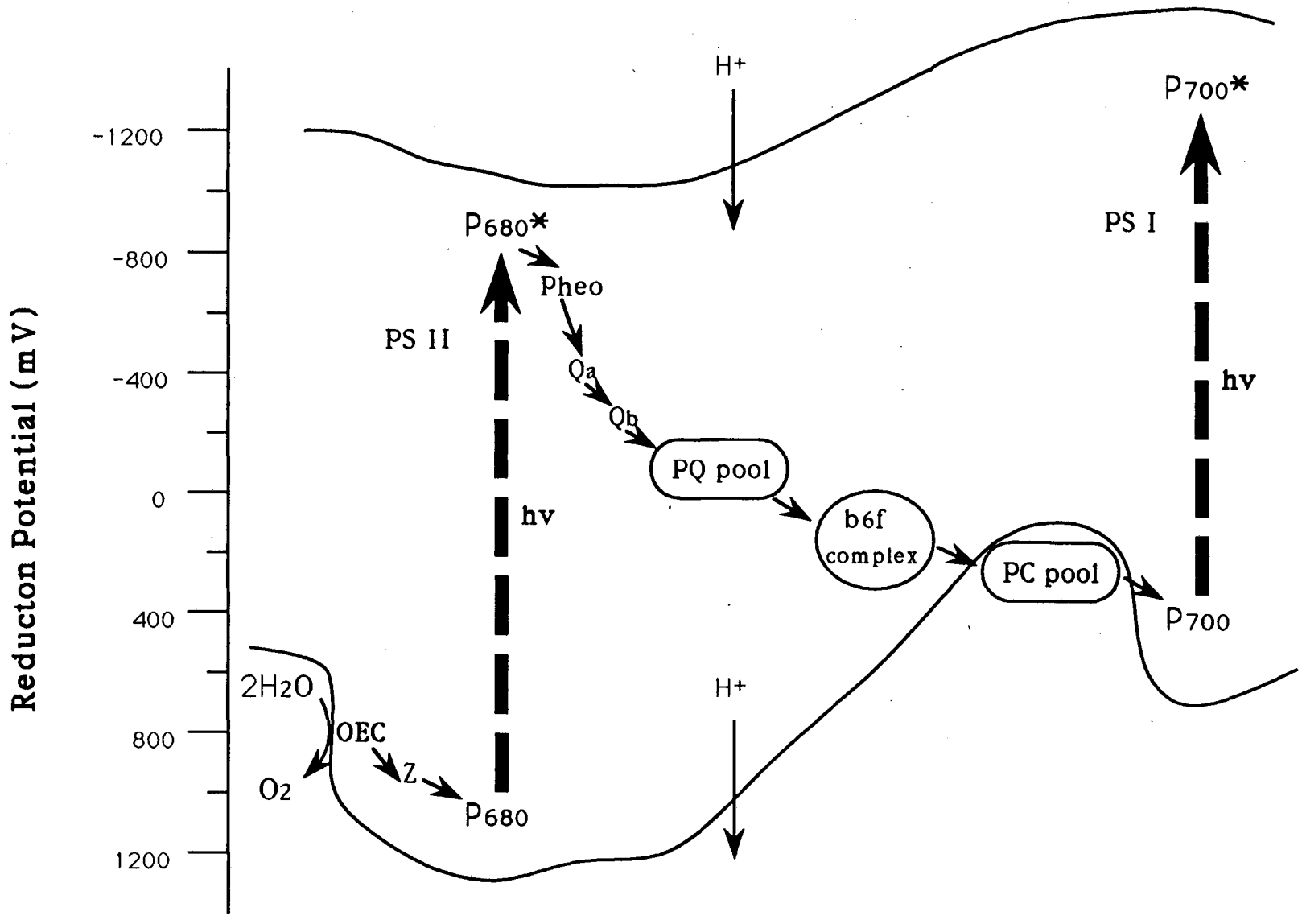
Reducton Potential (mV)
-1200
-800
-400
0
400
800
1200
H+
H+
P680*
Pheo
Qa
Qb
PQ pool
b6f
complex
PC pool
P700
P700*
PS I
hv
PS II
hv
2H2O
OEC
Z
O2
P680

plastoquinol. This plastoquinol is released from PS II and transfers electrons to a plastocyanin pool via the Cyt *b6f* complex (another integral membrane protein complex). Plastocyanin then transports electrons to PS I, which serves as an electron donor to bound ferrodoxin. Reduced ferrodoxin then transfers electrons to $NADP^+$ (nicotinamide-adenine dinucleotide phosphate) to form NADPH. The combined action of the two photosystems establishes a proton gradient which is used to synthesize ATP (adenosine triphosphate). NADPH and ATP are used by the organism in the fixation of carbon dioxide to synthesize carbohydrates.

The two photosystems capture photon energy by the excitation of chlorophyll molecules in associated light-harvesting complexes. This excitation is then transferred to the reaction center of the appropriate photosystem, where charge separation takes place. This charge separation is a one electron process which is linked to multiple electron processes by charge accumulation. The details of charge separation and charge stabilization by PS II and the oxygen-evolving complex (OEC), whose localization is the focus of the work presented in this thesis, are described in the next section.

Photosystem II

The transfer of excitation from the light-harvesting antenna to the reaction center of PS II results in excitation of a chlorophyll *a* complex known as P680. The number corresponds to the absorption maximum of this chromophore. Excitation of P680 is indicated by the vertical arrow for PS II in Figure 1-1. This excitation results in a large change in the reduction potential of P680 to form $P680^*$ (the excited state of P680). This excited electron is transferred to an intermediate pheophytin *a* molecule. A quinone molecule (Q_a) accepts one electron from this intermediate pheophytin *a* and transfers it to a

second quinone molecule (Q_b). Q_b acts as a two-electron gate in that it receives a second electron from Q_a after a second excitation of P680. This doubly reduced Q_b binds two protons and is released by PS II as a plastoquinol. The membrane-soluble plastoquinol then transfers electrons to PS I as described earlier.

The transfer of an electron away from $P680^*$ towards the reducing side of the thylakoid membrane produces an electron deficiency, or "hole," in P680. This "hole" is filled by electron donation from a nearby tyrosine residue called Y_Z (previously known as Z). This oxidized species, Y_Z^+, then extracts an electron from the OEC. The OEC acts as a four-electron gate on the oxidizing (lumenal) side of the thylakoid membrane. These four oxidizing equivalents are created by four separate excitations of P680 and transferred sequentially to the OEC through Y_Z. The OEC was proposed to cycle through four intermediates which accumulate these four oxidizing equivalents. It was proposed to involve the four Mn ions found tightly bound to PS II which are required for oxygen evolution. The OEC is discussed in greater detail in the section titled "oxygen-evolving center" later in this chapter.

All of the chromophores and electron-transfer components of PS II are bound by the protein components of PS II. A schematic of the oxygen-evolving core proteins of PS II is presented in Figure 1-2. This diagram depicts the proteins necessary for oxygen evolution under physiological conditions. The majority of light-harvesting proteins, which are present in PS II membrane preparations, are not shown. The two largest proteins shown, CP43 and CP47, are tightly associated light-harvesting proteins. The functions of CP43 and CP47 are not well understood, but they are present in all of the PS II preparations that evolve oxygen. The D1 and D2 proteins have been shown to function as the reaction center of PS II and bind the electron-transfer components of PS II as well as the Mn of the OEC. These two proteins, their amino acid sequences and their functions will be discussed in depth in sections that follow. The function of Cyt *b*-559 is also

Figure 1-2: Schematic of PS II proteins

This schematic of the oxygen-evolving core proteins of PS II depicts the proteins necessary for oxygen evolution under physiological conditions. The D1 and D2 proteins have been shown to function as the reaction center of PS II and bind the electron-transfer components of PS II as well as the Mn of the OEC. In addition to the four Mn per reaction center, Cl^- and Ca^{2+} are cofactors required for oxygen evolution. Dashed lines represent the thylakoid membrane boundaries.

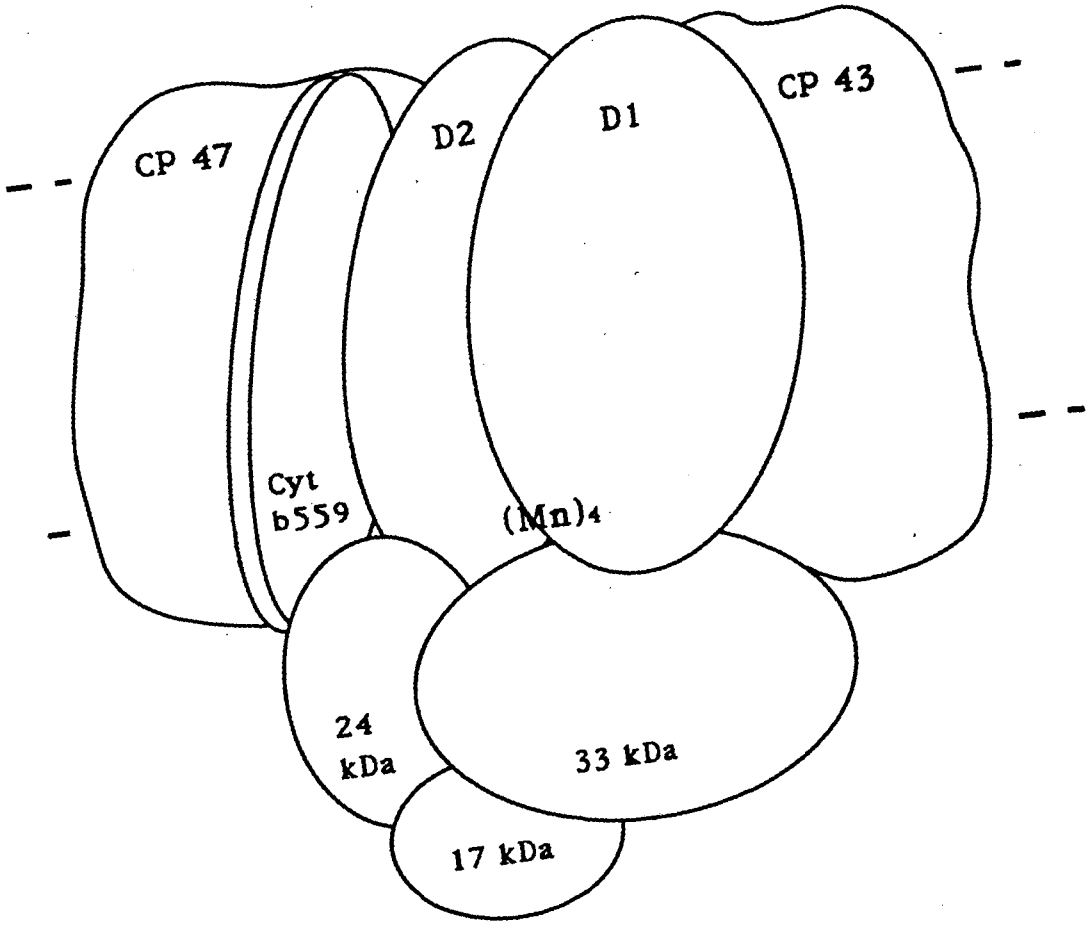
CP 47
D2
D1
CP 43
Cyt
b559
(Mn)4
24
kDa
33 kDa
17 kDa

unclear, but it is always found tightly associated with the D1 and D2 proteins. There is one copy of Cyt *b*-559 per reaction center and it spans the thylakoid membrane. Each Cyt *b*-559 contains a 5 kDa polypeptide, a 9 kDa polypeptide and a bridging heme group. Finally, there are three extrinsic polypeptides of 17, 24 and 33 kDa. The 17 kDa protein is thought to provide or create tight Cl^--binding sites. The 24 kDa protein is thought to provide or create tight Ca^{2+}-binding sites. These two proteins are not essential for oxygen evolution and can be replaced by increasing the concentrations of Cl^- and Ca^{2+}, respectively. The 33 kDa protein is not absolutely essential, but is necessary for full oxygen-evolving activity and protects the OEC Mn from reductants in the medium. The 33 kDa protein provides few, if any, ligands to this Mn. Additionally, a 20 kDa polypeptide and several small polypeptides of <5 kDa with unknown functions have been shown to be associated with various PS II preparations and have been omitted from this figure for clarity.

Reaction center of PS II

The assignment of the specific proteins which function as the reaction center of PS II has been a source of controversy until recently. One of the proposed models focussed on the protein known as CP47 (Nakatani et al., 1984). The issue was clarified when a strong sequence homology between the herbicide-binding protein of PS II from higher plants and blue-green algae (also known as the Q_b^-binding protein or the D1 protein) and the L subunit of the reaction center of the photosynthetic, but non-oxygen evolving, purple, non-sulfur bacteria *Rhodobacter capsulatus* was demonstrated by Hearst and Sauer (1983, 1984). Hearst (1986) also described the homology of the D2 protein of PS II with the M subunit of the reaction center of *Rb. capsulatus* (deduced from nucleotide sequence of its gene) published by Youvan et al. (1984). There was also a much stronger homology

present between the two proteins of the same reaction center, that is between the L and M subunits of *Rb. capsulatus* as well as between the D1 and D2 proteins of PS II. Based on these sequence homologies, Hearst (1986) suggested that the D1 and D2 proteins (encoded by chloroplast genes *psbA* and *psbD*, respectively) function as the reaction center proteins of PS II in analogy to the L and M subunits of purple bacteria. Based on affinity-labeling of the L subunit of *Rhodopseudomonas viridis* and the D1 protein of PS II by the reactive herbicide azidoatrazine in combination with sequence homologies of the D1 and D2 proteins with the L and M subunits of *Rps. viridis*, respectively, Michel and Deisenhofer (1986) independently came to the same conclusion.

The assignment of the D1 and D2 proteins as the core of the PS II reaction center was strengthened by the high resolution (3 Å) X-ray crystal structure of the photosynthetic bacterial reaction center of *Rps. viridis*. This structure has been published along with detailed discussions of the chromophore locations (Deisenhofer et al., 1984) and the arrangement of protein subunits (Deisenhofer et al., 1985). This work was recognized in 1988 by the award of the Nobel Prize in Chemistry to Drs. Johann Deisenhofer, Robert Huber and Hartmut Michel. Their research provided the first high-resolution X-ray crystal structure of an integral membrane protein and was a significant contribution to the photosynthesis field. Of overall importance in the structure are the near-symmetry of the two highly homologous bacterial reaction center proteins L and M. This observation is consistent with the proposal that the homologous D1 and D2 proteins constitute the PS II reaction center. Also, the L and M proteins bind the reaction center pigments involved in electron translocation across the membrane. An analogous role for binding of pigments by the D1 and D2 proteins within the PS II reaction center can be proposed based on similarity of the chromophores identified to be active in electron transport through the bacterial and PS II reaction centers. It should be noted that the crystal structure (Deisenhofer et al., 1985) shows much intertwining of all 3 bacterial reaction center proteins (the L and M

subunits discussed above, and the H subunit, for which no clearly analogous PS II protein has been identified, although several have been proposed). The extent of intertwining appears to be greatest in the loop regions on the lumenal and stromal sides of the membrane and implies that no PS II reaction center protein which is required for full oxygen-evolving activity can be completely dismissed as providing at least a few ligands to the Mn cluster of the OEC. The identification of the proteins and specific amino acids which provide these ligands to the active Mn is of great interest.

More recently, Nanba and Satoh (1987) isolated a PS II complex consisting of the D1 and D2 proteins and Cyt *b*-559. They propose this complex to be the reaction center of PS II. The pigment composition of this complex was reported to be 5 chlorophyll *a*, 2 pheophytin *a* and 1 ß-carotene. This is quite similar to the 4 bacteriochlorophyll *a*, 2 bacteriopheophytin *a* and 1 carotene composition of the purple bacterial reaction center. The complex, however, has no bound quinones or Mn and does not evolve oxygen. They also describe that "this complex is highly active in the photoreversible accumulation of reduced pheophytin *a* exhibiting the characteristic kinetics and spectrum of the photosystem II reaction center." In addition to the D1 protein, the D2 protein, the large and small protein subunits of Cyt *b*-559, this reaction center preparation was shown to contain a polypeptide with apparent molecular weight of 4.5-4.8 kDa (Ikeuchi and Inoue, 1988; Webber et al., 1989). This small protein is encoded by the chloroplast genome (*psbI* gene, 4.2 kDa calculated molecular weight of the gene product) as are the other 4 proteins of the isolated reaction center. Ikeuchi and Inoue (1988) found a stoichiometry for the 4.2 kDa protein relative to the 2 subunits of Cyt *b*-559 of approximately 1:1:1, indicating that there is one copy of the 4.2 kDa protein per reaction center complex based on the recent assignment of one Cyt *b*-559 per copy of D1 or D2 protein in the isolated reaction center preparation.

The reaction center complex preparation described by Nanba and Satoh (1987) has been the focus of many recent investigations, all of which are consistent with the

assignment of the D1 and D2 proteins as binding the PS II reaction center pigments. The reaction center complex was characterized by absorption, linear dichroism and circular dichroism spectroscopy (Newell et al., 1988), from which a perpendicular orientation of the reaction center long axis to the membrane plane was postulated (by comparison to the larger oxygen-evolving PS II core complex). These authors also give evidence indicating exciton coupling between chlorophyll molecules, consistent with the primary donor P680 being an exciton-coupled Chl dimer. The spectral properties of these preparations were studied further and are discussed by Tetenkin et al. (1989). The structured radical signal which accumulates after illumination at low temperature in the presence of sodium dithionite was assigned to the anion radical of pheophytin *a* by EPR and absorption spectroscopies (Frank et al., 1989). The presence of a spin-polarized triplet EPR signal after illumination at low temperature was reported as evidence for charge separation in the reaction center complex (Telfer et al., 1988; Ghanotakis et al., 1989). Using time-resolved fluorescence, Mimuro et al. (1988) calculated rate constants for the charge separation and charge recombination events, which differ only slightly from the rates measured for other PS II preparations. Study of the electron-transport properties (Chapman et al., 1988) indicates that silicomolybdate, but not artificial quinones, can function as an electron acceptor in these preparations. They also showed that $MnCl_2$, NH_2OH, KI and diphenylcarbazide (DPC) can act as electron donors to the reaction center complex. These exogenous electron acceptors and electron donors facilitate the study of electron transfer through the reaction center complex. Finally, Seibert et al. (1989) demonstrated that the full high-affinity Mn-binding site as measured by the Mn^{2+} inhibition of DPC-stimulated DCIP photoreduction described by Hsu et al. (1987) is present in the isolated reaction center complex. They also attempted to photoactivate this preparation using the procedures described by Tamura and Cheniae (1987) without success. These studies provide further evidence that the reaction center of PS II is largely limited to the proteins present in this preparation and provide strong support for the central role of the D1 and D2 proteins within

this structure. Although the results are also consistent with the binding of active Mn, there has been no demonstration of any oxygen-evolving activity by this complex. This lack of oxygen evolution indicates a possible requirement for additional proteins or cofactors to confer full activity.

Oxygen-Evolving Complex

The structural characterization and specific location of the OEC Mn cluster of PS II have been areas of intense research and controversy. Early evidence located the Mn to the interior of the thylakoid membranes within the chloroplast, meaning the lumenal side of these thylakoid membranes. The OEC Mn cluster has been shown to be associated with the PS II complex, released in the inhibition caused by several chemical treatments, involved in the *in vivo* reconstitution of oxygen evolution and necessary for the photoactivation of Mn-depleted PS II preparations *in vitro*. All of these developments have been reviewed by Brudvig et al. (1989). The genetic and biochemical explanations for the location of the Mn cluster are discussed in the next section of this chapter. More recent chemical evidence for assignment of the D1 and D2 proteins as providing the ligands that actually bind the OEC Mn, and some evidence as to the actual physical location of the Mn cluster, are discussed following that section. The spectroscopic evidence for Mn involvement is reviewed by Dismukes (1988), Brudvig et al. (1989) and others, and is described below with relevance to the structure and oxidation states of the Mn cluster within the OEC.

The early phenomenological description of the OEC was mainly based on observations and theoretical proposals by Joliot and Kok. The cyclical nature of maxima in oxygen evolution upon excitation with short flashes of light was described by Joliot et al. (1969). The maximum amount of oxygen evolved for dark-adapted spinach chloroplasts or algae samples occurred after the third flash. Thereafter, the maxima were spaced every

fourth flash and eventually damped out to a constant level. Kok et al. (1970) interpreted these results using a kinetic model of charge accumulation within an oxygen-evolving complex. This complex was proposed to involve the intrinsic Mn found to be required for oxygen evolution. The OEC was proposed to cycle through the accumulation of oxidizing equivalents and the oxidation of water as depicted in the S-state scheme (Figure 1-3). The S-state scheme describes the accumulation of one oxidizing equivalent during each of the transitions from S_0 to S_4 with a spontaneous decay from S_4 to S_0, at which point the O_2 molecule is released.

Evidence for Mn involvement in charge accumulation has been obtained using several different techniques, including EPR and X-ray absorption spectroscopies. The earliest EPR evidence was found by Dismukes and Siderer (1981) who described a "multiline" EPR signal of approximately 19 Mn hyperfine lines which was formed after a single flash of light. This signal was similar to the 16-line EPR spectrum described for an antiferromagnetically coupled Mn dimer previously described by Cooper et al. (1978) and was evidence for a change in the magnetic properties of the Mn complex upon illumination. This signal was assigned to the S_2 state of the Kok S-state scheme based on the assumption that dark-adapted samples reside mainly in the S_1 state because of the three flashes required for the first maxima in oxygen evolution during flash kinetic measurements. It was also shown that the Mn cluster actually changes oxidation state during the S_1 to S_2 transition as described by Goodin et al. (1984). They showed high resolution Mn X-ray edge spectra for samples poised in the S_1 and S_2 states and compared them to edge spectra of model compounds. The change in edge position from S_1 to S_2 for PS II samples correlated well with the change observed for model compounds having an increase in oxidation state of one unit.

Other spectroscopic evidence, mainly from EXAFS, has been useful in proposing structural models of the OEC Mn cluster. In addition, ultraviolet difference spectra taken

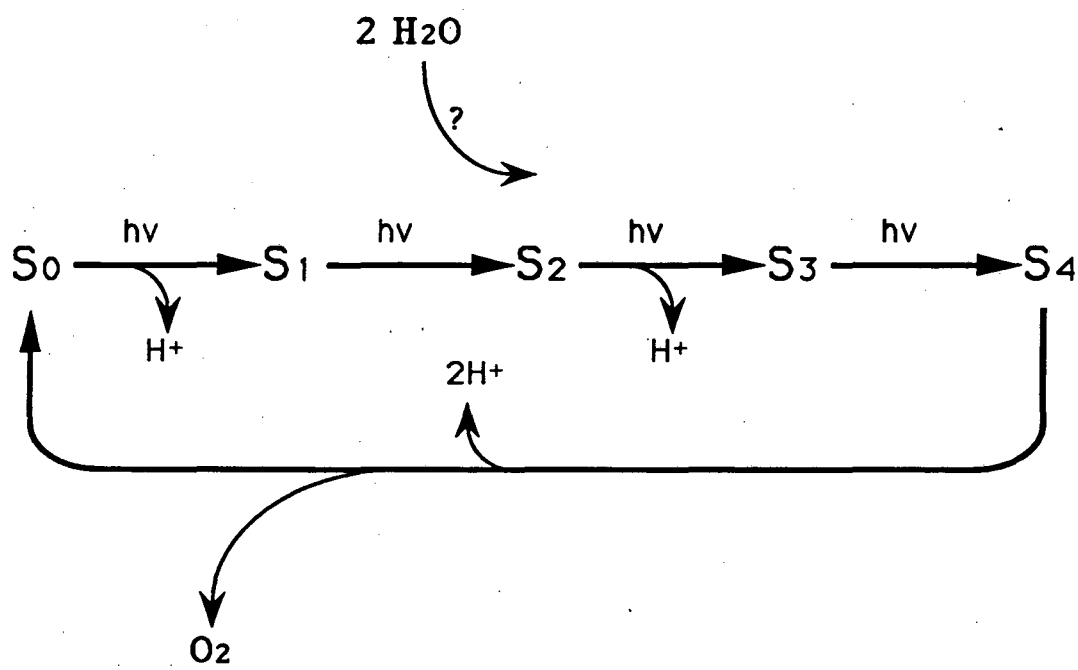

Figure 1-3: S-state scheme

Scheme proposed by Kok et al. (1970) using a kinetic model of charge accumulation within the oxygen-evolving complex. The S-state scheme describes the accumulation of one oxidizing equivalent (corresponding to the absorption of a photon by the primary donor) during each of the transitions from S_0 to S_4. A spontaneous decay occurs from S_4 to S_0, at which point the O_2 molecule is released. The proton release pattern and the binding of two water molecules are also shown.

during flash-induced S-state transitions have been used to formulate models of the oxidation states of the Mn within the OEC (Dekker et al., 1984; Renger and Weiss, 1986; Saygin and Witt, 1987). These experiments are apparently very difficult, and the results and their interpretations are neither clear cut nor consistent and will, therefore, not be further discussed here. Results of EXAFS using PS II membrane preparations were reported by Yachandra et al. (1986). This study showed a Mn cluster containing at least two Mn separated by 2.7 Å, which is consistent with di-μ-oxo bridging. The same distance was obtained from EXAFS of PS II preparations poised in the S_1 and S_2 states (Yachandra et al., 1987). More recently, Guiles et al. (1990b) have compared Mn XAS of PS II preparations in the S_3 state to those in the S_2 state. They concluded that a Mn oxidation does not take place during the S_2 to S_3 transition. They proposed a redox active ligand, possibly a histidine residue, to store this oxidizing equivalent and be located near the Mn cluster. In a study comparing the Mn XAS of PS II preparations prepared in a modified S_0 state (by hydroxylamine treatment) to those in the S_1 state, Guiles et al. (1990a) concluded that a Mn oxidation is likely during the S_0 to S_1 transition. These reports, along with recent EXAFS and Mn K-edge data, are reviewed (Sauer et al., 1991) and are most consistent with the four Mn oxidation states as: S_0 state (II, III, IV, IV), S_1 state (III, III, IV, IV), S_2 state (III, IV, IV, IV) and S_3 state (III, IV, IV, IV).

More recently, results from EPR and ESEEM have added information useful in modeling possible structures for the Mn cluster and describing ligands to the OEC Mn. Originally, one of the proposals for the source of the broad, featureless, g=4.1 EPR signal associated with the S_2 state was a mononuclear Mn(IV) ion (Hansson et al., 1986). This proposal has been dismissed based on Mn-hyperfine structure observed on the g=4.1 EPR signal of oriented PS II preparations (Kim et al., 1990). This structure indicates that more than one Mn ion must be magnetically coupled to produce this signal. This result is consistent with proposals assigning both the multiline and the g=4.1 EPR signals to

different conformations of the same multinuclear Mn cluster. Additionally, DeRose et al. (1991) have provided evidence for at least one histidine ligand to the EPR-active Mn. They applied ESEEM techniques to PS II preparations isolated from thermophilic cyanobacteria grown on [^{15}N]. These samples showed a change in nitrogen modulation from [^{14}N]-grown cyanobacterial preparations.

Studies of the power saturation and relaxation properties of signal II EPR signals have indicated a close spatial relationship between the radicals responsible for signal II (Y_D^+ and Y_Z^+) and the Mn cluster of PS II. These radicals have been recently identified by site-specific mutations of PS II membrane proteins using the unicellular cyanobacterium *Synechocystis* 6803. This organism is a facultative photoheterotroph which can grow on glucose without the presence of functional PS II. Debus et al. (1988a) changed Tyr-160 of the D2 protein to phenylalanine by site-directed mutagenesis of a *psbD* gene in *Synechocystis*. This mutant assembles a functional PS II complex as demonstrated by the ability to grow photosynthetically and evolve oxygen, but it lacks the stable EPR signal assigned to the D^+ radical. They concluded that D is Tyr-160 of the D2 protein and renamed it Y_D. They also suggested, based on a continuation of the C_2 symmetry of the PS II reaction center pigments towards the oxidizing side of P680, that the intermediate electron donor from Mn to $P680^+$, known as Z, is Tyr-161 of the D1 protein. To test this hypothesis, Debus et al. (1988b) changed Tyr-161 of D1 to phenylalanine by site-directed mutagenesis of a *psbA* gene in *Synechocystis*. The mutant assembles PS II as shown by its ability to produce the EPR signal assigned to the D^+ radical discussed above. It is unable to grow photosynthetically or evolve oxygen and has altered fluorescence properties. The altered fluorescence properties can be interpreted as a disruption in the forward electron transfer to $P680^+$ (the transfer rate is slowed by several orders of magnitude compared to wild-type). These data provide strong support for the the assignment of Tyr-161 of the D1 protein as Z (now called Y_Z), the intermediate electron

donor from the Mn complex to $P680^+$. Studies of the spectroscopic properties of the Y_D^+ and Y_Z^+ radical species, their interactions with the Mn cluster and possible oxidation states of the Mn cluster are discussed below.

The power saturation and relaxation properties of the EPR signals indicated a close spatial relationship between the radicals responsible for signal II (Y_D^+ and Y_Z^+) and the Mn cluster of PS II and have also provided insight into the structure and possible valence of the ions of the Mn cluster. Styring and Rutherford (1988) described the changes in low temperature power saturation of D^+ caused by the S-state transitions of the Mn cluster. They observed that the D^+ signal is easier to saturate after Mn-removal by Tris washing. This observation indicates a cross relaxation between D^+ and an efficient relaxer in the presence of Mn, which they suggest to be the OEC Mn cluster. They prepared samples in various S-states by illumination with a series of flashes and measured the microwave power for half-saturation of the D^+ signal. This power for half-saturation varied with flash number and was most consistent with a description of the Mn cluster as mixed-valent and paramagnetic for S_0 and S_3 (in addition to S_2) while the Mn in S_1 is more diamagnetic. They proposed the simplest reasonable model for the ions responsible for Y_D^+ relaxation to be S_0 [Mn(II)-Mn(III)], S_1 [Mn(III)-Mn(III)], S_2 [Mn(III)-Mn(IV)] and S_3 [Mn(III)-Mn(IV)], and suggested that more complex models are possible for a tetrameric Mn cluster.

Evelo et al. (1989) used electron spin echo spectroscopy to study the spin-lattice relaxation time of the EPR signal attributed to D^+, the stable tyrosine radical of PS II reaction centers. They studied the temperature dependence and average relaxation time for PS II preparations with the intact OEC poised at various S-states by illumination with a series of flashes. They found the spin-lattice relaxation curves to be biphasic, indicating a bi-exponential relaxation of D^+. They attributed this behavior to structural heterogeneity distinguished by two, magnetically non- or weakly coupled Mn ions that differ in relaxation time. The average relaxation time depends strongly on the S-state of the OEC, being

slowest for S_0, fastest for S_1 and intermediate for S_2 and S_3 (which are approximately equal). The temperature dependence in the range of 5-30 K for the relaxation of D^+ indicates that there are oxidations of Mn in the OEC in going from S_0 to S_1 and S_1 to S_2, but not for the S_2 to S_3 transition (consistent with the XAS data discussed earlier). They observed a strong dipolar contribution to the relaxation of only the S_0-state, indicating a paramagnetic species (different from the S=1/2 species in the S_2-state) which couples strongly to D^+ and is a much faster relaxer than the Mn cluster of the S_2-state. Finally, they proposed oxidation states for the 4 OEC Mn based on their data where: A) Two of the four Mn ions form a binuclear cluster which is antiferromagnetically coupled and are (2^+, 3^+, S=1/2) in S_0, (3^+, 3^+, S=0) in S_1, (3^+, 4^+, S=1/2) in S_2 and (3^+, 4^+, S=1/2) in S_3. Their interpretation is consistent with conclusions reached from X-ray spectroscopy (Sauer et al., 1991) and cw EPR (Styring and Rutherford, 1988) data. B) The other two Mn ions have oxidation states which differ by one unit (based on different relaxation properties) but do not change during any of the S-states from S_0 to S_3. Either (2^+, 3^+) or (3^+, 4^+) would agree with their results, but (4^+, 4^+) is favored by the X-ray spectroscopy data described earlier (Sauer et al., 1991).

Location of Mn-binding: genetic and biochemical evidence

As previously discussed, the reaction center of PS II has been assigned to the D1 and D2 proteins in analogy to the L and M subunits of purple bacteria (Hearst, 1986; Michel and Deisenhofer, 1986). Electron donation from the Mn cluster of the OEC to the reaction center primary donor (P680) goes through a redox-active tyrosine residue (Y_Z). In order to have efficient electron transfer, the Mn cluster of the OEC, Y_Z and P680 must be in close proximity to each other. The most likely location for Mn-binding would therefore be the lumenal side of the D1 and/or D2 reaction center proteins. Notably, if one

combines information on helical regions with the sequence alignments of the D1 protein with the L subunit and the D2 protein with the M subunit, it is apparent that the lumenal loops of D1 and D2 are significantly longer and contain more amino acids capable of ligating metal ions than the corresponding regions of L and M. This is strong support for Mn-binding in these regions of the D1 and D2 proteins.

A second line of evidence for the D1 and D2 proteins as the PS II reaction center came from Metz and Bishop (1980). They identified a low-fluorescent mutant (LF-1) of the green alga *Scenedesmus obliquus* containing a PS II reaction center functional in electron transport which did not evolve oxygen. PS II membranes preparations of this mutant bound only approximately 40% of the Mn bound by the wild-type (WT) membranes. Metz et al. (1980) demonstrated that the defective PS II protein had a slower electrophoretic mobility (higher apparent molecular weight) on LDS-PAGE than the corresponding WT protein. This 36 kDa LF-1 protein was correlated to a 34 kDa WT protein both of which were photoaffinity labeled by the PS II inhibitor azido[^{14}C]atrazine (Metz et al., 1985). The LF-1 PS II had active electron acceptor functions and contained a reaction center functional in electron transport, as characterized by the EPR spectra of radicals formed upon illumination (Rutherford et al., 1988). The defective protein was identified as the D1 protein of PS II (Metz et al., 1986; Taylor et al., 1988), while the D2 protein was apparently unchanged from its WT counterpart (Taylor et al., 1988). The D1 protein was shown to function on both the oxidizing and reducing sides of PS II, providing the first experimental evidence that D1 is a reaction center protein (Metz et al., 1986). This D1 protein has been proposed to assemble into PS II without proper processing of the carboxyl end (Metz et al., 1986; Diner et al., 1988; Taylor et al., 1988) which somehow blocks incorporation of the full complement of Mn required for oxygen evolution. These characteristics of the LF-1 mutant provide further evidence for Mn-binding in the region near the carboxyl end of the D1 protein.

A final biochemical property which assigns the D1 protein as part of the PS II reaction center is its fast, light-dependent, turnover *in vivo* (Edelman and Reisfeld, 1978; Silverthorne and Ellis, 1980). The D1 protein was also shown to exhibit rapid light-dependent *in vitro* degradation (Mattoo et al., 1984; Ohad et al., 1985). In the *in vitro* system, there was no turnover since protein synthesis is not present in isolated thylakoid membrane preparations. The biochemical reason for the turnover was proposed to be replacement of proteins damaged by the extremely high oxidizing potential of the higher oxidation states of Mn generated within the Mn-cluster of the OEC. The rapid degradation of the D1 protein, therefore, is consistent with the D1 protein as the primary site for binding of OEC Mn. The D2 protein was also shown to turnover more rapidly than other reaction center proteins, although slower than the D1 protein (Hundal et al., 1990). The pathway of the cleavage leading to D1 turnover was described by Greenberg et al. (1987). They identified the primary *in vivo* degradation product of the D1 protein as a 23.5 kDa fragment after exposure of *Spirodela oligorrhiza* cells to photoinhibiting light conditions. They also demonstrated that this 23.5 kDa fragment contained the amino-terminus of the D1 protein, proposed the cleavage site to be near the quinone-binding site of D1 (between helices IV and V, adjacent to a "PEST-like region" as defined by Rogers et al., 1986), and showed that the degradation of this 23.5 kDa fragment was much faster than the initial cleavage of the D1 protein. During photoinhibiting light conditions, a correlation was shown between the release of 4 Mn ions (per D1 protein lost) and the degradation of the D1 protein itself (Virgin et al., 1988). They also explained a correlation between the inhibition of oxygen evolution and loss of EPR multiline signal, both of which were much faster than the D1 protein degradation. Recently, Hundal et al. (1990) have reported the degradation of the D1 protein *in vitro*, by using isolated thylakoid membrane preparations, to be consistent with the *in vivo* degradation. They showed that concomitant with degradation of D1 protein, the 17, 24 and 33 kDa extrinsic proteins were released. Also, they showed that the previously described release of 4 Mn per D1 protein during D1 degradation occurs in

parallel with D1 loss even in the absence of the three extrinsic polypeptides. All of these data are consistent with the D1 protein providing the majority, if not all, of the amino acids that act as terminal ligands required to bind the active OEC Mn of PS II.

Location of Mn-binding: chemical and spectroscopic evidence

Several compounds, including benzidine, DPC, Mn^{2+} and I^- can act as exogenous electron donors to PS II membrane preparations lacking the endogenous OEC Mn complex. Upon illumination of PS II membrane preparations (from which Mn had been removed by Tris treatment) in the presence of $[^{125}I]^-$, the D1 protein was shown to be heavily labeled (Ikeuchi and Inoue, 1987). They assigned the D1 protein migration on SDS-PAGE by comparison to azido[^{14}C]atrazine labeling and immunoblotting with anti-D1 and anti-D2 rabbit antisera. Although the D1 protein was consistently the heaviest labeled protein for several different plants and a cyanobacterium, they also note weak labeling of the D2 protein and/or CP47 in some instances. In another study utilizing the same methods to label spinach PS II membranes, Takahashi and Satoh (1989) identified the fragment of the D1 protein that becomes photoaffinity labeled by [^{125}I] as Ile-143 to Met-172 based on the overlap of labeled fragments identified from different protease digestions. They deduced the specific amino acid labeled to be Tyr-161 on D1, which has been proposed to correspond to Z, the intermediate electron donor to P680 (Debus et al., 1988a). Even more interesting, is the light-dependent labeling of the D1 protein by [^{125}I] when Cl^--depleted PS II membranes retaining the active OEC Mn are incubated with $[^{125}I]^-$ (Ikeuchi et al., 1988). They noted preliminary enzymatic mapping, but the specific fragment or amino acid labeled had not been identified. They proposed the labeled amino acid residue would be in a region in close proximity to the OEC Mn. Finally, they concurred with the proposal of

the D1 protein as the location of Z, the OEC Mn-binding site and also the site of Cl^- binding.

Several experiments using [^{14}C]-DEPC have been used to examine the relationship of photoactivation and Mn-binding to specific PS II polypeptides. Tamura et al. (1989a) showed the connections between photoactivation of PS II membranes (by photoligation of Mn as described in Chapter 7), chemical modification by DEPC, the involvement of histidine residues on D1 (and possibly D2) and the Mn^{2+}/DPC competition assay developed by Hsu et al. (1987) described in Chapter 8. Tamura et al. (1989a) also showed evidence for specific histidine modification by DEPC under their reaction conditions. Many PS II proteins were radioactively labeled by [^{14}C]-DEPC in their experiments, but labeling of the D1 protein and the D1/D2 protein dimer were suppressed by photoligated Mn (involvement of the D2 protein was not confirmed or eliminated due to heavy labeling of the light-harvesting proteins in the corresponding region of the gel). Seibert et al. (1989) proposed that the high-affinity Mn-binding site measured by the Mn^{2+} inhibition of DPC-stimulated DCIP photoreduction can be divided into at least two different components. Using DEPC (the histidine chemical modifier described above) they show that half of the Mn-binding site of WT *Scenedesmus* (or spinach or wheat) preparations is blocked after modification. Another important result was the demonstration that the full high-affinity Mn-binding site is present in the isolated reaction center complex (D1/D2/Cyt *b*-559/4.2 kDa proteins), limiting the possible proteins which might provide these ligands to Mn. In their most recent publication, Preston and Seibert (1991b) combined two amino acid chemical modifiers (DEPC, which modifies histidines, and EDC, which modifies carboxyl-containing residues) with protease treatments in order to better define the high-affinity Mn-binding site using the DPC/Mn^{2+} non-competitive inhibition assay for DCIP photoreduction (Preston and Seibert, 1991a). Basically, their data indicate that the DEPC-sensitive and EDC-sensitive halves of the high-affinity site can each be divided into two

components which demonstrate differential sensitivity to the proteases used, therefore indicating four separately identifiable components. Although they propose the four components located by the Mn^{2+}/DPC assay to be ligands involved in photoligation of Mn during photoactivation and/or binding the functional OEC Mn, they also provide some alternative explanations (discussed in Chapter 8), all of which are still consistent with the involvement of the D1 protein in Mn-binding.

As discussed earlier, Debus et al. (1988a) showed that the stable EPR signal assigned to the D^+ radical arises from Tyr-160 of the D2 protein, and renamed it Y_D^+. Also, Debus et al. (1988b) demonstrated that the intermediate electron donor from Mn to $P680^+$, known as Z^+, is Tyr-161 of the D1 protein, and renamed it Y_Z^+. Studies of the properties of these two radicals and their spectroscopic interactions with P680 and the Mn cluster of the OEC have provided further evidence on the location of the Mn complex in PS II. Hoganson and Babcock (1989) studied the EPR spectrum of $P680^+$ in PS II membranes at room temperature using repetitive flash excitation. Under their conditions, oxygen evolution was inhibited, which extended the lifetime of the P680 radical into the 150-200 μs range, allowing observation of this transient EPR signal. Using different treatments, they compared the broadening of the $P680^+$ EPR spectrum in the presence of either the reduced or oxidized forms of Y_Z. They discussed in depth the assignment of their observed EPR signal to $P680^+$, describing evidence based on narrower EPR line width relative to those of other PS II radical signals and on optical studies of $P680^+$ decay kinetics. Both sets of references support their assignment. They also thoroughly explained various theories used to estimate the distance between the two radicals. They attributed the observed 1 G broadening of the $P680^+$ spectrum by Y_Z^+ (relative to the spectrum of $P680^+$ with Y_Z in its diamagnetic state) to a magnetic dipole-dipole interaction between the two radicals. Based on their calculations, they estimated the center-to-center distance between $P680^+$ and Y_Z^+ to be 10-15 Å.

Several studies of the power saturation and relaxation properties of their EPR signals have indicated the spatial relationship between the radicals responsible for signal II (Y_D^+ and Y_Z^+) and the Mn cluster of PS II. Yocum et al. (1981) demonstrated that the removal of Mn by Tris washing resulted in slower relaxation of Z^+ than observed in the presence of the intact Mn cluster. They concluded that the Mn cluster was situated close to Z^+ and was responsible for the faster relaxation of Z^+ in its presence. Rutherford et al. (1988) studied the EPR properties of the LF-1 mutant of *Scenedesmus obliquus* which lacks the Mn cluster and described a slower D^+ EPR signal relaxation relative to the Mn-containing *Scenedesmus* wild-type. They suggested that Z^+ and D^+ may be located more equivalently with respect to the Mn cluster than had previously been proposed. Finally, Styring and Rutherford (1988) described the changes in low temperature power saturation of D^+ caused by the S-state transitions of the Mn cluster. They observed that D^+ is easier to saturate after Mn-removal by Tris washing. They proposed a cross relaxation between D^+ and an efficient relaxer in the presence of Mn, which they suggested to be the Mn cluster. They prepared samples in various S-states by illumination with a series of flashes and measured the microwave power for half-saturation of the D^+ signal. This power for half-saturation varied with flash number and, from this information, they proposed possible models for the OEC Mn cluster.

Evidence of the location of Y_D within the reaction center was provided by Innes and Brudvig (1989). They studied the effect of adding the free-radical-relaxing agent dysprosium ion and its complexes with EDTA on the spin-lattice relaxation of PS II free radicals. They described the effects on the microwave power saturation of the EPR signal attributed to D^+ and used the results to determine its location within the membrane. They approximated the PS II protein surface to be planar and obtained distances from Y_D to the membrane surface in thylakoid, PS II membrane and Tris-washed PS II membrane preparations. They calculated a distance from the stromal membrane surface to D^+ of 26 Å

and a distance of 27 Å to the lumenal membrane surface after removal of the 17, 24 and 33 kDa extrinsic proteins. They calculated the height of the extrinsic protein unit to be about 14 Å. From these results, they proposed a membrane thickness of approximately 53 Å in the absence of extrinsic proteins. These results agree with distances predicted from analogy of the D1 and D2 proteins of PS II with the L and M subunits of purple bacteria described earlier. The height of the extrinsic protein unit calculated by Innes and Brudvig is comparable, but not identical, to the approximately 20 Å measured by freeze-etch electron microscopy (Seibert et al., 1987).

Recent studies have focused on the relationship between the tyrosine radicals, Y_D^+ and Y_Z^+, and the Mn cluster at different oxidation levels through the S-state cycle. As discussed earlier, Evelo et al. (1989) used electron spin echo spectroscopy to study the spin-lattice relaxation time of the EPR signal attributed to D^+. They studied the temperature dependence and average relaxation time for PS II preparations with the intact OEC poised at various S-states by illumination with a series of flashes. In addition to the oxidation states during the S-state cycle, they calculated a distance from D^+ to the OEC Mn cluster of 30-40 Å which they explained as being consistent with the results of Innes and Brudvig (1989) described above. Hoganson and Babcock (1988) measured the light-induced EPR spectrum of Y_Z^+ in intact PS II membranes using time-resolved techniques. They did their measurements at room temperature with flowing samples and exogenous electron acceptors (DCBQ or 1 mM ferricyanide) to maintain oxygen-evolving activity. The time-resolved spectrum of Y_Z^+ recorded for these active PS II membranes was very similar to the steady-state spectrum of the stable tyrosine radical Y_D^+ and the same as the steady-state Y_Z^+ spectrum in inhibited PS II membranes, regardless of whether Mn was still present. The similarity to the Y_D^+ signal is discussed as arising from very similar orientations of the two tyrosine radicals within the membrane bound protein complex. The similarity in line shape of the Y_Z^+ signal in different preparations implies that the interaction between Mn and Y_Z^+

is weak and does not perturb the spin distribution on this tyrosine radical. Based on these results, they conclude that the distance from Y_Z^+ to the nearest Mn ion must be greater than 10 Å (and they may be separated by 2 or more amino acid residues). They also demonstrate that Y_Z is the intermediate electron donor between Mn and P680 for the S-state transitions S_1 to S_2, S_2 to S_3 and S_3 to S_0 (they claim that S_0 to S_1 occurs too quickly for them to measure, but probably goes through Y_Z also). They also describe decay kinetics of Y_Z^+ that vary with the S-state of the OEC and are indicative of the Mn location being close to Y_Z.

Finally, several studies have addressed the effects of the Mn cluster in preventing the accessibility by exogenous reductants to the tyrosine radicals, Y_D^+ and Y_Z^+. Sivaraja and Dismukes (1988) investigated the flash-induced reactions of NH_2OH with PS II by equilibrium titrations with NH_2OH and the monitoring of odd-electron species by EPR spectroscopy. They characterized and presented a plausible model for the reversible reactions of NH_2OH with the S_1 and S_2 states of PS II at low (10-100 μM) NH_2OH concentrations. At slightly higher NH_2OH concentrations, they proposed a structural change of the electron acceptors which blocks electron transfer from Q_a^- to Q_b. Additionally, at high concentrations of NH_2OH (1-2 mM) there was a parallel release of Mn and loss of oxygen evolution, which was best explained by a cooperative loss of about 2 Mn ions per reaction center. The stable tyrosine radical signal attributed to Y_D^+ is completely removed by 1.5 mM NH_2OH, and this reduction of Y_D^+ occurs only following the release of Mn. This suggests that bound OEC Mn ions block the access of NH_2OH to Y_D and, presumably, also Y_Z. Ghanotakis et al. (1984a) had previously shown that after Mn-depletion by any of several methods, the kinetic behavior of Z^+ is altered, as demonstrated by a change in its EPR properties and its becoming more accessible to reduction by exogenous electron donors. The EPR signal of Z^+ after Mn removal required low microwave power in order to observe saturation, while Z^+ in the presence of bound

OEC Mn saturated only at much higher microwave power. Ghanotakis et al. (1984a) discussed the increased lifetime of the Z^+ radical into the 100 ms time-range, and its decrease by the addition of reductants such as benzidine. They proposed that the OEC Mn must be located near Z and sterically protects Z^+ from reduction by exogenous reductants. Recently, Hoganson et al. (1989) reported measurements of rates of YZ^+ reduction by exogenous reductants such as benzidine and Mn^{2+}. They used flash photolysis techniques to create the YZ^+ radical and measured its room temperature reaction kinetics with reductants by monitoring its EPR signal. They observed the same kinetics in the presence or absence of the 33 kDa extrinsic protein for membranes depleted of Mn. The rate of YZ^+ reduction was found to be linear with benzidine concentration (indicative of second order kinetics). The rate of YZ^+ reduction was also linear with Mn^{2+} at pH 6 and low Mn concentration (also second order kinetics), but reached a maximum level at concentrations five times that of the reaction center. At pH 6, The Mn^{2+} effect was inhibited by K^+, Ca^{2+} and Mg^{2+} (indicating an electrostatic interaction). The rate was biphasic for Mn^{2+} at pH 7.5, for which they described two components. The fast component may represent pre-flash binding of Mn^{2+} at one of the native Mn-binding sites (the first step in assembly of the Mn complex by photoactivation). The slow component may be diffusion controlled (and give the second order kinetics seen at pH 6). They concluded that the intrinsic OEC Mn are required in order to establish the barrier which prevents reductants from reaching YZ^+.

Some examples of antibody effects on other enzymes

Although several studies using antibodies to PS II protein components have been reported, none of them examined the effects of antibodies on the enzymatic activity of the oxygen-evolving complex. Other studies in much simpler systems have provided evidence

of inhibition of enzyme activities by antibodies. Some of these activities are associated with electron transport, redox reactions or oxidase activities. A few of the more relevant examples are described here.

Nisimoto et al. (1973) raised an antiserum against NADH:hemeprotein oxidoreductase using the enzyme purified from extracts of whole cells of *Rhodospirillum rubrum*. Incubation of chromatophores and purified protein with this antiserum inhibited the activity of NADH-cytochrome *c*2 reduction for both preparations. They showed that the enzyme bound in chromatophore membranes was functional in the donation of electrons from NADH to the cyclic electron transport system of the photosynthetic bacterium. Using an antibody to yeast cytochrome *b*5, Ohba et al. (1979) also demonstrated inhibition of the NADH-cytochrome *c* reductase and the NADH-dependent desaturase activities of yeast microsomes.

The purified NADPH-cytochrome *P*-450 reductase isolated from rat liver microsomes was used by Guengerich et al. (1981) to elicit polyclonal rabbit antibodies. These antibodies were shown to inhibit the enzyme's ability to reduce cytochrome *c* and cytochrome *P*-450 to different extents, depending on the source of enzyme. Takayama, et al. (1984) raised rabbit antibody against guinea-pig liver NADPH-cytochrome *P*-450 reductase. This antibody was shown to dose-dependently inhibit the superoxide (O_2^-)-generating activity of a membrane fraction isolated from leukocytes to approximately 50% of the total activity. Fukuhara et al. (1988) studied a blood neutrophyl-derived flavin enzyme involved in O_2^--generating oxidase activity. They demonstrated that incubation with polyclonal antibodies raised against the isolated protein caused a maximum inhibition of 54% of the O_2^--generating activity of the membrane-solubilized oxidase.

Goals of this work

The work described in this thesis combines several chemical, biochemical and immunological techniques into a series of experiments aimed at clarifying the structure of the oxygen-evolving complex of PS II. Specifically, the possibility of protein regions and/or amino acids serving as terminal ligands to the OEC Mn was investigated using antibodies raised to selected lumenal regions of the D1 and D2 proteins of the PS II reaction center. The selection of peptides to be used, along with the synthesis, purification and characterization of those peptides, are presented in Chapter 2. The eliciting of polyclonal antibodies to the different peptides and the characterization of the antibodies produced are presented in Chapters 3 and 4. In Chapter 4, the binding of the antibodies to the corresponding denatured protein was demonstrated by western blots of PS II membrane preparations separated by SDS-PAGE. To confirm antibody binding to intact PS II membrane preparations and to characterize this binding with respect to extrinsic protein composition and Mn presence, a solution antibody binding assay was used (Chapter 6). The effects of antibodies on several functions of the OEC were determined and are described in Chapters 5, 7 and 8. These three studies examine antibody effects on different aspects of Mn activity as the catalytic site for water oxidation. The ability of antibodies to compete with previously bound Mn was determined for PS II membrane preparations of varying extrinsic protein composition, all of which retain Mn before antibody addition, by measurement of the rate of oxygen evolution (Chapter 5). The ability of an antibody to block the binding and subsequent photoligation of Mn^{2+} is presented in Chapter 7 using a procedure to photoactivate PS II membrane preparations from which the active Mn had been removed. Finally, experiments which assayed the antibody effect on Mn^{2+} inhibition of diphenylcarbazide (DPC) to 2,6-dichlorophenol indophenol (DCIP) photoreduction are described in Chapter 8. These experiments address whether bound antibody can block any

of the four components of the high-affinity Mn-binding site that become available in the presence of DPC.

2. PEPTIDES

Introduction

In this chapter the peptides which correspond to lumenal regions of the D1 and D2 proteins of PS II that were chosen for synthesis, the rationale for their choice, the synthetic procedures used, the purification of the various peptides and, finally, the analysis of their composition and sequence are described. To summarize, the regions of the D1 and D2 proteins chosen as potentially Mn-binding had to fit several criteria as well as possible. First, they had to be exposed on the lumenal side of the thylakoid membrane according to the five transmembrane helix models proposed by Trebst (1986) and later confirmed by the antibody studies of Sayre et al. (1986). Secondly, the peptides had to contain as many potential Mn-binding residues as possible. And, lastly, the peptides preferred were regions of high homology among oxygenic organisms, but low homology with the anoxygenic photosynthetic bacteria as described in Chapter 1 and, in more detail, below.

Much has been published regarding the location of the OEC Mn cluster of PS II. Early evidence located the Mn to the interior of the thylakoid membranes within the chloroplast, meaning the lumenal side of these thylakoid membranes. Next, the OEC Mn was shown to be associated with the PS II complex. The active Mn was shown to be released by several chemical treatments which caused inhibition of oxygen evolution. Mn was also shown to be involved in the *in vivo* reconstitution of oxygen evolution and necessary for the photoactivation of Mn-depleted PS II preparations *in vitro*. All of these properties are reviewed by Brudvig et al. (1989). The spectroscopic evidence for Mn involvement is reviewed by Dismukes (1988), Brudvig et al. (1989) and others, and is described below with relevance to the ligand environment and in more detail in Chapter 1.

The five transmembrane helix models for the folding patterns of the D1 and D2 proteins are the models most consistent with studies of antibody binding to proposed interhelical regions (Sayre et al., 1986). These folding patterns and the protein incorporation into the thylakoid membrane were originally predicted by hydropathic analysis of the D1 and D2 proteins (Trebst, 1986). The spinach amino acid sequence of the D1 protein (Zurawski et al., 1982) and the pea amino acid sequence of the D2 protein (Rasmussen et al., 1984) are pictured in Figure 2-1 in a folding pattern similar to that presented by Michel and Deisenhofer (1988). The processing site near the C-terminus of the D1 protein as determined by Takahashi et al. (1988) is depicted as an "X" between alanine residues 344 and 345. The 9 amino acid C-terminal fragment is omitted from further diagrams, such as the one shown in Figure 2-4 which is explained below.

The sequence homologies of the D1 and D2 proteins with the L and M subunits of *Rb. capsulatus* which allowed Hearst (1986) and others to suggest that the D1 and D2 proteins function as the reaction center proteins of PS II are thoroughly discussed in Chapter 1. Of more importance here, are the regions of divergence of the D1 and D2 polypeptides from the L and M subunits of the non-oxygen evolving organisms. These regions tend to be highly conserved amongst oxygen evolving organisms and are often sequence insertions relative to the purple bacterial sequences. In Figures 2-2 and 2-3, comparisons of the L and M sequences, as originally described by Hearst (1986), with the spinach sequences for the D1 and D2 proteins, are shown. The amino acid conservation between the D1 and D2 protein sequences of several higher plants and several cyanobacteria is described in detail by Gingrich et al. (1988, 1990). The regions of the five proposed transmembrane helices for the D1 and D2 proteins are marked in the figures and correspond to those described for the L and M subunits by Michel and Deisenhofer (1988) but placed on the sequence alignments proposed by Hearst (1986). The regions of interest in potential Mn ligation are both of the C-terminal stretches and those loop regions

Figure 2-1: Folding pattern of the D1 and D2 proteins

The five transmembrane helix models for the folding patterns of the D1 and D2 proteins are shown as predicted by Trebst (1986). The proposed protein incorporation into the thylakoid membrane is indicated with the membrane boundaries shown as horizontal dashed lines. The *spinacia oleracea* amino acid sequence of the D1 protein (Zurawski et al., 1982) and the *pisum sativum* amino acid sequence of the D2 protein (Rasmussen et al., 1984) are pictured in a folding pattern similar to that presented by Michel and Deisenhofer (1988). The "X" between alanine residues 344 and 345 near the C-terminus of the D1 protein indicates the processing site as determined by Takahashi et al. (1988).

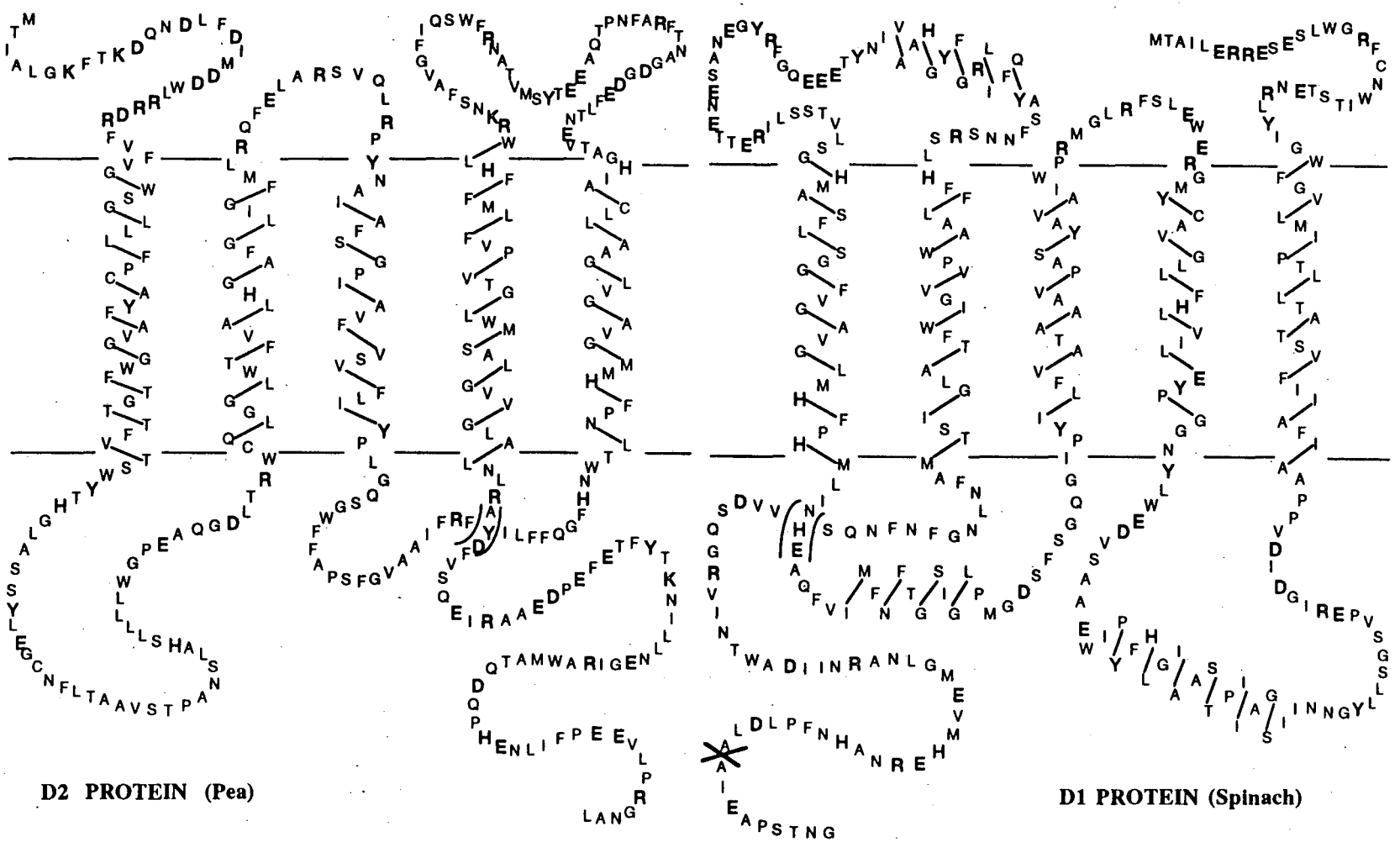

D2 PROTEIN (Pea)

D1 PROTEIN (Spinach)

Figure 2-2: Sequence comparison of D1 to L subunit

Amino acid sequence comparison of the spinach D1 protein with the purple bacterial L subunit, as originally described by Hearst (1986). The *spinacia oleracea* amino acid sequence is given for the D1 protein (Zurawski et al., 1982). The *Rb. capsulatus* amino acid sequence is given for the L subunit (Youvan et al., 1984). The marked and numbered regions of the five proposed transmembrane helices for the L subunit correspond to those described by Michel and Deisenhofer (1988).

```
Spinach D1 protein:    MT.AILERRE SESLWGRFCN WITSTENRLY IGWFGVLMIP
Rb. Caps. L subunit:   MALLSFERKY RVPGGTLIGGSLFDFWVGPFY VGFFGVTTI.

TLLTATSVFI IAFIAAPPVD IDGIREPVSG SLLYGNNIIS GAIIPTSAAI GLHFYPIWEA
..FFATLGFLLILWGAAMQGT WNP....... .......... ........QL ISIFPPPVEN
 Helix I

ASVDEWLYNG GPYELIVLHF LLGVACYMGR EWELSFRLGM RPWIAVAYSA PVAAATAVFL
GLNVAALDKG GLWQVITVCA TGAFCSWALR EVEICRKLGI GFHIPVAFSM AIFAYLTLVV
                       Helix II                         Helix III

IYPIGQGSFS DGMPLGISGT FNFMIVFQAE HNILMHPFHM LGVAGVFGGS LFSAMHGSLV
IRPMMMGSWG YAFPYGIWTH LDWVSNTGYTYGNFHYNPFHM LGISLFFTTA WALAMHGALV
                                                     Helix IV

TSSLIRETTE NESANEGYRF GQEEETYNIV AAHGYFGRLI FQYASFNNSR SLHFFLAAWP
LS......AA NPVKGKTMRT PDHEDT.... ....YFRDLM GYSVGTLGIH RLGLLLALNA
                                                         Helix V

VVGIWFTALG ISTMAFNLNG FNFNQSVVDS QGRVINTWAD IINRANLGME VMHERNAHNF
VFWSACCMLV SGTIYFDLWS DWWYWWV... ...NMPFWAD .......... ..........

PLDLAAIEAP STNG
.......MAG GING
```

Figure 2-3: Sequence comparison of D2 to M subunit

Amino acid sequence comparison of the spinach D2 protein with the purple bacterial M subunit, as originally described by Hearst (1986). The *spinacia oleracea* amino acid sequence is given for the D2 protein (Holschuh et al., 1984; Alt et al., 1984). The *Rb. capsulatus* amino acid sequence is given for the M subunit (Youvan et al., 1984). The marked and numbered regions of the five proposed transmembrane helices for the M subunit correspond to those described by Michel and Deisenhofer (1988).

Spinach D2 protein: MTIAVGKFTK DEKDLFDSMD DWLRRDRFVF VGWSGLLLFP
Rb. Caps. M subunit: MAEYQNFFNQ VQVAGAPEMG LKEDVDTFER TPAGMFNILG

CAYFALGGWF TGTTFVTSWY THGLASSYLE GCNFLTAAVS TPANSLAHSL LLLWGPEAQG
WMGNAQIGPI YLGIAGTVSL AFGAAWFFTI GVWYWYQAGFDPFIFMRDLFFFSLEPPPAEYG
Helix I

DFTRWCQLGG LWAFVALHGA FALIGFMLRQ FELARSVQLR PYNAIAFSGP IAVFVSVFLI
LAIAPLKQGG VWQIASLFMA ISVIAWWVRV YTRADQLGMG KHMAWAFLSA IWLWSVLGFW
Helix II Helix III

YPLGQSGWFF APSFGVAAIF RFILFFQGFH NWTLNPFHMM GVAGVLGAAL LCAIHGATVE
RPILMGSWSV APPYGIFSHL DWTNQFSLDHGNLFYNPFHGL SIAALYGSAL LFAMHGATIL
Helix IV

NTLFEDGDGA NTFRAFNPTQ AEETYSMVTA NRFWSQIFGV AFSNKRWLHF FMLFVPVTGL
AVTRFGGERE LEQIVDRGTA SERAALFWRWTMGWNATMEG. ...IHRWAIW MAVMVTLT..
Helix V

WMSALGVVGL ALNLRAYDFV SQEIRAAEDP EFETFYTKNI LLNEGIRAWM AAQDQPHENL
.....GGIGI LLSGTVVDNW YVWAQVHGYA PVTP

IFPEEVLPRG NAL

(between helices I and II and between helices III and IV of both proteins) which connect two transmembrane helices to each other on the lumenal side of the thylakoid membrane. Notice the particularly long sequence insertions between helices I and II of the D1 protein, and the C-terminal extensions on both the D1 and D2 proteins.

The proposals for which amino acids are capable of providing terminal ligands to the OEC Mn cluster are based on several lines of evidence, summarized here and described in more detail below. The spectroscopic evidence for the structural proposals of the Mn cluster have provided insight into possible amino acid ligands as summarized by Dismukes (1988). Early work used mainly EPR and X-ray absorption spectroscopy (EXAFS and XANES). More recently, improved sample preparations, application of the early spectroscopic methods to these samples and the introduction of pulsed EPR techniques (ESEEM and ENDOR) has provided higher resolution data which allows a more detail description of the OEC Mn complex. From the inorganic chemistry viewpoint, Pecoraro (1988) reviews the theoretically possible and chemically most probable groups that may act as ligands to Mn (oxyanions and imidazole groups). He also reviews the biochemical evidence, including comparison of other proteins which contain metal atom cofactors which has provided precedence for metal ion coordination within proteins, clues as to the amino acid residues preferred as ligands and likely structures of metal atom complexes within proteins.

In addition to the nitrogen groups from the peptide backbone, all of the amino acids which are theoretically possible candidates to provide ligands to Mn are: arginine, asparagine, aspartic acid, cysteine, glutamine, glutamic acid, histidine, lysine, methionine, serine, threonine and tyrosine. Of these, cysteine, methionine, serine and threonine can be excluded based an chemical reasoning as described by Dismukes (1988). The remaining amino acids, arginine, asparagine, aspartic acid, glutamine, glutamic acid, histidine, lysine

and tyrosine are still possible ligand donors and are included in the diagram in Figure 2-4. This figure diagrammatically represents the five transmembrane helix models as depicted with the complete amino acid sequences in Figure 2-1. In Figure 2-4, proposed transmembrane helices are shown as numbered, darkly outlined, rectangles. Lightly outlined, unnumbered, rectangles represent other potential helical regions. Symbols represent the approximate location of the possible Mn-ligating amino acids which are predicted to be on the lumenal side of the membrane. Combining ESEEM results from DeRose et al. (1991) with EXAFS results, both discussed in Chapter 1, the most probable composition of amino acid ligands to the Mn cluster would be 1 or 2 histidines with the rest mainly aspartic and glutamic acids, with possibly the deamination products (aspartic and glutamic acids) of asparagine and glutamine. To simplify the diagrams, only lumenal histidine and carboxyl-containing amino acids (aspartic and glutamic acids), with the position number of histidines labeled explicitly, have been shown in further figures representing the D1 and D2 proteins in order to demonstrate relative positions. All of the possible amino acid ligands are represented schematically in Figure 2-4 and the actual sequences are shown in Figure 2-1.

Efforts were concentrated on lumenal regions of mainly the D1 protein for several reasons. First, the sequence and composition of potential Mn-binding amino acids were examined as just described. Secondly, the LF-1 mutant of *Scenedesmus obliquus* identified by Metz and Bishop (1980) was shown to be deficient in oxygen evolution and to lack approximately two of the four functional Mn. The LF-1 mutant was shown to have one altered protein which migrated slower on PAGE (Metz et al., 1980) which was later identified to be the D1 protein (Metz et al., 1986). Finally, the D1 protein was shown to turn over very quickly (Edelman and Reisfeld, 1978; Silverthorne and Ellis, 1980), possibly due to damage from the highly oxidizing environment surrounding the Mn cluster. This turnover was later shown to occur after an initial cleavage at the reducing side of the

Figure 2-4: Diagram of D1 and D2 with all possible Mn ligands labeled

Diagrammatic representation of the five transmembrane helix models as depicted with the complete amino acid sequences in Figure 2-1. The approximate location of the lumenal amino acids (arginine, asparagine, aspartic acid, glutamine, glutamic acid, histidine, lysine and tyrosine) which are possible ligand donors to Mn are represented by the given symbols. Proposed transmembrane helices are shown as numbered, darkly outlined, rectangles. The thylakoid membrane boundaries are shown as horizontal dashed lines and the position number of histidines are labeled explicitly.

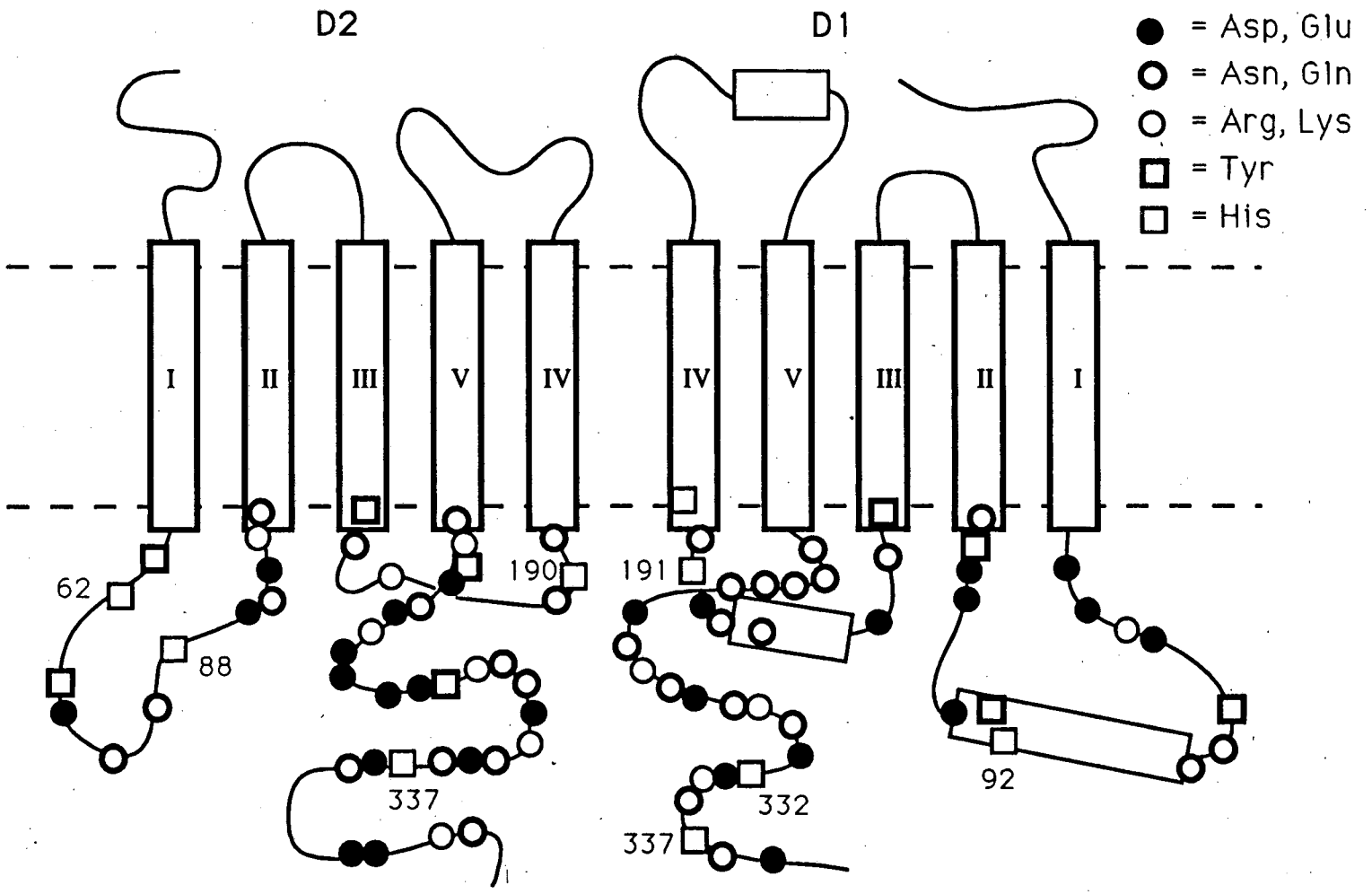
D2
D1
= Asp, Glu
= Asn, Gln
= Arg, Lys
= Tyr
= His
I
II
III
V
IV
IV
V
III
II
I
62
88
190
191
337
332
337
92

membrane near the quinone binding site (Greenberg et al., 1987). Although these authors describe the pathway for turnover of the D1 protein, the reason for the necessity of this turnover is still unclear and may be a requirement to replace D1 proteins damaged by Mn on the oxidizing side of the complex.

Several segments of the D1 and D2 proteins meeting the criteria described above were chosen for synthesis and are outlined on the schematic given in Figure 2-5. In this and following diagrams of the D1 and D2 proteins, circles or ovals surround the approximate regions of interest, which are further discussed as appropriate. The regions outlined in Figure 2-5 were chosen before the prediction of potential Mn-binding segments published by Dismukes (1988). The regions that were chosen here and those that Dismukes predicted were similar, with the C-terminal regions of D1 and D2 emphasized. But, regions closer to the C-terminus of both mature proteins and in the loop region connecting helices I and II of the D1 protein, all of which were excluded by Dismukes, were favored in this study. The C-terminus of D1 above residue 338 was eliminated by Dismukes based on the cleavage of 12 to 16 residues of the protein sequence determined from the DNA sequence to form the mature functional protein as explained by Marder, et al. (1984). The actual cleavage was later shown to remove only 9 residues (Takahashi et al., 1988), leaving the C-terminus of D1 intact to residue 344. Similarly, the 28 C-terminal residues of D2 were excluded by Dismukes based on *Clamydomonas reinhardtii* sequences published by Rasmussen, et al. (1984) and Rochaix, et al. (1984). These sequences appeared to show a lack of homology for oxygen-evolving organisms as analyzed by Zurawski, et al. (1982). The sequence was later corrected (Erickson, et al., 1986) and shown to be highly homologous and absent in the non-oxygen evolving photosynthetic organisms, therefore, considered here as a potential Mn-binding region.

Figure 2-5: Diagram of D1 and D2 showing regions to be synthesized

Diagrammatic representation of the five transmembrane helix models with outlines surrounding segments of the D1 and D2 proteins which were chosen for synthesis. In this and further figures representing the D1 and D2 proteins, only lumenal histidine and carboxyl-containing amino acids (aspartic and glutamic acids) are shown, with the position number of histidines labeled explicitly.

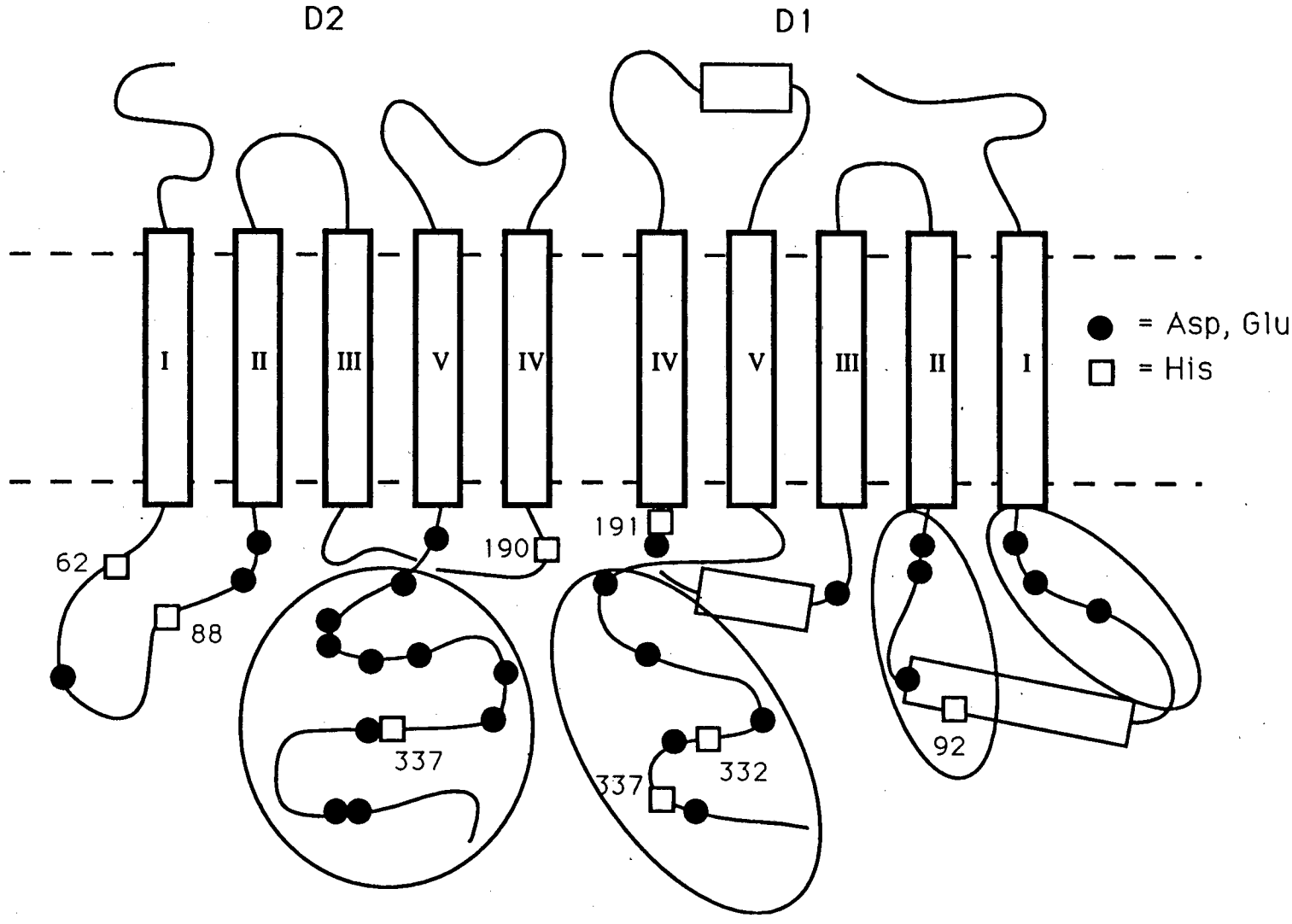
D2
D1
I
II
III
V
IV
IV
V
III
II
I
= Asp, Glu
= His
62
88
190
191
337
337
332
92

Procedures

Peptide synthesis

Peptides were synthesized at the Melvin Calvin Laboratory, with the guidance of David Koh, on an Applied Biosystems Model 430A Peptide Synthesizer using the Merrifield solid phase method and t-Boc chemistry as originally described by Merrifield (1963) and later reviewed by Kent and Clark-Lewis (1985). Hydrogen fluoride cleavage and deprotection was performed by the custom synthesis group led by Dr. Anita Hong at Applied Biosystems, Foster City, California using the method of Tam, et al. (1983).

Peptide purification

Peptide purification was done by reverse phase high performance liquid chromatography (HPLC) on C18 columns using either a Waters or a Rainin HPLC system. A two solvent gradient system was used as described by Rivier et al. (1984). The solvents used were Solvent A: 0.1% trifluoroacetic acid (TFA) in 100% water and Solvent B: 0.09% TFA in 60% acetonitrile, 40% water. Initially, a crude peptide was dissolved in a small volume (usually 5-20 ml) of Solvent A, containing 1 M acetic acid or 6-8 M urea when needed. Filtration using 2 ml microfilters (Rainin) was always performed prior to loading samples onto HPLC columns. A small fraction (100-300 μl) of this filtered solution was loaded onto an analytical C18, 300Å pore size, 1/4 inch diameter column (Rainin) at a flow rate of 0.5 to 1.0 ml/min. The solution was allowed to load onto the column for 20 min while flowing 100% Solvent A. The linear gradient used for this initial analysis started at 100% A and reached 100% B in 60 min. After this time, the column was flushed for 20 min with 100% B and then changed back to 100% A over 10 min. The effluent was monitored continuously by absorption at 220 nm. The elution position of the major peak was used to define a shallower gradient for better separation. The shallower

gradients incorporated this analytical elution percentage between their midpoint and two thirds point. Another analytical sample was loaded as above at 100% A for 20 min. The amount of Solvent B was then increased in 10-20 min from 0 to 35% (a common gradient starting point, which was anywhere from 25 to 45% B depending on the peptide). The gradient proceeded from 35% B to 65% B (again, 65% B was common, but the endpoints fell somewhere in the range of 40 to 80% B) in 60 or 90 min. Finally, the solvent was changed to 100% B in 10-20 min and allowed to flow for an additional 20 min before returning to 100% A in 10 min. This profile was then used for preparative runs on larger bore columns (C18, 300Å pore size, 1 inch diameter column from Rainin or Waters) using flow rates of 4 to 10 ml/min. For these runs, however, the volumes of filtered peptide solution ranged from 2 to 20 ml and were loaded as multiple injections or through a third solvent pump. The timing of the 20 min at 100% A did not begin until after completion of loading. For these larger samples, the effluent was monitored at 235 nm and the major peak by absorption was collected and pooled as fractions of differing purity (in the cases of several runs of the same peptide or separation into several fractions during a single run). This solution was then dried in a Speed-Vac to remove the organic solvents and acids and, if needed, lyophilized to remove any remaining water.

Peptide characterization

Peptide composition was verified by amino acid analysis at the Melvin Calvin Laboratory, with the guidance of David Koh, using a system consisting of Applied Biosystems' Model 420A Amino Acid Derivatizer, 130A Separation System and 900A Control/Data Analysis Module. Samples containing 100-500 pmole of a particular peptide were placed in small tubes, dried by lyophilization and the tubes inserted into vials containing 6 M HCl (sequencing grade) and sealed with solid covers containing Teflon seals. These samples were acid hydrolyzed by heating overnight at 200°C. After carefully removing the lid (in a hood) while still hot to avoid HCl condensation, the small tubes were

removed and the hydrolysate redissolved in the volume required of distilled water to have 10-20 pmole of peptide per 20 µl. Nine 20 µl samples were placed on thoroughly cleaned glass filter discs and run on the amino acid analyzer following three samples of amino acid standard (10 µl of 1:100 dilution of stock from Bio Rad). The position of amino acid peaks of the standard were compared to previous standard runs for assignment to specific amino acids. The detector response to each amino acid was then calibrated to peak height or peak area by use of known standard concentrations. These calibrations were then used to assign the peaks of a hydrolyzed peptide and to calculate the amount (in pmole) of each amino acid present in that sample of peptide. These amounts were finally converted to ratios and compared to the theoretical amino acid composition of each peptide. This procedure was used to verify peptide composition, but gave no information as to peptide sequence.

Peptide sequences were confirmed by fast atom bombardment (FAB) mass spectrometry performed under the guidance of Dr. Judy Leary at the Chemistry Department, University of California at Berkeley. This method was under development at the time these sequences were analyzed. The correct sequences of synthesized peptides were easily confirmed. When fragmentation patterns of the purified peptide did not match the predicted sequence, it was not possible to assign a unique sequence. For these reasons, peptides whose sequences were not confirmed by mass spectrometry were resynthesized and repurified.

Results and Discussion

The sequences of the five peptides chosen for synthesis (along with the numbers of the starting and ending amino acids of the corresponding spinach protein) are shown in Figure 2-6. These sequences come from the spinach sequence of the D1 protein (Zurawski

Name	Sequence
D1-a	321-INR-ANL-GME-VMH-ERN-AHN-FPL-DLA-344
D1-b	319-DII-NRA-NLG-MEV-MHE-R-334
D1-c	56-PPV-DID-GIR-EPV-SGS-LLY-GNN-76
D1-d	90-GLH-FYP-IWE-AAS-VDE-WLY-N-108
D2-a	300-VSQ-EIR-AAE-DPE-FET-FYT-KN-319

Figure 2-6: Sequences of peptides synthesized

Sequences of the five peptides chosen for synthesis (along with the numbers of the starting and ending amino acids of the corresponding spinach protein). These sequences correspond to segments of the *spinacia oleracea* amino acid sequences of the D1 protein (Zurawski et al., 1982) and the D2 protein (Holschuh et al., 1984; Alt et al., 1984).

et al., 1982) and the pea sequence of the D2 protein (Rasmussen et al., 1984). The peptides were successfully synthesized and deprotected as described above. Their approximate positions on the intact proteins are outlined on the schematic in Figure 2-7.

Peptide purification was done by reverse phase HPLC on C18 columns as described above. Generally, an analytical HPLC trace of a peptide showed one major, relatively sharp peak accounting for 75-95% of the total absorbance at 220 nm and eluted at a solvent composition in the region between 35% B and 65% B (with the remaining percentage made up with solvent A). The analytical HPLC trace of peptide D1-a was different in that there were three broad overlapping peaks whose sum accounted for 90-95% of the total absorbance at 220 nm. The largest peak accounted for only 60% of the absorbance, and the next two peaks absorbed approximately equally the remaining 30-35%. Peptide D1-a proved impossible to purify, even with different column types and a variety of different solvent systems (not described here). During purification attempts, three crude peptides (D1-a, D1-c and D1-d) were used for a first attempt at antibody production using C8 HPLC beads as the carrier and adjuvant (see Chapter 3). When the crude products from a peptide synthesis were used as antigen, only a few sequences in addition to the desired peptide are available to elicit antibodies. These would primarily include amino acid deletions and products of early termination (peptides missing portions of the N-terminus), which would not create major complications in further assays. The region of D1 corresponding to peptide D1-a was resynthesized as a slightly shorter peptide (D1-b) which was successfully purified. Of the five peptides shown in Figure 2-6, only D1-a could not be purified. The other four peptides (D1-b, D1-c, D1-d and D2-a) all showed good analytical HPLC traces and were successfully purified as described earlier. The crude yield of peptide following deprotection was generally 1-2 mg, depending on the length and composition of the specific peptide. The final yield of peptide following preparative HPLC were more variable and ranged from 50 to 200 μg, this time depending

Figure 2-7: Diagram of D1 and D2 showing synthesized peptide regions

Diagrammatic representation of the five transmembrane helix models with the approximate positions of the synthesized peptides outlined on the intact proteins. As described in Figure 2-5, only lumenal histidine and carboxyl-containing amino acids (aspartic and glutamic acids) are shown, with the position number of histidines labeled explicitly.

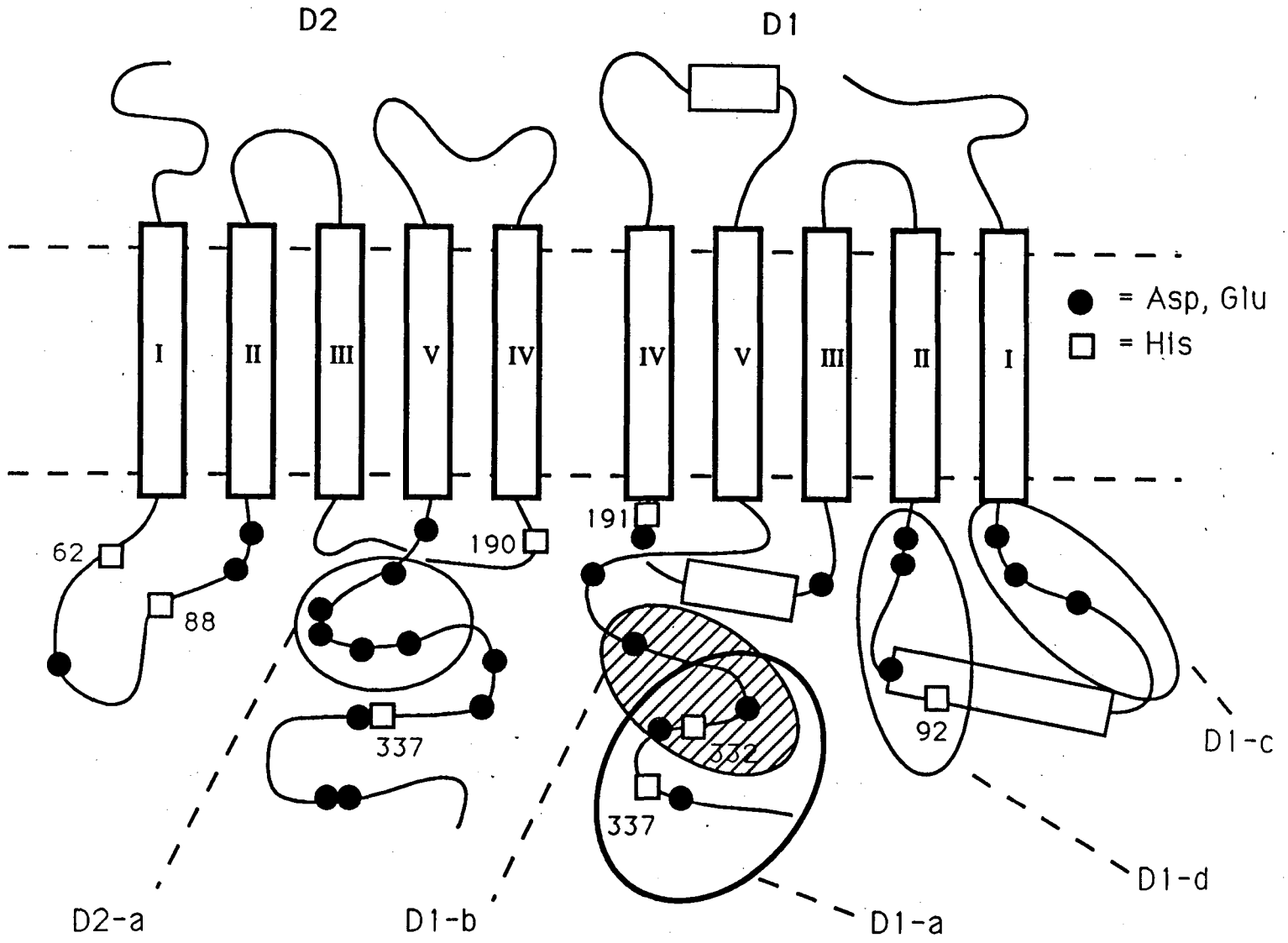
D2
D1
I
II
III
V
IV
IV
V
III
II
I
= Asp, Glu
= His
62
88
190
191
337
332
337
92
D2-a
D1-b
D1-a
D1-d
D1-c

on the required purity and solubility behaviors of the individual peptide. The purity of the central fractions collected from the major peaks was very high as shown by no residual peaks on final analytical HPLC traces. These central fractions were used for subsequent antibody production, see Chapter 3.

Peptide composition was verified by amino acid analysis using the equipment described above. Since peptide D1-a proved impossible to purify, it was not further characterized. For an example of the results of amino acid analysis, the composition of peptide D1-b is shown in Table 2-1. At this point, it should be noted that amino acid composition is always affected by the acid hydrolysis procedure used. The best procedure available at the time, which was described earlier, was chosen. The predicted effects of this hydrolysis procedure on the yield of individual residues as described by Pickering and Newton (1990) are shown in Table 2-2. To summarize, the most quantitatively reproducible residues are: Ala, Arg, Gly, His, Ile, Leu, Lys, Phe, Pro and Val. Two residues, Asn and Gln, are converted to Asp and Glu, respectively and quantitatively. Therefore, the experimental Asp value represents the sum of Asn and Asp found in the peptide, and similarly for the Glu value. The residues whose yield may vary, depending on procedural variations are Cys, Met, Trp and Tyr. Finally, the yield is predictably less than 100% for Ser and Thr (see Table 2-2). Generally, the yield of Ser is 90% and the yield of Thr is 95%. Using these corrections to calculate corrected experimental amino acid compositions gave values which agree more closely with the predicted amino acid contents of known proteins. As an example, the final column of Table 2-3 shows the amino acid composition for peptide D1-b as corrected for all of these expected variations. As can be seen, the experimental sequence matches quite well with the predicted sequence when hydrolysis effects are considered. This was also the case for the other three peptides analyzed (D1-c, D1-d and D2-a) as is shown in Tables 2-4, 2-5 and 2-6. One of these peptides (D1-c), however, had shown an anomalous amino acid composition and

Table 2-1

Amino acid composition of purified D1-b peptide, whose sequence was DII-NRA-NLG-MEV-MHE-R. The given experimental amino acid ratios are not corrected for the effects of acid hydrolysis on amino acid composition.

Amino Acid	Predicted AA Ratios	Experimental AA Ratios
Ala	1	0.97
Arg	2	1.87
Asn	2	0
Asp	1	3.15
Glu	2	2.13
Gly	1	1.00
His	1	0.98
Ile	2	2.21
Leu	1	1.08
Met	2	0.80
Val	1	0.98

Table 2-2

Effects of acid hydrolysis on amino acid composition as described by Pickering and Newton (1990). This information incorporates known effects of acid hydrolysis on individual amino acids and will be used for the calculation and explanation of corrected amino acid compositions from the experimental amino acid ratios.

Amino Acid	Percentage Observed	Corrections and comments
Ala	100%	
Arg	100%	
Asn	0%	becomes 100% Asp
Asp	100%+	Asp + Asn
Cys	<70%	x 1.43
Gln	0%	becomes 100% Glu
Glu	100%+	Glu + Gln
Gly	100%	
His	100%	
Ile	100%	
Leu	100%	
Lys	100%	
Met	<50%	x 2.00
Phe	100%	
Pro	100%	
Ser	90%	x 1.11
Thr	95%	x 1.05
Trp	<50% (we see 0%?)	x 2.00
Tyr	<80%	x 1.25
Val	100%	

Table 2-3

Corrected amino acid composition of purified D1-b peptide, whose sequence was DII-NRA-NLG-MEV-MHE-R. These corrected amino acid ratios incorporate the known effects of acid hydrolysis on amino acid composition as described in Table 2-2.

Amino Acid	Predicted AA Ratios	Experimental AA Ratios	Corrected AA Ratios
Ala	1	0.97	
Arg	2	1.87	
Asn	2	0	
Asp	1	3.15	1+2?
Glu	2	2.13	
Gly	1	1.00	
His	1	0.98	
Ile	2	2.21	
Leu	1	1.08	
Met	2	0.80	1.60?
Val	1	0.98	

Table 2-4

Corrected amino acid composition of purified D1-c peptide, whose sequence was PPV-DID-GIR-EPV-SGS-LLY-GNN. These corrected amino acid ratios incorporate the known effects of acid hydrolysis on amino acid composition as described in Table 2-2.

Amino Acid	Predicted AA Ratios	Experimental AA Ratios	Corrected AA Ratios
Arg	1	1.16	
Asn	2	0	
Asp	2	4.17	2+2?
Glu	1	0.97	
Gly	3	2.88	
Ile	2	2.00	
Leu	2	2.20	
Pro	3	3.14	
Ser	2	1.81	2.01
Tyr	1	0.81	1.01
Val	2	2.03	

Table 2-5

Corrected amino acid composition of purified D1-d peptide, whose sequence was GLH-FYP-IWE-AAS-VDE-WLY-N. These corrected amino acid ratios incorporate the known effects of acid hydrolysis on amino acid composition as described in Table 2-2.

Amino Acid	Predicted AA Ratios	Experimental AA Ratios	Corrected AA Ratios
Ala	2	2.21	
Asn	1	0	
Asp	1	2.01	1+1?
Glu	2	2.05	
Gly	1	1.00	
His	1	0.92	
Ile	1	0.83	
Leu	2	2.09	
Phe	1	1.02	
Pro	1	0.97	
Ser	1	0.84	0.93
Trp	2	0	?
Tyr	2	0.80	1.00
Val	1	0.88	

Table 2-6

Corrected amino acid composition of purified D2-a peptide, whose sequence was VSQ-EIR-AAE-DPE-FET-FYT-KN. These corrected amino acid ratios incorporate the known effects of acid hydrolysis on amino acid composition as described in Table 2-2.

Amino Acid	Predicted AA Ratios	Experimental AA Ratios	Corrected AA Ratios
Arg	1	1.14	
Asn	1	0	
Asp	1	2.18	1+1?
Gln	1	0	
Glu	4	5.22	4+1?
Ile	1	1.00	
Lys	1	0.98	
Phe	2	1.92	
Pro	1	1.07	
Ser	1	0.87	0.97
Thr	2	1.85	1.94
Tyr	1	0.81	1.01
Val	1	0.90	

unexplainable mass spectrometry results after its first synthesis (data not shown), so the results of a second synthesis are those described above and in Table 2-4.

Several peptide sequences were confirmed by fast atom bombardment (FAB) mass spectrometry. This method was under development at the time these sequences were analyzed. For this reason, correct sequences were easily confirmed, but it was much more difficult to determine sequences when the experimental fragmentation pattern did not match the predicted pattern. The largest weight peak corresponded to the molecular weight of the intact, ionized peptide. Cleavage at any of the peptide backbone bonds surrounding a given amino acid yields a maximum of six different fragmentation patterns. There is one series for each of the two fragments caused by cleavage at one of the three backbone bonds per amino acid residue (see Figure 2-8). Any combination of these fragmentation patterns can be observed, depending on the specific peptide. In addition, a high background at nearly all molecular weights is caused by fragmentation of side groups and multiple cleavages. Of the four original peptides analyzed (D1-b, D1-c, D1-d and D2-a), only D1-c gave unexplainable fragmentation patterns and a molecular weight much smaller than expected. The other three peptides and the second synthesis of peptide D1-c gave appropriate molecular weights and fragmentation patterns in agreement with those computed from the expected sequence.

In summary, the five peptides whose sequences are shown in Figure 2-6, were successfully synthesized and deprotected as described earlier. These peptides were purified by reverse phase HPLC on C18 columns. Peptide D1-a proved impossible to purify, but the other four peptides (D1-b, D1-c, D1-d and D2-a) were successfully purified. The amino acid compositions of the purified peptides were verified by amino acid analysis and confirmed by fast atom bombardment mass spectrometry. Attempts to elicit antibodies using these five peptides are described in the next chapter.

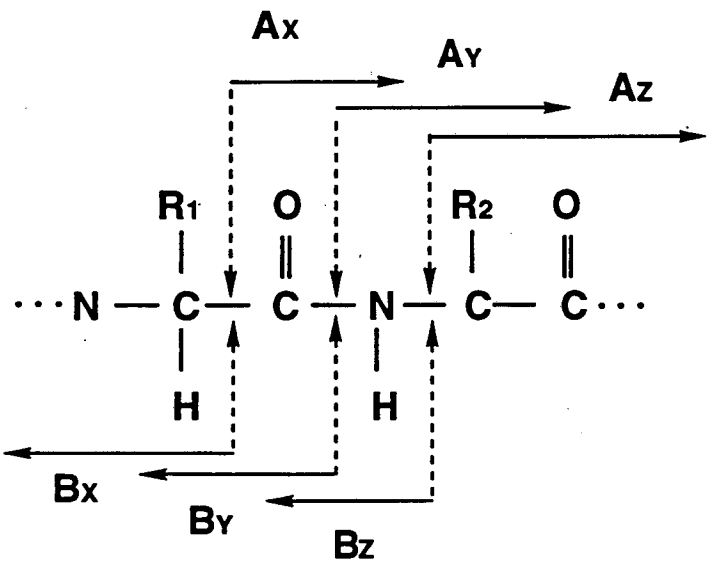

Figure 2-8: Possible peptide fragmentation patterns

Cleavage at any of the peptide backbone bonds surrounding a given amino acid yields a maximum of six different fragmentation patterns. There is one series for each of the two fragments caused by cleavage at one of the three backbone bonds per amino acid residue. The possible fragmentation patterns involving two amino acid side chains (R_1 and R_2) within a protein are given and all backbone atoms are shown explicitly.

3. ANTIBODIES

Introduction

The sequences of the successfully synthesized peptides discussed in the previous chapter are shown in Figure 2-6. The approximate positions of these peptides on the intact D1 and D2 proteins are outlined on the schematic in Figure 2-7. This chapter describes attempts to elicit polyclonal antibodies in New Zealand White rabbits using these five peptides as the antigens. There were several attempts to produce antibodies using the two methods described below. In each attempt, two to four different rabbits were used per peptide in order to increase the chances of antibody production.

Initially, crude peptides were noncovalently coupled to C8 HPLC beads and injected subcutaneously. The C8 HPLC beads are thought to act as carrier and adjuvant for these peptides. In a fashion similar to reverse phase HPLC, the hydrophobic regions of the peptides bind noncovalently to the C8 beads and are released slowly under physiological conditions. Free peptides would be destroyed quickly after injection. But, this attachment to the C8 beads, protects the peptides, allowing them to be detected by the immune system and to possibly produce antibodies that recognize the peptide. This procedure was used first due to its simplicity and reported prior success rate of approximately 50% of peptides leading to polyclonal antibodies (Dr. J. Allison, Immunology Dept., UC Berkeley, CA, personal communication). This procedure successfully produced antibodies against one peptide, D1-a. The other peptides used in this procedure were D1-c and D1-d, neither of which elicited antibodies detectable by western blotting analysis as discussed in the next chapter.

The second procedure was much more involved, but resulted in successful antibodies against two other peptides, D1-b and D2-a, which were not elicited by the first procedure. Briefly, the second procedure involved covalent conjugation of peptides to PPD (the purified protein derivative of tuberculin bacillus), injection into the surgically exposed popliteal lymph node, and booster shots subcutaneously into the area of the same lymph node (see detailed procedure below). All of these steps, including conjugation of peptides to PPD and the use of Freund's adjuvants, were used in order to increase the antigenicity of the peptides as much as possible. PPD has been characterized as a protein which has strong activation of the immune system without many antibodies being produced against itself. Therefore, peptides conjugated to PPD should benefit from this enhanced immune response and more readily produce antibodies that will recognize it. It should be noted that even this, the procedure most likely to elicit antibodies against small peptides, produced antibodies against only 2 of the 4 peptides injected. This was consistent with the successful production of polyclonal antibodies by approximately 50% of the peptides, as expected (Dr. J. Allison, Immunology Dept., UC Berkeley, CA, personal communication).

Procedures

Antibody production

Polyclonal antibodies were raised in New Zealand White rabbits by one of two methods:

1) Crude peptides which were deprotected and cleaved from the support resin were noncovalently coupled to C8 beads which act as carrier and adjuvant. Approximately 0.1 μg of peptide was incubated with 100 μg of C8 beads for 4 hours with constant gentle mixing at room temperature. The beads were allowed to settle and the supernatant

removed. The beads were then washed twice with phosphate buffered saline (PBS) and resuspended in 500 µl of PBS. These suspensions were injected subcutaneously at 2 week intervals for 3 injections per rabbit following procedures provided by Dr. J. Allison (Immunology Dept., UC Berkeley, CA).

2) Approximately 5 µg of purified (see previous chapter) peptides were covalently coupled to 500 µg of PPD (the purified protein derivative of tuberculin bacillus) by incubation with glutaraldehyde as previously described (Reichlin, 1980; Lachmann et al., 1986). Primary injections consisted of 100 µg of conjugate in 200 µl PBS which were emulsified with an equal volume of Complete Freund's Adjuvant. This mixture was injected into the surgically exposed popliteal lymph node (Sigel, 1983) with the assistance of the veterinary staff from the Office of Laboratory Animal Care (OLAC) at the University of California, Berkeley. Boosts 4 and 6 weeks later contained 100 µg of conjugate in 200 µl of PBS emulsified with an equal volume of Incomplete Freund's Adjuvant and were subcutaneous mainly in the region of the same lymph node. In both procedures, rabbits were bled before injections and two or more weeks after the last injection. The whole blood was allowed to clot, centrifuged at low speed and the supernatant (serum) was retained.

Assay for antibody presence

Antibodies were assayed by western blotting analysis using spinach PS II membrane preparations as the target proteins run on polyacrylamide gel electrophoresis (PAGE). The details of these procedures are described in the next chapter.

Pre-immune Fab's

Pre-immune IgG antibody binding fragments (Fab's), for use in solution binding assays, were made by procedures provided by R. Storrs (Chemistry Dept., UC Berkeley,

CA). Rabbit pre-immune serum was diluted 1:1 with 0.01 M phosphate buffered 0.15 M saline (PBS) and centrifuged (10,000 x g, 15 min) to clarify. The IgG fraction was precipitated by dropwise addition of an equal volume of room temperature saturated ammonium sulfate, pH 7.4, stirring for an additional hour and centrifugation as above. The pellet was resuspended in 1/4 of the original volume of PBS:saturated ammonium sulfate (1:1, v/v) to wash, centrifuged as above and repeated. At 0-4°C, the pellet was dissolved in 2/3 of the original serum volume of PBS and dialyzed against 20 volumes of Fab Buffer (0.1 M phosphate buffer, pH 7.2, 4 mM EDTA) overnight at 4°C without stirring and then for 4 h with stirring after a change of buffer. After dialysis, the retentate was centrifuged as above to remove insoluble protein. The weight of IgG was estimated by UV absorption at 280 nm (1.37 OD/mg per ml). Dithiothreitol (DTT) was added to 1 mM final concentration. Digestion with papain (1% by weight) was performed for 2 to 4 h with gentle agitation at 37°C. Finally, chromatography through Sephadex G-50 fine (equilibrated with Fab Buffer), with monitoring at 280 nm, quenched the digestion and separated antibody fragments from papain. Fab's and Fc's elute in the void volume, while papain comes out later.

Results and Discussion

The method utilizing crude peptide mixtures non-covalently coupled to C8 HPLC beads was used twice. The first series used only one peptide, D1-a, injected into 2 rabbits. Both rabbits successfully produced antibodies (anti-D1-a) which recognized the D1 protein on western blots of spinach PS II membrane preparations. The binding of this particular antibody was first demonstrated using ELISA techniques with the immunizing peptide as the substrate target (data not shown). Although this assay gave positive results, recognition of the D1 protein was required and, therefore, western blotting techniques

became the primary assay for antibody presence. Discussion of this assay and the specific results are deferred to the next chapter, and the results described there will be used as conclusions of the presence or lack of antibody here without further elaboration. The second series using the C8 HPLC beads used 2 crude peptides (D1-c and D1-d) injected into 4 rabbits each. All of these rabbits failed to produce antibodies as assayed by western blotting.

The second method, involving coupling of peptides to PPD and injection into the popliteal lymph node, was used once with 4 peptides (D1-b, D1-c, D1-d and D2-a) injected into 3 rabbits each. Two of these peptides, D1-b and D2-a, successfully elicited antibodies (anti-D1-b and anti-D2-a) that recognized the D1 and D2 proteins, respectively, on western blots of spinach PS II membrane preparations. Both of these antibodies gave positive results on western blots at greater dilutions than did anti-D1-a, indicating that they are either stronger binding antibodies or that their serum concentration is greater.

Pre-immune IgG antibody binding fragments (Fab's) were successfully prepared using the procedure described above. The antibody fragment peak was collected as several fractions. The OD at 280 nm was measured and the fraction with highest protein concentration was used for the solution binding experiments described in Chapter 6.

4. WESTERN BLOTTING ASSAYS

Introduction

Western blotting was used for several purposes. It was first used to analyze the serum taken from individual rabbits for the presence of antibody. ELISA techniques using the immunizing peptide as antigen had given reasonable positive results for anti-D1-a, but did not address whether the antibodies recognized the intact D1 protein. Mainly for this reason, western blotting analysis was used as the primary screening method for the remainder of antibody analyses. The procedure used for these analyses involved comparison of pre-immune serum binding versus "immune" serum binding at several different dilutions in order to control for nonspecific binding of the primary and secondary antibodies and developing time with the final substrate. These blots were performed on membrane strips cut from a blot of a polyacrylamide gel electrophoresis (PAGE) of PS II membranes. The strips were processed in separate compartments of a Bio-Rad 25-well western blotting tray in order to minimize cross contamination. Alkaline phosphatase-labeled secondary antibodies were used to detect primary antibody presence.

The second procedure which was used appeared to be more sensitive and provided greater discrimination with lower background binding. It was not used for the primary screening due mainly to the requirement for [^{125}I] containment which would have been difficult using the Bio-Rad blotting tray. This assay was therefore used as final confirmation of antibody specificity as well as to determine binding to different types of preparations (see below). The main difference in this procedure involved the binding of [^{125}I]-labeled secondary antibody and its detection by autoradiography.

Procedures

PS II membrane preparation

PS II membrane fragments were prepared from spinach leaves essentially as described by Berthold, et al. (1981), but including modifications from Ford and Evans (1983), Rutherford et al. (1984) and Dr. J.-L. Zimmermann (Service Biophysique, CEN-Saclay, France). Spinach leaves (4-6 bunches) obtained from local markets were washed using de-ionized water and then deveined. They were then placed in a Waring blender with 200 ml of cold Grinding Medium (50 mM Hepes pH 7.5, 1 mM EDTA, 0.4 M NaCl, 4 mM $MgCl_2$, 5 mM sodium ascorbate, 0.2 % BSA, the last 2 added shortly before grinding) per bunch of spinach. They were ground with a short pulse and then 10 s on medium speed. The mixture was filtered through 2 layers of cheesecloth and then 16 of layers cheesecloth and immediately centrifuged (10 min, 6000 x g, 4°C, Sorvall GS3 or GSA rotor). The grinding and filtering steps were performed in a cold room (4°C) as quickly as possible to keep protease damage to a minimum. Further steps were performed on ice under dim light and all buffers were ice cold. The pelleted chloroplasts were resuspended using a small paint brush into 40 ml (per bunch) of Washing Medium (150 mM NaCl, 8 mM $MgCl_2$, 50 mM Hepes pH 7.5) and centrifuged as above. The pellet containing broken chloroplasts was resuspended into a small volume of Resuspension Medium (50 mM MES-NaOH pH 6.0, 15 mM NaCl, 10 mM $MgCl_2$). The Chl concentration was measured using acetone extracts and following the method described by Arnon (1949). Generally, a yield of 100-150 mg Chl for 4-6 bunches of spinach was found at this point in the procedure. Triton X-100 detergent was dissolved in Resuspension Medium and added to make the final mixture 25 mg Triton/mg Chl and 2 mg Chl/ml solution. The mixture was incubated at 4°C with gentle stirring for 20 min in complete darkness. The PS II-enriched membrane fragments were pelleted by

centrifugation (30 min, 35000 x g, 4°C, Sorvall SS34 rotor). They were resuspended in Resuspension Medium and centrifuged (1 min, 2000 x g, 4°C, Sorvall SS34 rotor) to remove excess starch. This pellet was discarded and the supernatant was centrifuged again (30 min, 35000 x g, 4°C, Sorvall SS34 rotor). The final pellet contains oxygen-evolving PS II membranes and was generally resuspended at >2 mg Chl/ml in SMN Buffer (0.4 M sucrose, 20 mM MES-NaOH pH 6.5, 15 mM NaCl, 10 mM $MgCl_2$). An average final yield was 60-100 mg Chl from 4-6 bunches of spinach. These PS II membrane preparations had oxygen evolution rates of 450-550 μmol O_2/mg Chl per h and were stored in aliquots at -80°C until used.

Tris treatment of PS II membranes

As described by Preston and Seibert (1991a), spinach PS II membranes were Mn-depleted (Tris-treated) by centrifugation (30,000 x g, 10 min) and resuspending at 500 μg Chl/ml in 1.0 M Tris-HCl pH 9.4, 0.4 M sucrose. The mixture was incubated for 30 min under room lights at 4°C with occasional mixing. The membranes were collected by centrifugation (30,000 x g, 10 min), washed once in SMN Buffer and resuspended in the same buffer.

Carboxypeptidase A treatment of PS II membranes

Carboxypeptidase A-treated PS II membranes were prepared as described in Preston and Seibert (1991b). Carboxypeptidase A type II from bovine pancreas (E.C. 3.4.17.1) was purchased from Sigma (St. Louis, MO) and used as provided. After thawing, Tris-treated PS II membranes at 200 μg Chl/ml were incubated for 1 h with the protease at 20°C in the dark in Digestion Buffer (0.4 M sucrose, 20 mM MES-NaOH pH 6.5, 20 mM NaCl). Carboxypeptidase A was used at a concentration of 2:1 w/w enzyme:Chl with the addition of 1 mM phenylmethylsulfonyl fluoride to inhibit endopeptidase activity. The conditions for this protease treatment were selected to ensure

that the reaction proceeded to completion. At the end of the treatment, the protease was inhibited by the addition of 20 volumes of ice cold Digestion Buffer containing 1 mM 1,10-phenanthroline. The membranes were collected by centrifugation (10 min, 35000 x g, 4°C, Sorvall SS34 rotor), washed once in Digestion Buffer and resuspended in SMN Buffer.

Polyacrylamide Gel Electrophoresis

Polyacrylamide gel electrophoresis of the desired preparations, usually spinach PS II membranes, were run using [^{14}C]-methylated protein standards (Amersham CFA.626) or unlabeled low molecular weight protein standards (Bio-Rad) for calibration of molecular weights. The gels used contained 0.1% sodium dodecyl sulfate (SDS) and 6 M urea and were run following the "discontinuous buffer" procedures described by Laemmli (1970) as modified for PS II proteins (Ljungberg et al., 1986) and incorporating suggestions made by N. Bowlby (Dept. of Cell. and Molec. Biol., Univ. of Michigan, Ann Arbor). The gels were either 15% acrylamide or 10-20% acrylamide gradient separating gels, both with 6% acrylamide stacking gels. The 4x Stacking Gel Buffer (0.5 M Tris pH 6.8, 6.5 M urea) differed from the 4x Separating Gel Buffer (1.5 M Tris pH 8.8, 6.5 M urea) as required for this system. Samples were diluted 1:1 (v/v) with 2x loading buffer (urea, SDS, glycerol, DTT and bromphenol blue in Stacking Gel Buffer) and incubated for 1-24 h at 4°C before loading. The 20 x 20 cm gels were run for 40-50 hours at 50-60 V (constant voltage, room temp.). Often, gels were stained for 4 h (0.2% w/v coomassie brilliant blue R-250 in 45% v/v methanol and 10% v/v acetic acid) followed by rapid destaining for 1-2 h (45% v/v methanol and 7% v/v acetic acid) and slow destaining overnight (10% v/v methanol and 7% v/v acetic acid).

Electroblotting

Electroblotting onto Immobilon-P Transfer Membranes (Millipore) was performed in a Bio-Rad trans-blot cell. Before blotting, the membranes were briefly immersed in

100% methanol, placed in distilled water for 5 min, and soaked for 15-20 min in Transfer Buffer (25 mM Tris base, 192 mM glycine, 15% v/v methanol, pH 8.2-8.3). All filters and the gels themselves were also soaked in Transfer Buffer for 15-20 min prior to placement in the electroblotting apparatus. The blotting cassette was assembled and placed in the apparatus (with the membrane side of the assembly facing the anode electrode). The apparatus was filled with Transfer Buffer and then run at 14 V overnight in the cold room (4°C).

Western Blotting

The procedures described by Towbin et al. (1979) were used, with some modifications, for western blotting. The blot was removed from the electroblotting apparatus and rinsed once with distilled water. A portion of the blot was cut and stained for 10 min (0.2% w/v coomassie brilliant blue R-250 in 45% v/v methanol and 10% v/v acetic acid) followed by rapid destaining for 5-10 min (45% v/v methanol and 7% v/v acetic acid). The remainder of the membrane was rinsed once with PBS (0.01 M phosphate buffer, 0.15 M NaCl) and placed in heat-sealable bags which were cut open and resealed between each wash or incubation. It was then blocked for 2 h (5% BSA, PBS). After washing once for 5 min (0.1% BSA, 0.05% Tween-20, PBS), it was incubated for 2 to 4 h with antiserum at 1:100 to 1:1000 dilution (in 1% BSA, 0.05% Tween-20, PBS). Following 3 washes as above, it was incubated with [^{125}I]-labeled secondary antibody (goat-anti-rabbit IgG, Amersham IM.134) at 1:1000 dilution in 1% BSA,.0.05% Tween-20, PBS. Finally, it was washed 3 times as before, rinsed with distilled water, dried, and autoradiographed using Kodak film and 1 or 2 intensifying screens at -70°C.

For enzymatic detection, the procedure was similar to that described above. After rinsing, strips of the Immobilon-P blot were cut to fit into a Bio-Rad 25-well western blotting tray, in which all incubations were performed with 4-5 ml of solution per well on a

shaker platform at room temperature. If the membrane ever dried out, it was re-wet in methanol for 5 s or 5% Tween-20 for 15-20 min and then rinsed briefly with distilled water. The strips of membrane were rinsed once with TBS (20 mM Tris-HCl pH 7.4, 0.9% NaCl). They were then blocked for 2 h (5% BSA, TBS). After washing once for 5 min (0.1% BSA, 0.05% Tween-20, TBS), they were incubated for 2 to 4 h with antiserum at 1:100 to 1:1000 dilution (in 1% BSA, 0.05% Tween-20, TBS). Following 3 washes as above, they were incubated with alkaline phosphatase-labeled secondary antibody (Bio-Rad) at 1:3000 dilution in 1% BSA, 0.05% Tween-20, TBS. After washing 3 times as above, a final wash was performed with TBS. The freshly prepared substrate (0.56 mM BCIP, 0.48 mM NBT, 10 mM Tris-HCl pH 9.5) was then added. The blots were watched for color development (5-20 min) before quenching with two 5 min washes with distilled water. These blots were then photographed and/or stored in darkness to avoid fading.

Results and Discussion

Polyacrylamide gel electrophoresis was run as described above with several different sources of protein samples in order to perform a western blot to characterize the antibody raised against the D1-a peptide (anti-D1-a). The binding of this particular antibody had previously been demonstrated using ELISA techniques with the immunizing peptide as the substrate target (see Chapter 2), but specific recognition of the D1 protein was required. The gel was run in duplicate, one was stained with coomassie brilliant blue (Figure 4-1) and the other was used for western blotting (Figures 4-2 and 4-3). Each sample was run in duplicate to load different amounts of protein with the exception of the three DEPC-modified preparations, which contained the same amounts of protein treated with differing amounts of DEPC. In Figure 4-1, the samples expected to contain the D1 protein are: PS II membrane preparation from spinach (lane 2), oxygen-evolving spinach

Figure 4-1: PAGE of various PS II preparations

Polyacrylamide gel electrophoresis after staining with coomassie brilliant blue. The samples were: PS II membrane preparation from spinach (lane 2), oxygen-evolving spinach core preparations (lanes 3 and 4), spinach reaction center complex preparations (lanes 5 and 6), DEPC-modified spinach core preparations (lanes 8, 9 and 10), PS II membrane preparations from *Synechococcus* sp. (lanes 11 and 12) and partially purified reaction centers from *Rb. capsulatus* (lanes 13 and 14). Pre-stained protein standards of 17, 27, 39, 50, 75 and 130 kDa were run in lanes 1 and 15. Protein standards of 14.4, 21.5, 31, 45, 66.2 and 92.5 kDa were run in lane 7 and their approximate positions are marked on the right side of the figure. The positions of the D1 and D2 proteins are also marked. The stacking gel was 6% acrylamide and the separating gel was a 10 to 20% acrylamide gradient gel. The entire gel contained 6 M urea and 0.1 % SDS and was run for 40 h at 4°C at a constant voltage of 50 V.

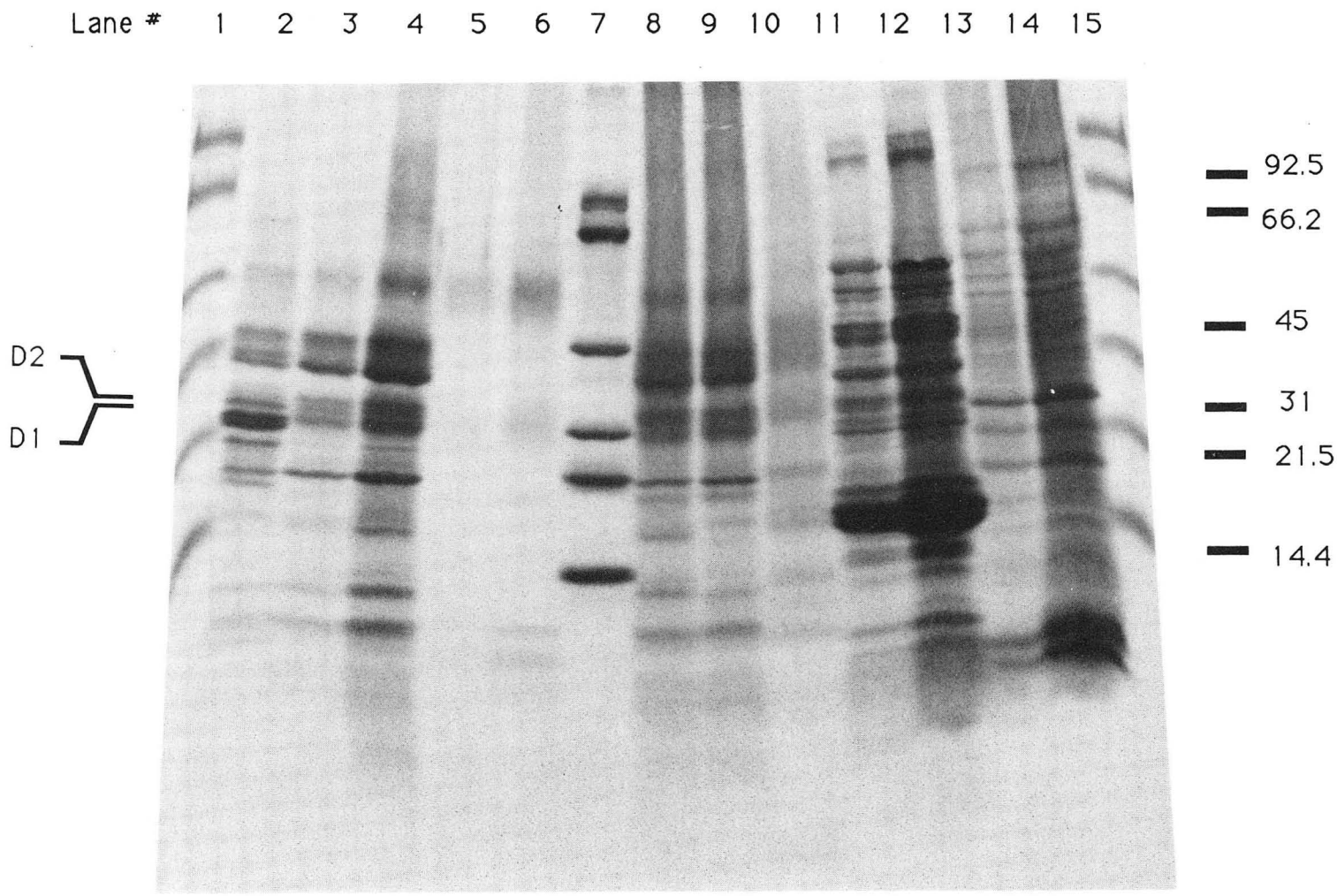
Lane # 1 2 3 4 5 6 7 8 9 10 11 12 13 14 15
D2
D1
92.5
66.2
45
31
21.5
14.4

core preparations (lanes 3 and 4), spinach reaction center complex preparations (lanes 5 and 6), DEPC-modified spinach core preparations (lanes 8, 9 and 10) and PS II membrane preparations from the thermophilic cyanobacterium *Synechococcus* sp. (lanes 11 and 12). Partially purified reaction centers from *Rhodobacter capsulatus* were used to examine potential cross-reactivity with the L, M and H subunits of the purple bacterial reaction center (lanes 13 and 14). Pre-stained protein standards of 17, 27, 39, 50, 75 and 130 kDa were run in lanes 1 and 15 as approximate molecular weight markers and to monitor progress during the electrophoretic process. As better molecular weight markers, protein standards of 14.4, 21.5, 31, 45, 66.2 and 92.5 kDa were run in lane 7. This lane also contained a small amount, not obvious by coomassie staining, of [^{14}C]-labeled protein standards of 14.3, 30, 46 (and/or 50), 69, 92.5 (and/or 100) and 200 kDa to be used as references in western blotting. These particular gels were run under conditions chosen to minimize the broadening of the bands corresponding to the D1 and D2 proteins. It was necessary to produce bands as sharp as possible in order for western blotting to distinguish between these two generally diffuse and closely spaced PAGE bands. The gels contained 6 M urea and 0.1 % SDS to maximize denaturation. The stacking gels were 6% acrylamide and the separating gels were 10 to 20% acrylamide gradient gels. These gels were run for 40 h at 4°C (in a cold room) at a constant voltage of 50 V. It should be noted that the bands corresponding to the D1 and D2 proteins (best seen in lane 3) are indeed very sharp, but their separation is fairly small, even after a 40 h electrophoresis, which is considered quite long for this type of PAGE. Also, the reaction center complex preparations (lanes 5 and 6) seem to show only slight staining at the positions expected for the D1 and D2 proteins, but show a darker, diffuse, region at approximately 50 kDa which corresponds to aggregation of the D1 and D2 proteins as described by Nanba and Satoh (1987) for this type of preparation.

Some discussion as to the choice of samples used and their protein compositions would be useful at this point. The spinach reaction center complex preparation was a gift from A. Williamson (Sauer research group, Chemistry Dept., UC Berkeley, CA). This reaction center complex preparation (Figure 4-1, lanes 5 and 6) corresponds to the preparation of simplest protein composition currently available, would be used for a few of the further studies, but does not evolve oxygen. As explained in Chapter 1, this preparation has the ability to perform charge separation as described by Chapman et al. (1988). As demonstrated by Seibert et al. (1989), this preparation contains the four components of the high-affinity Mn-binding site as measured by the assay for Mn^{2+} inhibition of DPC-stimulated DCIP photoreduction described by Hsu et al. (1987). This preparation contains the D1 and D2 reaction center proteins, the large and small protein subunits of Cyt *b*-559 and the 4.2 kDa polypeptide.

The spinach core preparation (Figure 4-1, lanes 3 and 4) is the smallest characterized oxygen-evolving preparation, would also be used for some of the experiments listed below, and provides the most predictably interpretable protein content and, hence, pattern after coomassie staining of the gel. This sample was provided by M. Latimer (Sauer research group, Chemistry Dept., UC Berkeley, CA). In addition to the D1 protein, the D2 protein, the large and small protein subunits of Cyt *b*-559 and the 4.2 kDa polypeptide, this preparation contains several other proteins which are apparently required for the expression of oxygen evolution. These proteins are CP43, CP47, the 33 kDa extrinsic polypeptide, a 20 kDa polypeptide and several small polypeptides of <5 kDa with unknown functions.

The PS II membrane preparation from spinach (Figure 4-1, lane 2) was the sample containing the most spinach PS II proteins. In addition to the proteins present in the oxygen-evolving spinach core preparation described above, this preparation contains two other extrinsic polypeptides of 17 and 24 kDa and a significant quantity of loosely

associated light-harvesting proteins (multiple overlapping bands in the 30 kDa region). This preparation was representative of the largest complex to be used in further experiments (oxygen evolution assays, Chapter 5; solution binding assays, Chapter 6; photoactivation assays, Chapter 7; and assay of high-affinity Mn-binding sites, Chapter 8).

The DEPC-modified spinach core preparations (Figure 4-1, lanes 8, 9 and 10) were from a collaboration with M. Latimer (Sauer research group, Chemistry Dept., UC Berkeley, CA). He was mainly interested in chemically labeling the PS II histidines with DEPC and identifying the sites of protein labeling in the presence and absence of the active Mn. Here the protein banding for different levels of chemical modification and the detectability of the D1 protein by western blotting was being examined. This work was not continued, but results of similar experiments were later published by Tamura et al. (1989a) and are described in Chapters 7 and 8.

The PS II membrane preparation from the thermophilic cyanobacterium *Synechococcus* sp. (Figure 4-1, lanes 11 and 12) was a kind gift from V. DeRose (also of the Sauer research group, Chemistry Dept., UC Berkeley, CA). She has done EPR and X-ray spectroscopies using this preparation and compared the results to those from spinach preparations (DeRose, 1990). This preparation was used here to test for cross-reactivity with the expectedly homologous PS II reaction center proteins of a cyanobacterium and to western blot a sample which contains more protein components than the spinach PS II membrane preparation (see Figure 4-1), including higher PS I contamination.

The partially purified reaction centers from *Rb. capsulatus* (Figure 4-1, Lanes 13 and 14) were a gift from G. Armstrong (Hearst research group, Chemistry Dept., UC Berkeley, CA) from preparations by S. Worland (Sauer and Hearst research groups, Chemistry Dept., UC Berkeley, CA). These samples were used to examine potential cross-reactivity, especially with the L and M subunits of the purple bacterial reaction center

which have been shown to exhibit homology to the D1 and D2 proteins of PS II (Hearst, 1986). The lumenal region of the D1 protein selected for the peptide which elicited this antibody was chosen to minimize use of regions homologous to the L subunit (see Chapter 2), so cross-reactivity was expected to be minimal.

Autoradiograms of a western blot using the antibody raised against the D1-a peptide (anti-D1-a) at 1:100 dilution with [^{125}I]-labeled secondary antibody for detection are shown in Figures 4-2 and 4-3. This western blot used the second gel of the pair described above, whose coomassie-stained partner is shown in Figure 4-1. These figures correspond to two exposures of the same western blot to emphasize different aspects of the results. Figure 4-2 is a 4 h exposure which demonstrates that there is one major band at approximately 30 kDa (identified to be the D1 protein, as described below) detected in 4 of the 5 samples expected to contain the D1 protein. The spinach samples are: PS II membrane preparation (lane 2), oxygen-evolving core preparation (lanes 3 and 4), and DEPC-modified oxygen-evolving core preparation (lanes 8 and 9, but not 10 where the majority of the protein was retained in the well). For the PS II membrane preparation from *Synechococcus* sp. (lanes 11 and 12), the most intensely labeled band is at approximately 28 kDa. The reaction center complex preparation (lanes 5 and 6) did not show labeling in this region at this exposure, probably due to its low initial concentration and the aggregation described earlier. The aggregate does show slight labeling in lane 6. The reaction center preparation from *Rhodobacter capsulatus* (lanes 13 and 14) also does not show cross-reactivity with the L, M and H subunits at this level of exposure, as expected.

A 14 h exposure of the same western blot described above is shown in Figure 4-3. The antibody raised against the D1-a peptide (anti-D1-a) binds strongest to a single band at the appropriate location for the D1 protein. This can be seen best by comparing the proteins in lane 3 (Figure 4-1) with the 31 kDa standard in lane 7 to determine the position of the D1 and D2 proteins. A description of the banding pattern of lanes 3 and 4 (Figure 4-

Figure 4-2: Western blot of gel in Fig. 4-1 using anti-D1-a

Autoradiogram of a western blot using the antibody raised against the D1-a peptide (anti-D1-a) at 1:100 dilution with [^{125}I]-labeled secondary antibody used for detection. This autoradiogram was a 4 h exposure of a western blot which used the second gel of the pair whose coomassie-stained partner is shown in Figure 4-1. Samples and gel conditions were identical to those given for Figure 4-1. Lane 7 also contained a small amount, not obvious by coomassie staining, of [^{14}C]-labeled protein standards of 14.3, 30, 50 and 64 kDa and their approximate positions are marked on the right side of this figure.

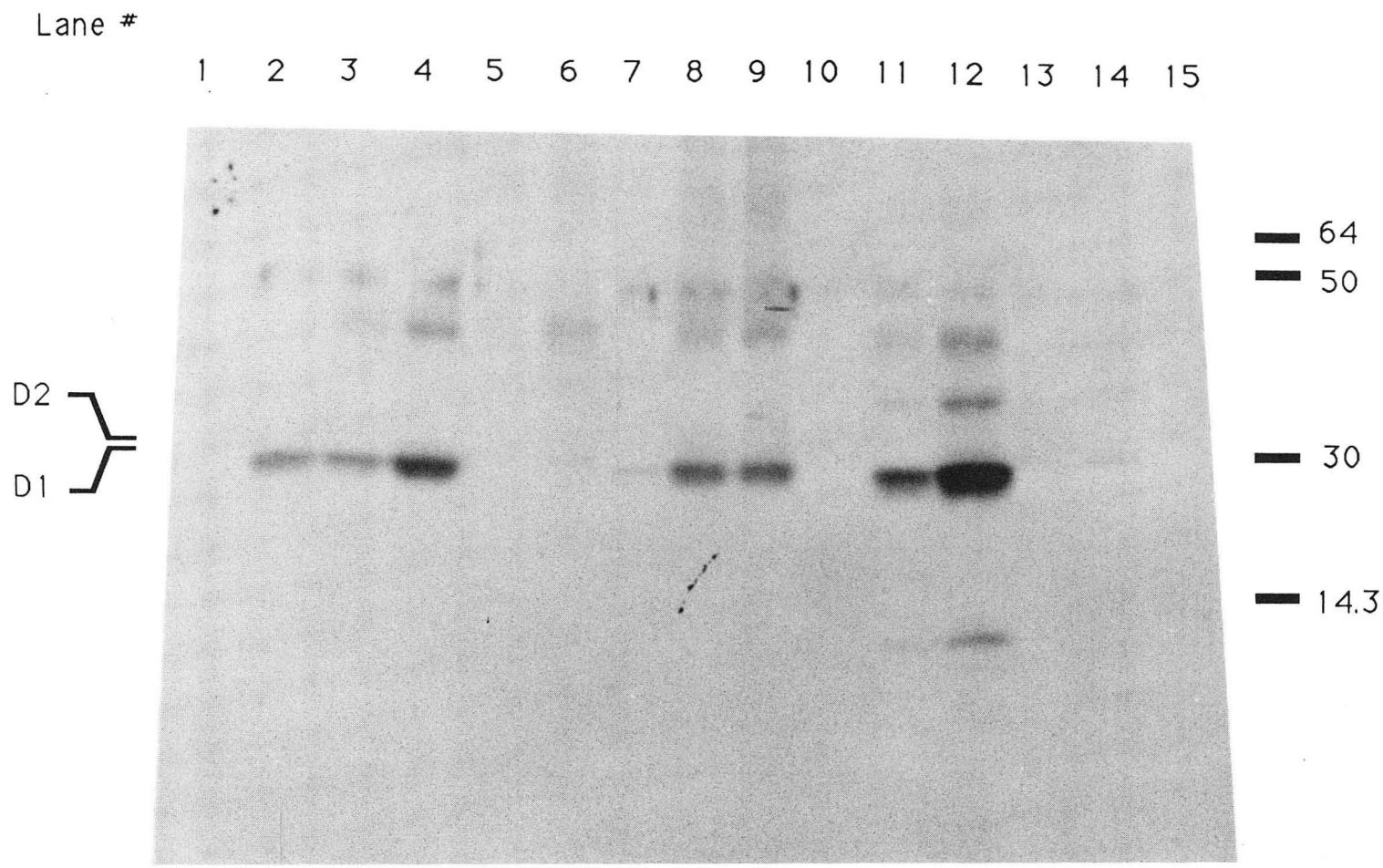
Lane #
1 2 3 4 5 6 7 8 9 10 11 12 13 14 15
D2
D1
64
50
30
14.3

Figure 4-3: Darker exposure of western blot of gel in Fig. 4-1 using anti-D1-a

Autoradiogram of a darker exposure of the western blot using anti-D1-a at 1:100 dilution with [^{125}I]-labeled secondary antibody used for detection. This autoradiogram was a 14 h exposure of the same western blot shown in Figure 4-2. Samples and gel conditions were identical to those given for Figure 4-1. Lane 7 also contained a small amount, not obvious by coomassie staining, of [^{14}C]-labeled protein standards of 14.3, 30, 50 and 64 kDa and their approximate positions are marked on the right side of this figure.

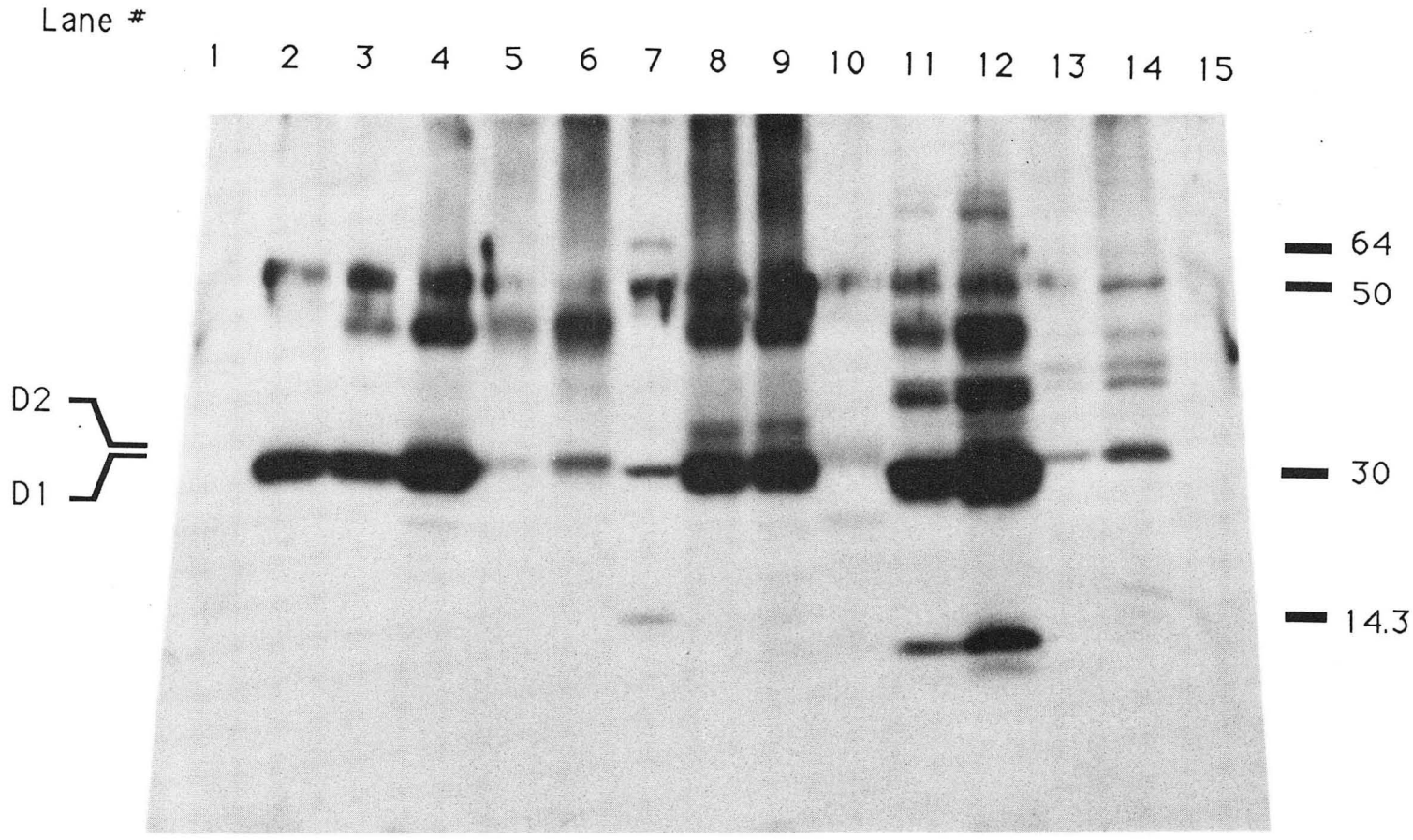
Lane #
1 2 3 4 5 6 7 8 9 10 11 12 13 14 15
D2
D1
64
50
30
14.3

1) will aid in this assignment. From the bottom, the first 2 clear bands below 14.4 kDa correspond to the small and large polypeptide subunits of Cyt *b*-559. Note that since this a gradient gel, the low molecular weight region is compressed relative to the migrations observed on linear gels. The next, faint, band is probably some remaining 17 kDa extrinsic protein. At approximately 20 kDa, a dark band corresponding to the 20 kDa protein which may serve a role analogous to the purple bacterial reaction center H subunit. Above this, a faint band is seen which is probably some remaining 24 kDa extrinsic protein. The next wide band is actually 3 or 4 bands on close inspection and correspond to remaining light harvesting proteins, the D1 protein, the D2 protein and the 33 kDa extrinsic protein (going up). The next group of bands, around the 45 kDa region, corresponds to CP43 and CP47 (the approximately 45 and 51 kDa proteins, respectively). Finally, the smears at 50 kDa and above represent aggregation products which contain the D1 and D2 proteins. Next, comparing this relationship to the position of the main labeled band in any lane (Figures 4-2 and 4-3) relative to the 30 kDa [^{14}C]-labeled standard in lane 7. A particularly good comparison is seen between lane 6 (Figure 4-3), containing the reaction center complex preparation, and the 30 kDa standard in lane 7. Note that this band is detected here in lane 6 even though it was not apparent after coomassie staining (Figure 4-1). The 30 kDa [^{14}C]-labeled standard appears as a faint coomassie band below the 31 kDa protein standard (see Figure 4-1).

The difference in overall background between the two exposures of the western blot (Figures 4-2 and 4-3) is the reverse of what one would expect and is courtesy of the photographic reproduction of the autoradiograms. Figure 4-3 also demonstrates background binding to bands in addition to the main D1 protein band, specifically to two bands in the 50 kDa region assigned to aggregation of the D1 and D2 proteins as described by Nanba and Satoh (1987). There is also binding to other bands, in particular, relatively strong binding to higher bands for *Synechococcus* sp. (possibly aggregation products) and

weak binding to several bands in *Rb. capsulatus*. This is consistent with results from several other groups which demonstrate somewhat specific background binding of rabbit antibodies to several bands in photosynthetic preparations from various organisms (L. McIntosh, MSU-DOE Plant Research Lab. and Biochemistry Dept., Michigan State Univ., East Lansing, MI, personal communication). This binding can be eliminated by increasing the stringency of the western protocol, as described below. Nevertheless, by far the major band detected is still the one corresponding to the D1 reaction center protein of PS II.

An analysis of the coomassie stained gel (Figure 4-1) and the autoradiograms of the corresponding western blot (Figures 4-2 and 4-3), makes it apparent that in addition to the sharpening of the bands corresponding to the D1 and D2 proteins, a greater separation between them would make analysis more straightforward. In order to maximize this separation between the D1 and D2 proteins and retain some sharpness in their bands, suggestions made by N. Bowlby (Dept. of Cell. and Molec. Biol., Univ. of Michigan, Ann Arbor), mainly pertaining to sample preparation and temperature control, were incorporated into the final PAGE protocol which is described above (see Procedures section). Heating was avoided and the gels maintained at approximately constant room temperature by circulating 20°C water through the apparatus's cooling unit. Before loading, samples were incubated overnight at 4°C after addition of an equal volume of "2x loading buffer" containing SDS, urea and glycerol. The commonly used short incubation with heating to 37°C caused increased aggregation and anomalous banding patterns and was replaced by this procedure.

Figure 4-4 shows coomassie stained gels which were products of the two best procedures developed. These are each half of two polyacrylamide gels run as explained above. The two gels differ in the acrylamide percentages, the left side of Figure 4-4 shows a 15% acrylamide gel while the right side of Figure 4-4 shows a 10-20% acrylamide gradient gel. All gels contained 6 M urea and 0.1 % SDS as before, the stacking gels were

Figure 4-4: PAGE examples of the best resolution for the D1 and D2 proteins

Polyacrylamide gel electrophoresis after staining with coomassie brilliant blue. The two gels differ in the acrylamide percentages, the left side shows a 15% acrylamide gel while the right side shows a 10-20% acrylamide gradient gel. All gels contained 6 M urea and 0.1% SDS, the stacking gels were 6% acrylamide and the gels were run for 40 h at a constant voltage of 50 V at controlled room temperature. Both gels have the same samples in corresponding lanes. The samples were: purified 33 kDa extrinsic protein (2nd lanes), oxygen-evolving spinach core preparation (3rd lanes), spinach reaction center complex preparation (4th lanes), PS II membrane preparation from *Synechococcus* sp. (6th lanes) and partially purified reaction centers from *Rb. capsulatus* (7th lanes). Pre-stained protein standards of 17, 27, 39, 50, 75 and 130 kDa were run in the and 8th lanes. Protein standards of 14.4, 21.5, 31, 45, 66.2 and 92.5 kDa were run in the 5th lanes and their approximate positions are marked between the two gels. The positions of the D1 and D2 proteins are also marked.

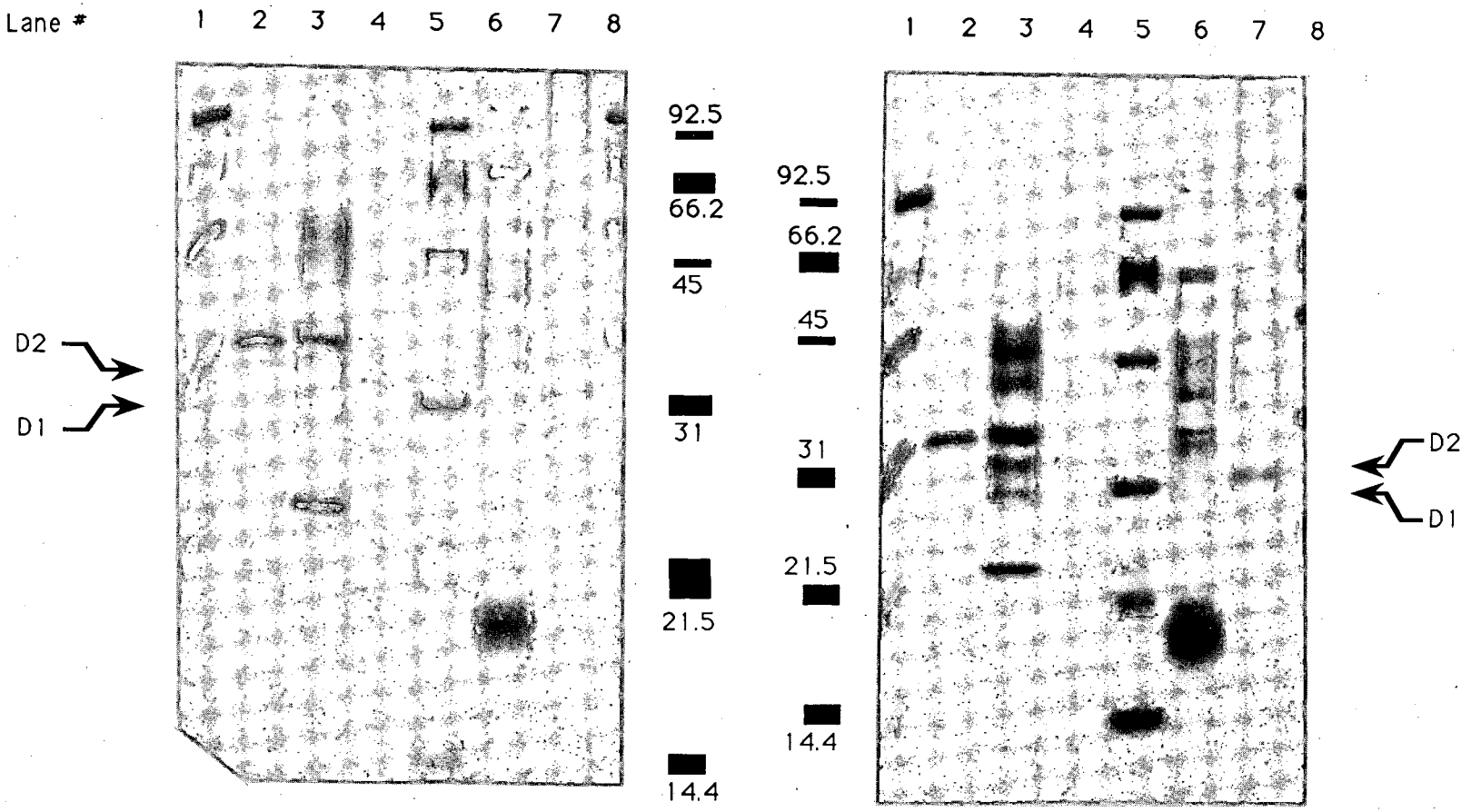
Lane #
1 2 3 4 5 6 7 8
D2
D1
92.5
66.2
45
31
21.5
14.4
92.5
66.2
45
31
21.5
14.4
1 2 3 4 5 6 7 8
D2
D1

6% acrylamide and the gels were run for 40 h at a constant voltage of 50 V, but this time at controlled room temperature. The samples run on the two gels shown in Figure 4-4 were some of those run on the gel shown in Figure 4-1, but only one sample of appropriate protein content was used. Both gels have the same samples in corresponding lanes. The samples in the 2nd lanes (Figure 4-4) were purified 33 kDa extrinsic protein for use in other experiments (see Chapters 5, 6 and 7). No other bands or background streaking were apparent, indicating a greater than 95% purity. The other samples were: oxygen-evolving spinach core preparation (3rd lanes), spinach reaction center complex preparation (4th lanes), PS II membrane preparation from the thermophilic cyanobacterium *Synechococcus* sp. (6th lanes) and partially purified reaction center preparation from *Rb. capsulatus* (7th lanes). Pre-stained protein standards of 17, 27, 39, 50, 75 and 130 kDa were again run in the 1st and 8th lanes as approximate molecular weight markers and to monitor progress during the electrophoretic process. And, as better molecular weight markers, protein standards of 14.4, 21.5, 31, 45, 66.2 and 92.5 kDa were run in the 5th lanes. These lanes also contained a small amount, not obvious by coomassie staining, of [^{14}C]-labeled protein standards of 14.3, 30, 46 (and/or 50), 69, 92.5 (and/or 100) and 200 kDa to be used as references in western blotting.

A new oxygen-evolving spinach core preparation was used for the gels in Figure 4-4, and the simpler banding pattern shows greater purity. From the bottom, the first dark band corresponds to the 20 kDa protein which may serve a role analogous to the purple bacterial reaction center H subunit. The small and large polypeptide subunits of Cyt *b*-559 have run off the bottom of the gel in the left side of Figure 4-4, while only the large subunit is seen below 14.4 kDa in the right side of Figure 4-4. The next set of bands correspond to the D1 protein, the D2 protein and the 33 kDa extrinsic protein (going up). As can be seen in both gels of Figure 4-4, the bands corresponding to the D1 and D2 proteins are very well resolved in these gels, although at some sacrifice in their sharpness. The next group of

bands, around the 45 kDa region, corresponds to CP43 and CP47 (the approximately 45 and 51 kDa proteins, respectively). The smears at 50 kDa and around 64 kDa again represent aggregation products which contain the D1 and D2 proteins. Noticeably, the purity of this preparation is quite high, as demonstrated by the lack of bands corresponding to light harvesting proteins and the 17 and 24 kDa extrinsic proteins. All further PAGE gels run for western blotting purposes followed these procedures, but usually used spinach PS II membrane preparations as the samples. Gels of 15% acrylamide were preferentially used due to the better separation of the D1 and D2 proteins, even though more small polypeptides were sacrificed.

Thus far, the goal was to develop a western blotting procedure that could be used to screen sera for antibodies raised against additional peptides and, concurrently, characterize the binding properties of anti-D1-a with respect to several sources of photosynthetic reaction centers. The characterization of anti-D1-a is described in the previous paragraphs and the corresponding figures. The gel procedures described earlier, examples of which are shown in Figure 4-4, were then used to run gels without lane divisions (one wide lane) loaded only with PS II membrane preparations. The 15% acrylamide gels, with SDS and urea as above, were run for 40-45 h at a constant voltage of 50 V at controlled room temperature. Approximate gel migration was obtained by coomassie staining of one inch cut from an end of the original gel before blotting (Figure 4-5, lane 1). The rest was electroblotted onto an Immobilon-P membrane overnight as previously described. The membrane was removed, rinsed in distilled water and allowed to dry. It was cut into 1/4 inch strips parallel to the running direction, labeled, placed in wells of a Bio-Rad blotting tray, re-wet with methanol (5-10 s) or 5% Tween-20 (15-20 min) and rinsed with distilled water. Blotting continued as described earlier for detection with alkaline phosphatase-labeled secondary antibody. Generally, three wells corresponding to one rabbit's serum contained immune serum at 1:100 dilution, immune serum at 1:1000 dilution and pre-

Figure 4-5: Western blots using enzymatic detection

Qualitative results of screening of sera from four rabbits. The strips are western blots using antibodies raised against several peptides. Alkaline phosphatase-labeled secondary antibody was used for the detection. The 15% acrylamide gels, with SDS and urea as in Figure 4-4, were loaded only with PS II membrane preparation and were run for 40-45 h at a constant voltage of 50 V at controlled room temperature. One inch cut from an end of the original gel before blotting was coomassie stained (lane 1). Lanes 2-5 correspond to sera from two rabbits immunized with the D1-b peptide. Lanes 6-9 correspond to sera from two rabbits immunized with the D2-a peptide. Lane 2 is a 1:100 dilution and lane 3 is a 1:1000 dilution of serum from the same rabbit. Similarly for the pairs of lanes 4 and 5, 6 and 7 as well as 8 and 9. The position of the D1 protein was obtained from blotting with anti-D1-a (not shown) and the expected position of the D2 protein was estimated from the coomassie stained gel portion.

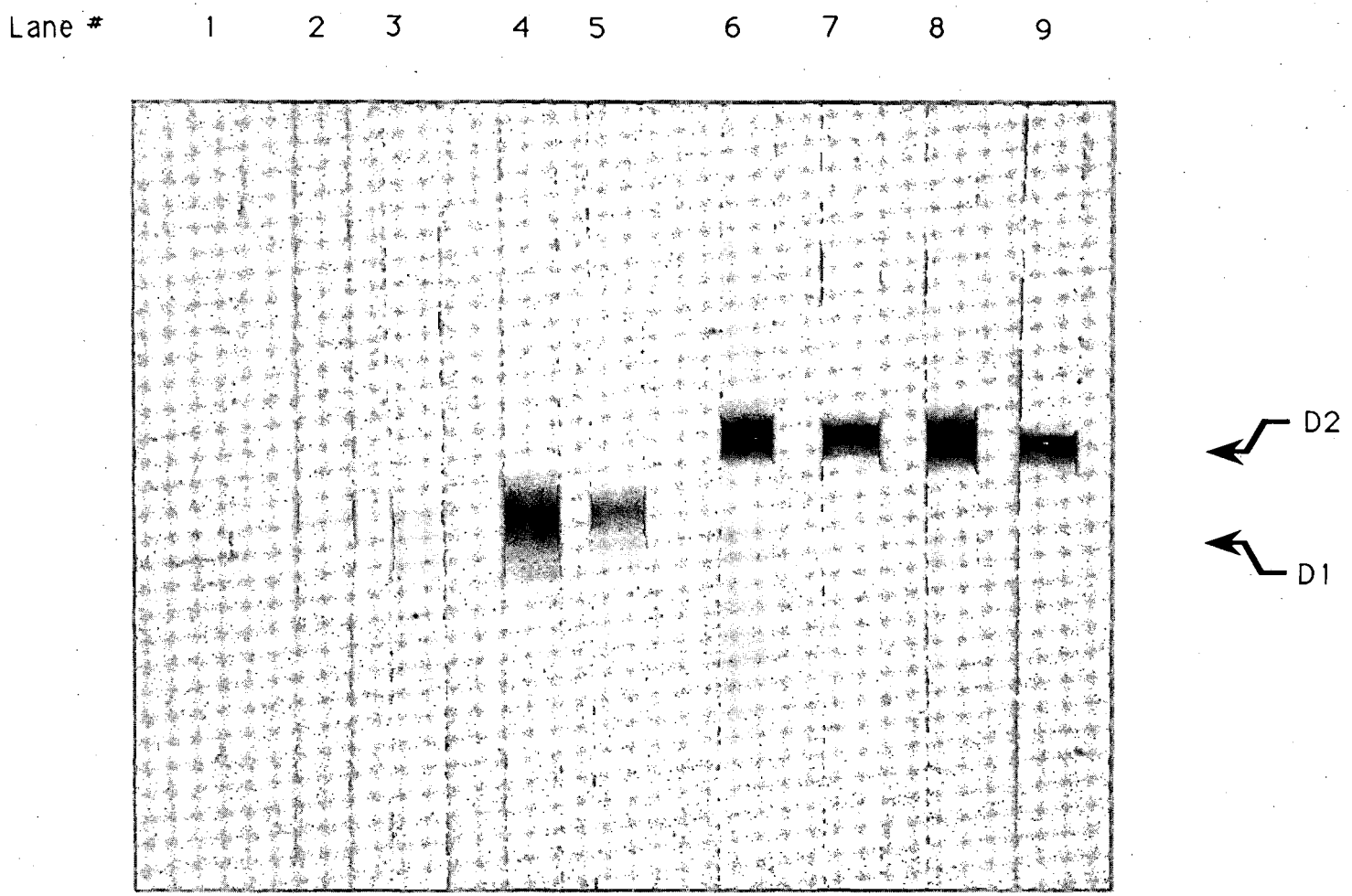
Lane #
1
2
3
4
5
6
7
8
9
D2
D1

immune serum at 1:100 dilution. An example of the results for four rabbits is shown in Figure 4-5. The pre-immune lanes were left off this figure due to no detection of cross-reaction after longer incubations with the substrate (which increases the background) for any of the four sets. Lanes 2-5 correspond to sera from two rabbits immunized with the D1-b peptide. Lanes 6-9 correspond to sera from two rabbits immunized with the D2-a peptide. Lane 2 is a 1:100 dilution and lane 3 is a 1:1000 dilution of serum from the same rabbit. Similarly for the pairs of lanes 4 and 5, 6 and 7 as well as 8 and 9. The position of the D1 protein was obtained from blotting with anti-D1-a (not shown) and the expected position of the D2 protein was estimated from the coomassie stained gel portion. As can be seen, lanes 2 and 3 show weak binding to the D1 protein. Lanes 4 and 5 shows stronger binding to the D1 protein (this serum was used as anti-D1-b). Lanes 6, 7, 8 and 9 all show strong binding to the D2 protein (the serum used in lanes 8 and 9 was used as anti-D2-a). This procedure gives qualitative results because of variability between different wells, mainly due to the length of time allowed for color development. Nevertheless, it made possible the assay of many samples of rabbit serum in order to find ones that indeed recognized the desired proteins and which could be further characterized using the [^{125}I]-labeled secondary antibody procedure, an example of which is described below.

The two peptides successfully used to generate antibodies against the D1 protein contain one segment in common (from Ile 321 to Arg 334) and differ mainly in that peptide D1-a contains an extra 10 amino acids on the carboxyl end. Carboxypeptidase A presumably removes the C-terminus of the D1 protein, stopping at Arg 334. Therefore, the binding sites for the three antibodies (anti-D1-a, anti-D1-b and anti-D2-a) were better characterized by comparison of binding to carboxypeptidase A-treated PS II membranes relative to untreated PS II membranes in western blots. Autoradiograms of three western blots using the three antibodies are shown in Fig 4-6. Samples were PS II (lanes 2, 5 and 8) and carboxypeptidase A-treated PS II (lanes 3, 6 and 9) membrane preparations. Lanes

Figure 4-6: Western blots of PS II and carboxypeptidase A-treated PS II preparations

Autoradiograms of three western blots of PS II membrane preparations (lanes 2, 5 and 8) and carboxypeptidase A-treated PS II membrane preparations (lanes 3, 6 and 9). Antibodies raised against the carboxyl ends of the D1 and D2 proteins were used. Blotting was with anti-D1-a (lanes 1-3), anti-D1-b (lanes 4-6) and anti-D2-a (lanes 7-9). Secondary antibody labeled with [^{125}I] was used for detection. Lanes 1, 4 and 7 contained [^{14}C]-labeled protein standards of 14.3, 30 and 46 kDa. The positions of these standards, which are marked to the left of each blot, were determined from a set of autoradiograms exposed for a longer period of time than the ones shown.

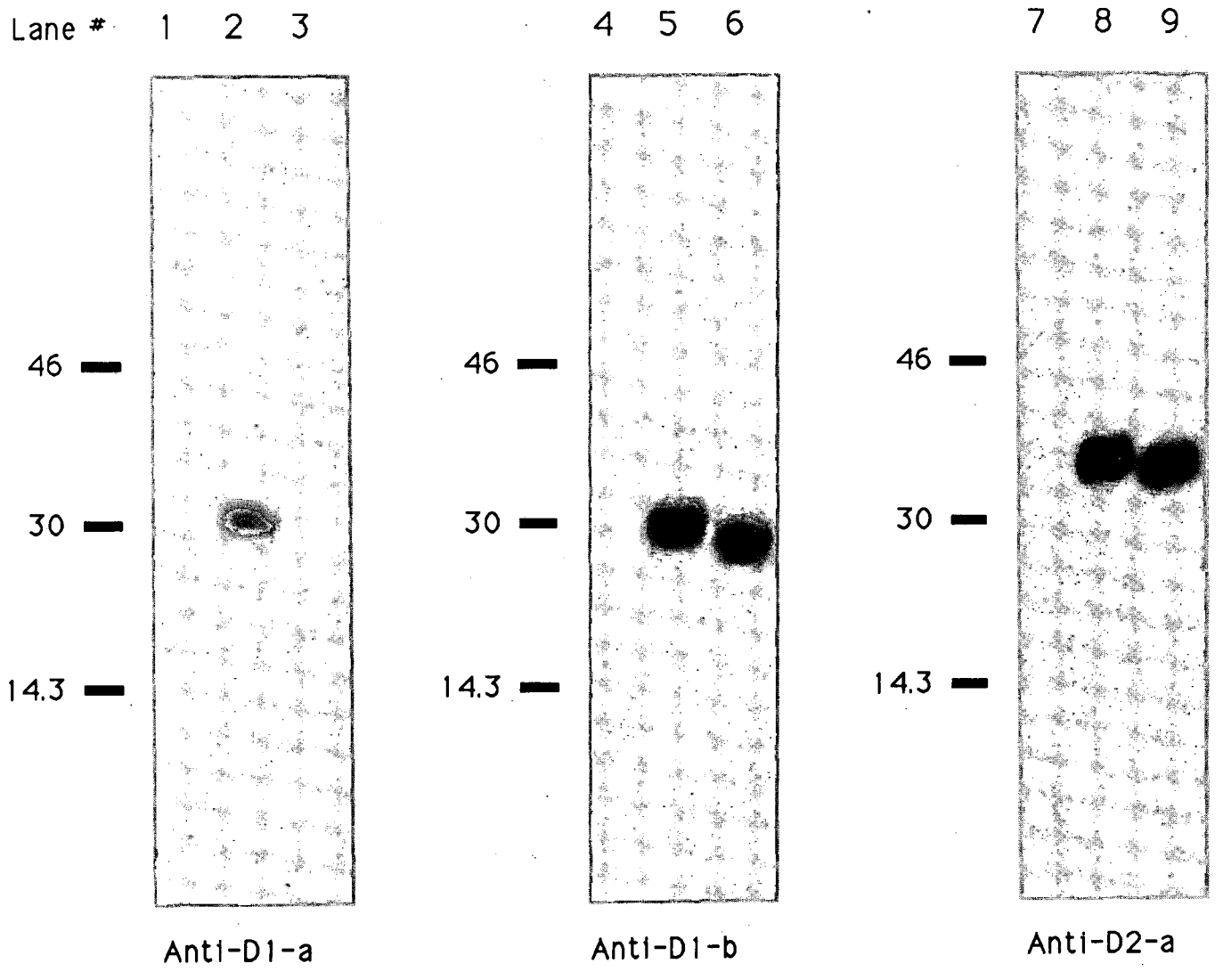
Lane # 1 2 3
4 5 6
7 8 9
46
30
14.3
46
30
14.3
46
30
14.3
Anti-D1-a
Anti-D1-b
Anti-D2-a

1, 4 and 7 contained [^{14}C]-labeled protein standards which are seen faintly here, but whose positions were determined from autoradiograms exposed for a longer period of time than the ones shown. Blotting was with anti-D1-a (lanes 1-3), anti-D1-b (lanes 4-6) and anti-D2-a (lanes 7-9). Western blotting indicates that all three of these antibodies bound to their corresponding denatured protein (D1 or D2) as expected (Figure 4-6). Anti-D1-b and anti-D2-a showed reactivity at greater dilution than anti-D1-a (not shown). The antibody to the D1-a peptide (anti-D1-a) did not, however, bind to denatured PS II membranes in which a small fragment of the D1 protein had been removed by treatment with carboxypeptidase A. The other two antibodies, anti-D1-b and anti-D2-a still bound. For these samples, the D2 protein shows slightly increased electrophoretic mobility relative to that in untreated PS II membranes. The D1 protein shows a greater increase in mobility after carboxypeptidase A treatment, consistent with the digestion of more residues from the C-terminus of the D1 protein than from the C-terminus of the D2 protein. The lack of binding of anti-D1-a to the carboxypeptidase A-treated PS II membranes can be interpreted to mean that the binding site detected by this western blotting procedure is to the carboxyl side of Arg 334. The binding sites of anti-D1-b and anti-D2-a cannot be further characterized using these results.

5. OXYGEN EVOLUTION ASSAYS

Introduction

The first set of experiments performed in order to see if antibodies had any effect on the functioning of the oxygen-evolving complex (OEC) of PS II was the measurement of oxygen evolution rates of PS II membrane preparations after a preincubation with antibody. Since all preparations which were used contained the intact OEC Mn, the mechanism of action upon antibody addition would presumably have been the displacement of Mn or alteration of the structure in such a manner as to change oxygen evolution rates.

As can be seen in the results section, many different PS II membrane preparations were used, mostly testing one of the antibodies (anti-D1-a). The reason for sequentially using the different preparations was to initially maximize oxygen evolution rates which would increase the accuracy of observed antibody effects. The oxygen evolution rates are highest for preparations whose lumenal side is the most intact. As one removes extrinsic polypeptides, the OEC becomes increasingly labile and exhibits generally decreasing rates of oxygen evolution. To maximize oxygen evolution, these preparations have increasing requirements for addition of cofactors such as Cl^- and Ca^{2+}. The lumenal side of these preparations becomes increasingly accessible upon removal of the extrinsic proteins, facilitating antibody binding and potentially making the OEC more easily affected by the binding of antibodies.

The spinach PS II membrane preparations used here have the following extrinsic polypeptide composition: PS II membranes contain all three (17, 24 and 33 kDa) proteins still bound. NaCl-treated PS II membranes lack the 17 and 24 kDa proteins, but retain the 33 kDa protein. $CaCl_2$-treated PS II membranes lack all three extrinsic proteins, but have

been shown (Ono and Inoue, 1983b) to retain all of the Mn necessary for oxygen evolution when assayed with added Cl^- and Ca^{2+}. Urea-treated PS II membranes also lack the three extrinsic proteins and have been shown (Miyao and Murata, 1985) to retain the Mn necessary for oxygen evolution when assayed with added Cl^- and Ca^{2+}. The urea treatment must be done in the presence of high concentrations of NaCl (200 mM or greater) in order to retain the OEC Mn.

PS II membranes require nearly no added Cl^- or Ca^{2+} for 100% oxygen evolution activity. For NaCl-treated PS II membranes, the requirement is raised to 30 mM Cl^- and 5 mM Ca^{2+} for 100% activity (Miyao and Murata, 1984). $CaCl_2$-treated PS II membranes and urea-treated PS II membranes show a maximum of 20% activity with 200 mM Cl^- and 10 mM Ca^{2+} (Miyao, et al., 1987). This activity can be raised to almost 100% upon the addition of a two times or greater molar excess of purified 33 kDa protein prior to the measurement of oxygen evolution (Miyao and Murata, 1985).

In this chapter, results of assays for oxygen evolution using various PS II membrane preparations which had been preincubated with immune serum (anti-D1-a) are presented. Pre-immune serum was used as a control for nonspecific effects. The preparations used included PS II membranes, NaCl-treated PS II membranes, $CaCl_2$-treated PS II membranes and urea-treated PS II membranes. For preparations lacking the 33 kDa protein, assays were performed with and without the addition of purified 33 kDa protein. The results indicate that the antibodies have no deleterious effects on the Mn of the OEC. During prolonged incubations, it appears that anti-D1-a stabilizes the OEC Mn against release, allowing reconstitution of oxygen evolution upon addition of the 33 kDa protein.

Procedures

PS II membrane preparation

PS II membrane fragments were prepared from spinach leaves essentially as described by Berthold, et al. (1981), but including modifications from Ford and Evans (1983), Rutherford et al. (1984) and Dr. J.-L. Zimmermann (Service Biophysique, CEN-Saclay, France). The details of this preparation are presented in the previous chapter.

NaCl treatment of PS II membranes

2 M NaCl-extracted PS II membranes (NaCl-treated PS II membranes) lack 17 and 24 kDa extrinsic proteins and were prepared as described by Åkerlund, et al. (1982). After thawing, spinach PS II membranes were centrifuged (30,000 x g, 10 min). The membranes were resuspended at 500 μg Chl/ml in 2 M NaCl, 50 mM MES-NaOH pH 6.5, 0.4 M sucrose. The incubation was carried out for 30 min in darkness at 4°C with occasional mixing. The membranes were then collected by centrifugation (30,000 x g, 10 min). The treatment was repeated once, after which the membranes were washed twice in SMN Buffer and then resuspended in the same buffer to approximately 2-3 mg of Chl per ml.

$CaCl_2$ treatment of PS II membranes

1 M $CaCl_2$-extracted PS II membranes ($CaCl_2$-treated PS II membranes) were compositionally the same as 2.6 M urea, 200 mM NaCl-extracted PS II membranes (urea-treated PS II membranes, Miyao and Murata, 1985) and lack 17, 24 and 33 kDa extrinsic proteins. $CaCl_2$-treated PS II membranes and urea-treated PS II membranes can be prepared from intact PS II membranes or NaCl-treated PS II membranes. All of these samples were handled under dim green light in the cold room. After thawing, spinach PS

II membranes were centrifuged (30,000 x g, 10 min). The membranes were resuspended at 500 μg Chl/ml in 1 M $CaCl_2$, 50 mM MES-NaOH pH 6.5, 0.4 M sucrose. The incubation was carried out for 30 min in darkness at 4°C with gentle mixing. The membranes were then collected by centrifugation (30,000 x g, 10 min). The treatment was repeated once, after which the membranes were washed twice in SMN Buffer and then resuspended in the same buffer to approximately 2-3 mg of Chl per ml.

Urea treatment of PS II membranes

Urea-treated PS II membranes were PS II membrane preparations (or NaCl-treated PS II membranes) extracted with 2.6 M urea, 200 mM NaCl to remove the remaining extrinsic polypeptides. Into SM24 centrifuge tubes, SMNC50 Buffer (0.4 M sucrose, 50 mM MES-NaOH pH 6.5, 100 mM NaCl, 50 mM $CaCl_2$) was added to 0.5 ml of PS II membranes to bring the total volume to 8-10 ml and centrifuged (18,000 rpm=30,000 x g, 15 min, SS34 rotor with adaptor). The pellet was resuspended in 10 ml (2.6 M urea, 200 mM NaCl, 50 mM MES-NaOH pH 6.5) and incubated on a rocker for 30-40 min in the dark at 4°C. Then, this mixture was centrifuged, resuspended, incubated and centrifuged all as above. The pellet was resuspended into 8 ml of SMNC50 Buffer, centrifuged as above, resuspended in 1 ml final volume of SMNC50 Buffer and stored at -80°C in 0.5 ml aliquots.

Isolation of 17 and 24 kDa proteins

The 17 and 24 kDa proteins were isolated as a mixture from the NaCl-treated PS II supernatants of 2 washes of PS II membranes. These mixtures were centrifuged (30,000 x g, 10 min) and the supernatants were pooled together and concentrated by Amicon filtration using a YM-10 membrane. The NaCl was then removed by dialysis against 20 mM MES-NaOH pH 6.5. The absorption at 280 nm was taken to get the total protein concentration, which was then diluted to 0.5-1 μg of protein per ml with 20 mM MES-NaOH pH 6.5.

This preparation was then combined with an equivalent volume of 2x Buffer A (40 mM MES-NaOH pH 6.5, 0.8 M sucrose, 30 mM NaCl, 10 mM $MgCl_2$) and frozen in aliquots at -20°C until use.

Isolation of 33 kDa protein

The 33 kDa protein was isolated from the supernatants of 1 M $CaCl_2$ treatment of PS II membranes previously treated with NaCl. PS II membranes were treated twice as above with NaCl to remove the 17 and 24 kDa proteins. Following two washes with Buffer A, two 30 min incubations with 1 M $CaCl_2$ were done to remove the 33 kDa protein from the membranes. These mixtures were centrifuged (30,000 x g, 10 min) and the supernatants were pooled together and concentrated by Amicon filtration using a YM-30 membrane. The $CaCl_2$ was then removed by dialysis against 20 mM MES-NaOH pH 6.5. The absorption at 276 nm (20 per mM per cm, Miyao and Murata, 1984) was taken to get the total protein concentration, which was then diluted to 0.5-1 μg of protein per ml with 20 mM MES-NaOH pH 6.5. This preparation was then combined with an equivalent volume of 2x Buffer A (40 mM MES-NaOH pH 6.5, 0.8 M sucrose, 30 mM NaCl, 10 mM $MgCl_2$) and frozen in aliquots at -20°C until use.

Oxygen evolution assays

Each assay consisted of 30 μg chlorophyll (PS II, NaCl-treated PS II, $CaCl_2$-treated PS II, or urea-treated PS II) incubated with antisera or pre-immune serum for 1 to 4 h at 0-4°C in the dark. Incubation with pre-immune serum was used as a control for a measure of the possible nonspecific effects of serum addition on the assay. Experiments using reaction center cores or urea-treated cores were done as above with 6 μg chlorophyll (roughly the same number of reaction centers as for PS II experiments). Urea- or $CaCl_2$-treated samples were assayed with or without an additional incubation with 35 μg of 33 kDa protein for 30 min to 1 h before the assay. This amount of 33 kDa protein was

equivalent to a purified 33 kDa protein to Chl w/w ratio of 0.3 for PS II membranes and 2.0 for PS II core preparations (Murata, et al., 1984). These ratios correspond to absolute stoichiometries of purified 33 kDa protein to reaction center of approximately 2:1 for both preparations.

The incubated samples were then assayed with a Clark-type oxygen electrode (Yellow Springs Instr., Ohio). DCBQ (10 µl of 0.1 g/ml stock in DMSO) as acceptor was added in a final volume of 1.6 ml SMNC Buffer (0.4 M sucrose, 50 mM MES-NaOH pH 6.5, 50 mM NaCl, 50 mM $CaCl_2$). The cuvette was maintained at a constant temperature of 24°C and its contents magnetically stirred. Illumination from a slide projector was passed through a 360 nm cutoff filter and a spherical flask filled with water (focused the light and acted as a heat filter). The rate of oxygen evolution was calculated from the initial slope after applying continuous light, at or slightly above saturation levels.

Results and Discussion

This chapter describes a set of experiments aimed at characterizing possible direct antibody effects on the OEC of PS II reaction centers by studying the oxygen evolution of PS II-enriched membrane preparations of differing extrinsic polypeptide composition. Preincubations with anti-D1-a were compared to parallel preincubations with pre-immune serum in order to account for non-specific effects of the serum. In all tables, each rate of oxygen evolution represents the average of 3-5 measurements and has an accuracy of approximately ±10 µmol O_2/mg Chl per h. In Table 5-1, data from an experiment using various PS II membrane preparations treated by preincubation with anti-D1-a or pre-immune serum for 1-2 h is presented. Thereafter, in Tables 5-2 through 5-4, results from experiments using PS II membrane preparations depleted of the extrinsic proteins are presented. Treatment of PS II membranes with 2.6 M urea (+200 mM NaCl) or 1 M

$CaCl_2$ removes the three extrinsic polypeptides while leaving the OEC Mn cluster intact. These preparations evolve oxygen to only a small extent, but can be reconstituted to near 100% activity after incubation with purified 33 kDa protein. The effects of anti-D1-a on these preparations were investigated by varying the length of preincubation as well as the order of addition of sera and 33 kDa protein.

Table 5-1, shows the results from an experiment using PS II membrane preparations of varying extrinsic polypeptide composition. PS II membranes contain all three (17, 24 and 33 kDa) proteins still bound. PS II membranes incubated with anti-D1-a or pre-immune serum for 1-2 h showed no difference in oxygen evolution, both evolving near control PS II levels (476 μmol O_2/mg Chl per hr) when assayed in SMN Buffer containing low Cl^- and Ca^{2+} concentrations. NaCl-treated PS II membranes lack the 17 and 24 kDa extrinsic proteins. After incubation with anti-D1-a or pre-immune serum for 1-2 h, NaCl-treated PS II membranes showed no difference in oxygen evolution. Both treatments resulted in oxygen evolution of slightly more than 90% of the control PS II levels. This preparation was assayed for oxygen evolution in SMN Buffer containing at least 30 mM Cl^- and 5 mM Ca^{2+}. Finally, $CaCl_2$-treated PS II membranes were also incubated with anti-D1-a or pre-immune serum for 1-2 h. These $CaCl_2$-treated PS II membranes lack all three extrinsic proteins and also showed no difference in oxygen evolution for the two preincubations, both evolving at near 20% of control PS II levels when assayed in SMN Buffer containing 200 mM Cl^- and 10 mM Ca^{2+}.

The next experiment was performed in order to determine the required amount of purified 33 kDa protein necessary to reconstitute a substantial fraction of the oxygen evolution for PS II preparations lacking the 33 kDa protein. This was necessary so that these preparations could be assayed more reliably by addition of the 33 kDa protein after preincubation with antibody. The results in Table 5-2 are for oxygen evolution rates of samples containing 30 μg of chlorophyll assayed in SMN Buffer with 200 mM Cl^- and 10

Table 5-1

Oxygen evolution of various PS II membrane preparations following preincubations with anti-D1-a or pre-immune serum for 1-2 h. Prior to incubation with the antibodies, PS II membranes were treated with 2 M NaCl to remove the 17 and 24 kDa extrinsic polypeptides or treated with 1 M $CaCl_2$ to remove the 17, 24 and 33 kDa extrinsic polypeptides.

	Oxygen evolution (μmol O_2/mg Chl per h)		
Sample Type	No Preincubation	Anti-D1-a	Non-Immune
PS II membranes	476 (100%)	468 (98%)	460 (97%)
NaCl-treated PS II membr.	438 (92%)	445 (93%)	430 (90%)
$CaCl_2$-treated PS II membr.	104 (22%)	114 (24%)	95 (20%)

Table 5-2

Oxygen evolution of two PS II membrane preparations lacking all three extrinsic polypeptides. PS II membranes were treated with 1 M $CaCl_2$ or with 2.6 M urea, 200 mM NaCl to remove the 17, 24 and 33 kDa extrinsic polypeptides. Oxygen evolution was measured after incubations with increasing amounts of 33 kDa protein, but no antibody.

	Oxygen evolution (μmol O_2/mg Chl per h)	
Amount 33 kDa Added	$CaCl_2$-PS II	Urea-NaCl-PS II
0 μg	83 (18%)	105 (23%)
7 μg	166 (36%)	158 (34%)
17 μg	241 (52%)	299 (64%)
35 μg	249 (54%)	399 (86%)
50μg	249 (54%)	415 (89%)
67 μg	257 (55%)	432 (93%)

*Control untreated PS II membranes gave rate of 465 (100%)

mM Ca^{2+} following 1-2 h incubations with different amounts of purified 33 kDa protein. The oxygen evolution of $CaCl_2$-treated PS II membranes incubated with increasing amounts of 33 kDa protein ranged from 20% of control PS II evolution to about 55% with 35 μg or more 33 kDa added. For urea-treated PS II membranes, the rate of oxygen evolution relative to control PS II membranes ranged from 20% with 0 μg 33 kDa protein added to around 90% with 35 μg or more added. These results indicate that the $CaCl_2$ treatment damaged a large fraction of the reaction centers, rendering them unable to reconstitute oxygen evolution upon addition of 33 kDa protein. The urea treated samples gave results more consistent with those described by Miyao and Murata (1985). Therefore, urea-treated samples were used for the remainder of PS II experiments described in this chapter. The amount of purified 33 kDa protein added for these experiments and those described in Chapter 7 was equivalent to 35 μg of 33 kDa protein per 30 μg of chlorophyll.

Table 5-3 presents results of an experiment that examined several variables in the assay of oxygen evolution following preincubations with anti-D1-a or pre-immune serum. SMNC10 Buffer and SMNC50 Buffer refer to the assay buffers used, which were SMN Buffer with 10 mM or 50 mM $CaCl_2$, respectively. The lack of 33 kDa protein, or its addition following antibody incubation, are indicated by "NO 33" and "With 33," respectively. Two amounts of sera were added to different sets of samples, 1x and 4x indicates this variable. Each pair of urea-treated PS II membranes incubated with anti-D1-a or pre-immune serum for 1-2 h showed no difference in oxygen evolution, both samples of a pair evolving at about 30% of control PS II levels. This result is consistent for the two assay buffers as well as for the two amounts of added sera. Each pair of urea-treated PS II membranes incubated with anti-D1-a or pre-immune serum for 1-2 h and then 35 μg of purified 33 kDa protein added 1 h before assay showed similar rates of oxygen evolution. Within a pair, the two samples varied by approximately 5% of the control PS II rate, indicating that anti-D1-a does not inhibit the rebinding of the 33 kDa protein. Anti-D1-a

Table 5-3

Oxygen evolution of PS II membrane preparations lacking all three extrinsic polypeptides following preincubations with varying amounts of anti-D1-a or pre-immune serum for 1-2 h. Prior to incubation with the antibodies, PS II membranes were treated with 2.6 M urea, 200 mM NaCl to remove the 17, 24 and 33 kDa extrinsic polypeptides. Oxygen evolution was measured in several buffers after an incubation with or without purified 33 kDa extrinsic protein.

	Oxygen evolution (μmol O_2/mg Chl per h)			
Sample Type	SMNC10 NO 33	SMNC10 With 33	SMNC50 NO 33	SMNC50 With 33
No preinc.	125 (27%)	344 (75%)	137 (30%)	344 (75%)
Anti-D1-a	144 (32%)	394 (86%)	125 (27%)	344 (75%)
Pre-immune	150 (33%)	375 (82%)	125 (27%)	337 (74%)
4x Anti-D1-a	144 (32%)	419 (92%)	137 (30%)	319 (70%)
4x Pre-immune	119 (26%)	387 (85%)	119 (26%)	306 (67%)

*Control untreated PS II membranes gave rate of 456 (100%)

also does not appear to have any deleterious effects on the Mn cluster of the OEC. It is interesting to note that for all pairs of samples to which the 33 kDa protein was added there is a slightly greater rate of oxygen evolution for the anti-D1-a sample relative to the corresponding pre-immune serum sample. The samples assayed in SMNC10 Buffer gave generally higher rates, so this buffer was used for assays described in the next experiment.

The data in Table 5-4 is from an experiment which tested the antibody effects on the stability of the OEC Mn during prolonged incubations. This was examined because, for a given pair of samples during previous experiments, the one incubated with anti-D1-a consistently gave slightly higher rates of oxygen evolution than the sample incubated with pre-immune serum. Also, the removal of the 2 more loosely bound of the 4 OEC Mn by aging $CaCl_2$-treated membranes in low NaCl buffer had been described (Ono and Inoue, 1985; Cole et al., 1987). Urea-treated PS II membranes were incubated in SMN Buffer with anti-D1-a or pre-immune serum for 2-4 days. Then, 35 μg of purified 33 kDa protein was added 1 h before assay. For a pair of samples, higher oxygen evolution rates for the anti-D1-a sample was measured relative to the pre-immune serum sample (Table 5-4). This difference became more pronounced as the length of incubation increased and is much more apparent for the samples incubated with the 4x serum concentration. Also note that the difference is enhanced when the assay for oxygen evolution is performed after incubation with added 33 kDa protein. For this experiment, it appears that anti-D1-a is stabilizing the OEC Mn during the prolonged incubations, allowing reconstitution of oxygen evolution upon addition of the 33 kDa protein.

In summary, this chapter has shown that preincubation with anti-D1-a does not seem to markedly change the rate of oxygen evolution for any of the PS II membrane preparations examined. In PS II membrane preparations from which the 33 kDa protein was removed, preincubation with anti-D1-a has little effect on the rate of oxygen evolution.

Table 5-4, Days 1 and 2

Oxygen evolution of PS II membrane preparations lacking all three extrinsic polypeptides following preincubations with varying amounts of anti-D1-a or pre-immune serum for 0-4 days. Prior to incubation with the antibodies, PS II membranes were treated with 2.6 M urea, 200 mM NaCl to remove the 17, 24 and 33 kDa extrinsic polypeptides. Oxygen evolution was measured after an incubation with or without purified 33 kDa extrinsic protein. Note: This table is continued on the next page.

	Oxygen evolution (μmol O_2/mg Chl per h)			
Sample Type	Day 1: NO 33	Day 1: With 33	Day 2: NO 33	Day 2: With 33
No preinc.	125 (27%)	344 (75%)	106 (23%)	319 (70%)
Anti-D1-a	144 (32%)	394 (86%)	106 (23%)	375 (82%)
Pre-immune	150 (33%)	375 (82%)	106 (23%)	262 (58%)
4x Anti-D1-a	144 (32%)	419 (92%)	106 (23%)	312 (68%)
4x Pre-immune	119 (26%)	387 (85%)	75 (16%)	190 (42%)

*Control untreated PS II membranes gave rate of 456 (100%)

Table 5-4, Days 3 and 4

Oxygen evolution of PS II membrane preparations lacking all three extrinsic polypeptides following preincubations with varying amounts of anti-D1-a or pre-immune serum for 0-4 days. Prior to incubation with the antibodies, PS II membranes were treated with 2.6 M urea, 200 mM NaCl to remove the 17, 24 and 33 kDa extrinsic polypeptides. Oxygen evolution was measured after an incubation with or without purified 33 kDa extrinsic protein. Note: This table continues from the previous page.

	Oxygen evolution (μmol O_2/mg Chl per h)			
Sample Type	Day 3: NO 33	Day 3: With 33	Day 4: NO 33	Day 4: With 33
No preinc.	75 (16%)	219 (48%)	~0 (~0%)	167 (37%)
Anti-D1-a	75 (16%)	219 (48%)	28 (6%)	167 (37%)
Pre-immune	72 (16%)	187 (41%)	~0 (~0%)	103 (23%)
4x Anti-D1-a	69 (15%)	175 (38%)	9 (2%)	122 (27%)
4x Pre-immune	47 (10%)	125 (27%)	~0 (~0%)	19 (4%)

*Control untreated PS II membranes gave rate of 456 (100%)

The same result is obtained whether purified 33 kDa protein is added before or after the antibody incubation. The addition of purified 33 kDa protein is required to reach the maximal rate of oxygen evolution for these preparations. Finally, it appears that anti-D1-a stabilizes the OEC Mn during prolonged incubations, and allows reconstitution of oxygen evolution upon addition of the 33 kDa protein.

6. SOLUTION BINDING ASSAYS

Introduction

Solution binding assays were used in order to determine which antibodies actually bound to native PS II membranes in solution. Although the antibodies were shown to bind to the appropriate one of the D1 or D2 proteins on western blots, whether they bind in solution was examined because of the negative results in other solution studies such as oxygen evolution (Chapter 5) and initial studies of Mn photoactivation (Chapter 7).

This assay was adapted from the procedures of Sayre et al. (1986) who used it to study the orientation of the D1 and D2 proteins in the thylakoid membrane. More precisely, they elicited antibodies to peptides corresponding to regions of the D1 and D2 proteins which are not found in transmembrane helical regions as proposed by the 5 transmembrane helix model described by Trebst (1986) or the 7 transmembrane helix model detailed by Rao et al. (1983). Their peptides were chosen such that binding to closed thylakoid membranes vs inside-out thylakoid membranes would distinguish between the two proposed models. The model of Trebst (1986), containing 5 transmembrane helices was shown to be correct by this antibody analysis.

This procedure was modified by using isolated PS II membrane fragments instead of intact thylakoids. This allowed for the study of binding of antibodies to the preparations used for other experiments and to manipulate the extrinsic polypeptide composition, the cofactors added, and the digestion and processing of the C-termini of the D1 and D2 proteins.

Procedures

PS II membrane preparation

PS II membrane fragments were prepared from spinach leaves essentially as described by Berthold, et al. (1981), but including modifications from Ford and Evans (1983), Rutherford et al. (1984) and Dr. J.-L. Zimmermann (Service Biophysique, CEN-Saclay, France). The details of this preparation are presented in Chapter 4.

Other PS II preparations

Several other PS II membrane preparations were used here. All of them were prepared starting with the PS II membrane fragments described above. The details of the preparation of NaCl-treated PS II membranes and $CaCl_2$-treated PS II membranes are presented in Chapter 5. The details of the preparation of Tris-treated PS II membranes and carboxypeptidase A-treated PS II membranes are presented in Chapter 4.

NH_2OH treatment of PS II preparations

Immediately before starting the binding assay, samples of each membrane preparation were treated at 500 μg Chl/ml for 1 h with 2 mM hydroxylamine in SMN Buffer at 4°C in the dark with occasional mixing (to remove Mn without altering the extrinsic protein composition) as described by Tamura and Cheniae (1985). The membranes were then collected by centrifugation (30,000 x g, 10 min) and washed twice in SMNC Buffer before resuspension in the same buffer.

Solution assay for antibody binding

The procedure used in this study is a modified version from that of Sayre et al. (1986). Approximately 20 μg Chl of PS II membrane preparations (untreated, NaCl-treated, $CaCl_2$-treated, urea-treated, NH_2OH-treated, or carboxypeptidase A-treated) were

pre-incubated at 0.4 mg Chl/ml in SMN Buffer containing 80 mM NaCl, 2% BSA, 0.04% Tween-20, and 10-40% pre-immune Fab (prepared as described in Chapter 3) for 2 h. Twenty µl of antiserum (or pre-immune serum) was simultaneously pre-incubated in SMN Buffer containing 120 mM NaCl, 3% galactose, 3% BSA, and 0.06% Tween-20. This combination of incubations was needed to reduce nonspecific binding of pre-immune serum. Equal volumes of PS II membranes and antiserum were then mixed and incubated on ice for 2 to 4 h with periodic mixing. Each sample was then washed 3 times by centrifugation for 5 min in a microfuge at 4°C and then resuspended in SMN Buffer containing 200 mM NaCl, 2% BSA, 0.04% Tween-20. The secondary antibody, [^{125}I]-labeled donkey anti-rabbit Ig (Amersham IM.134), was added at 1:200 final dilution. After incubation for 2 to 4 h with periodic mixing, the samples were washed 3 times as above. Each membrane pellet was resuspended in SMN Buffer and equal fractions of approximately 5 µg Chl each were used for chlorophyll determination and gamma counting. Chlorophyll determination was done in 80% acetone (by adding 4 volumes of 100% acetone per volume of PS II) as described by Arnon (1949). Counts per minute (CPM) values for each sample were first normalized to 5 µg Chl and then corrected for non-specific [^{125}I] binding. This was done by subtracting values for pre-immune samples from their respective immune samples.

Results and Discussion

Several attempts were required in order to optimize the assay and get reproducible results with low background binding. The most important were: pre-incubation of the PS II preparation with pre-immune Fab, pre-incubation of the immune or pre-immune serum with galactose, the inclusion of Tween-20 and BSA in the incubation buffers and the addition of 200 mM NaCl to all wash buffers. After the assay, chlorophyll determination

of all samples was used to normalize CPM. All of these procedural changes are included in the final procedure described above.

The results from one of the first successful assays are given in Table 6-1. This experiment addressed the question of whether anti-D1-a bound differentially to PS II membranes with different extrinsic polypeptide compositions. Additionally, this experiment examined whether anti-D1-a bound differentially to the same PS II membrane preparations after incubation with the 33 kDa extrinsic protein. The 33 kDa extrinsic protein was added by incubation with purified 33 kDa protein as described in Chapter 5. Differing from the final procedure, this assay started with 10 μg Chl per sample and ended with analysis of final samples of approximately 2 μg Chl for counting of radioactivity and an equivalent amount for determination of Chl content. The difference in CPM between the immune and pre-immune samples were calculated after correction for the actual amount of sample by Chl determination. As can be seen from these differences, the sample lacking the 17 and 24 kDa proteins (NaCl-treated PS II membranes) binds 50% more [^{125}I], and therefore more antibody, than the sample of intact PS II membranes. Likewise, the sample lacking the 17, 24 and 33 kDa proteins (urea-treated PS II membranes) binds 200% more [^{125}I] than the sample of NaCl-treated PS II membranes. From these results, it appears that anti-D1-a binding is increased by the removal of the extrinsic proteins from PS II. For the samples pre-incubated with the 33 kDa extrinsic protein, generally little change or a decrease in binding (for urea-treated PS II membranes) is apparent. For intact PS II membranes, the change caused by 33 kDa protein pre-incubation is a slight increase of 13% of the original binding. For NaCl-treated PS II membranes, the binding to the 33 kDa protein pre-incubated sample is 14% lower than without treatment. The magnitude of these changes is on the order of the error inherent in these measurements. Finally, urea-treated PS II membranes pre-incubated with the 33 kDa protein show a decrease of 49% from the original sample. From these results, two types of binding sites (epitopes) for anti-D1-a on

Table 6-1

Binding in solution of anti-D1-a to PS II membrane fragments of varying extrinsic polypeptide composition. Prior to incubation with the antibodies, PS II membranes were treated with 2 M NaCl to remove the 17 and 24 kDa extrinsic polypeptides or treated with 2.6 M urea, 200 mM NaCl to remove the 17, 24 and 33 kDa extrinsic polypeptides. Subsequently, samples from each treatment were incubated with purified 33 kDa extrinsic protein. Finally, the membranes were incubated for 4 h with antibody and then with [^{125}I]-labeled secondary antibody as described in the Procedures section. The values given are CPM remaining associated with 2 μg Chl of PS II membranes.

Preparation	Difference	+33 kDa Difference
PS II	2,960	3,340
NaCl-PS II	4,430	3,790
Urea-PS II	13,300	6,740

the D1 protein as determined by these solution binding assays can be proposed. One of the epitopes is more exposed and seems to be available even in the presence of all three extrinsic polypeptides. The second epitope becomes available only upon removal of the 33 kDa protein and is obstructed by pre-incubation with the 33 kDa protein for preparations previously lacking it.

The results shown in Table 6-2 address the question of whether anti-D1-a binds differentially to PS II membranes with different extrinsic polypeptide compositions in the presence or absence of the Mn cluster. The Mn cluster was removed by treatment with 2 mM hydroxylamine which, as opposed to the common treatment with 5 mM hydroxylamine, was shown to remove most of the OEC Mn while retaining the major portion of the three extrinsic proteins (Tamura and Cheniae, 1985). This assay started with 25 μg Chl per sample and ended with analysis of final samples of approximately 5 μg Chl for counting of radioactivity and an equivalent amount for determination of Chl content. The difference in CPM between the immune and pre-immune samples was again calculated after correction for the actual amount of sample by Chl determination. As can be seen from these differences, the percentage change between the samples of different extrinsic protein composition is small, and far from results in Table 6-1. This may be best explained by the loss of Mn from the urea-treated PS II membranes of the experiment of Table 6-1. If this was the case, the results of Table 6-1 would be consistent with the results explained here and shown in Table 6-2. For the samples treated with hydroxylamine, a definite increase in binding is apparent. For intact PS II membranes, the increase caused by hydroxylamine treatment is 86% of the original binding. For NaCl-treated PS II membranes, the binding to the hydroxylamine treated sample is 114% higher than without treatment. Finally, urea-treated PS II membranes subsequently treated with hydroxylamine show an increase of 220% over the original sample. From these results, two types of binding sites (epitopes) for anti-D1-a on the D1 protein as determined by these solution binding assays can be

Table 6-2

Binding in solution of anti-D1-a to PS II membrane fragments of varying extrinsic polypeptide composition and varying Mn content. Prior to incubation with the antibodies, PS II membranes were treated with 2 M NaCl to remove the 17 and 24 kDa extrinsic polypeptides or treated with 2.6 M urea, 200 mM NaCl to remove the 17, 24 and 33 kDa extrinsic polypeptides. Subsequently, the Mn cluster was removed from samples of each extrinsic polypeptide composition by treatment with 2 mM hydroxylamine. Finally, the membranes were incubated for 4 h with antibody and then with [^{125}I]-labeled secondary antibody as described in the Procedures section. The values given are CPM remaining associated with 5 μg Chl of PS II membranes.

Preparation	Difference	NH_2OH Difference
PS II	4,130	7,680
NaCl-PS II	4,830	10,350
Urea-PS II	4,970	15,920

proposed. One of these epitopes is more exposed and seems to be available even in the presence of all three extrinsic polypeptides. The other, possibly more interesting, epitope becomes available only upon removal of the Mn cluster by treatment with hydroxylamine. The difference between the three PS II preparations after hydroxylamine treatment is consistent with the protection of this second epitope by the extrinsic proteins, particularly by the 33 kDa protein, as discussed earlier.

The results of solution antibody binding assays using Tris-treated, but not otherwise denatured, PS II membranes are shown in Table 6-3. The numbers given represent CPM for 5 μg of Chl after normalization for the actual amount of Chl in each gamma-counted sample and subtraction of the normalized background (as measured by the binding of pre-immune serum). The results of this assay show that all three antibodies were able to bind to Tris-treated PS II membranes in solution. However, anti-D1-a binding to PS II membranes treated with carboxypeptidase A was much reduced, as expected from the western blots in Figure 4-6. Treatment with carboxypeptidase A did not affect the binding of anti-D2-a to any great extent. On the other hand, the binding of anti-D1-b was slightly increased (~20%), indicating that the epitopes for both antibodies were still present and that the epitope for anti-D1-b was more exposed in this material. The solution binding assay shows that anti-D1-a binding to carboxypeptidase A-treated PS II membranes was reduced by about 50%. The difference in apparent binding of anti-D1-a to carboxypeptidase A-treated PS II membranes in the solution assay compared to the western blot (Figure 4-6) may be a result of several factors. Most importantly, the difference in stringency of the two procedures may allow detection in solution of weakly binding antibodies, which may not have been observed on the western blot. These experiments provide evidence that the strongest binding portion of the anti-D1-a serum binds to the carboxyl-terminal end (about 10 residues before the processing point) of the D1 protein. This portion of the anti-D1-a serum does not appear to share binding sites with anti-D1-b.

Table 6-3

Binding of anti-D1-a, anti-D1-b and anti-D2-a to PS II membrane fragments and carboxypeptidase A-treated PS II membrane fragments in solution. PS II membranes were Tris-treated to remove Mn and the three extrinsic polypeptides prior to carboxypeptidase A treatment and incubation with the antibodies. Subsequently, the membranes were incubated for 4 h with antibody and then with [^{125}I]-labeled secondary antibody as described in the Procedures section. The values given are CPM remaining associated with 5 μg Chl of PS II membranes.

Antibody Incubation	PS II	Carboxypeptidase A-treated PS II
anti-D1-a	7,430	3,810
anti-D1-b	8,530	10,880
anti-D2-a	8,770	7,130

The peptides against which the antibodies were raised share a common sequence (Ile 321 to Arg 334) and one of the binding sites for the anti-D1-a serum could be in this region, of low affinity and detected here by the solution binding assay while not apparent by western blotting (Chapter 4).

To summarize, it appears that anti-D1-a binding, as measured by the solution binding assay, is slightly increased by the removal of the extrinsic proteins from PS II. Two types of binding sites (epitopes) for anti-D1-a on the D1 protein as determined by the solution binding assays can be proposed. One of the epitopes is more exposed and seems to be available even in the presence of all three extrinsic polypeptides. The second epitope becomes available only upon removal of the 33 kDa protein and is obstructed by pre-incubation with the 33 kDa protein for preparations previously lacking it. Another separation into two types of binding sites (epitopes) for anti-D1-a on the D1 protein can be postulated relating to the presence of the Mn cluster. One of these epitopes is more exposed and seems to be available even in the presence of all three extrinsic polypeptides. The other, possibly more interesting, epitope becomes available only upon removal of the Mn cluster by treatment with hydroxylamine, and is probably the epitope detected by the assay of high-affinity Mn-binding sites (Chapter 8). Finally, PS II membranes treated with carboxypeptidase A were used in the solution binding assay to further characterize the three antibodies. The sites to which these three antibodies appear to bind are discussed above.

7. PHOTOACTIVATION ASSAYS

Introduction

The measurement of oxygen evolution rates from a variety of PS II preparations demonstrated that antibody binding had no adverse effects on the functioning of the intrinsic OEC Mn of PS II membranes (see Chapter 5). The only effect observed was the stabilization of the Mn complex by anti-D1-a during prolonged incubations of PS II membranes depleted of the 17, 24 and 33 kDa extrinsic polypeptides by $CaCl_2$ treatment. If a decrease in oxygen evolution rates had been seen, the antibody's mechanism of action on that particular PS II membrane preparation with the intact OEC Mn complex would have been displacement of Mn or alteration of the structure in such a manner as to change oxygen evolution activity. Since the antibodies produced no decrease in oxygen evolution, and the antibodies were shown to bind to PS II membranes in solution with the degree of binding increasing upon Mn removal (see previous chapter), the reverse experiment was tested. This was to first bind the antibodies to PS II membranes depleted of Mn and some or all of the three extrinsic proteins and then assay for the effect of the antibodies on the rebinding of Mn by measuring the extent of photoactivation of oxygen-evolving activity.

The photoactivation process in which the oxygen-evolving ability is restored to thylakoids that were prepared or treated in a fashion to remove the active Mn from its native location in the OEC of PS II has been known for quite some time. As explained by Blankenship et al. (1975), the procedure of Yamashita et al. (1971) can be used to reactivate Tris-washed chloroplasts, which do not initially evolve oxygen, to a final yield of 100% of the control rate of oxygen evolution. Tamura and Cheniae (1986) summarized the wide variety of preparation procedures and the various, often conflicting, results that were

available before they applied the photoactivation procedure to PS II-enriched membrane preparations. The early studies had used cultured algae, intact chloroplasts from leaves greened by widely spaced flashes, Tris-extracted chloroplasts or leaves in which the OEC Mn had been inactivated by NH_2OH treatment. These systems gave results which indicated a requirement for light in order to ligate Mn^{2+} and observe oxygen evolution. The requirements for protein synthesis, state of protein phosphorylation, involvement of PS I, presence of Ca^{2+} and/or stromal factors were not clearly delineated. Actually, the requirement of illumination, although apparent, had no well defined function. Among the possible explanations was that of Blankenship et al. (1975) indicating a light-driven transport of Mn^{2+} across the thylakoid membrane. The most convincing model from studies using intact thylakoid was presented by Ono and Inoue (1983a). They proposed a scheme involving 2 binding sites, one for Mn^{2+} and another for Ca^{2+}. They claimed that Mn^{2+} and Ca^{2+} could both inhibit each other's binding to the appropriate site and that photoactivation proceeded only when Mn^{2+} and Ca^{2+} were both in the correct binding site.

Tamura and Cheniae (1986), in the first report using PS II-enriched membrane preparations, began to better define the requirements for photoactivation of oxygen evolution ability by re-ligation of Mn^{2+}. They washed PS II membranes with $CaCl_2$ and then treated them with redox reagents in order to solubilize the 17, 24 and 33 kDa extrinsic polypeptides and the majority of OEC Mn. They showed that photoligation of Mn^{2+} required both light and approximately 50 mM Ca^{2+}. They observed an apparent competition between Mn^{2+} and Ca^{2+} for both the Mn- and Ca-binding sites. Both of these results agree with the data of Ono and Inoue (1983a) discussed above. The Mn^{2+} photoligation, as shown by Mn quantitation, was said to occur without the extrinsic proteins, but addition of the 33 kDa protein was required for expression of oxygen evolution. They claimed that their results excluded light-driven Mn^{2+} transport across

thylakoid membranes as the requirement for illumination in this system, indicating that light was required in the actual ligation of Mn to its site in the OEC of PS II. The following interesting data which they did not emphasize was also presented in this publication. They claimed maximum photoactivation of 50% (at 4°C) and 75% (at 23°C). They explained that this <100% yield was not a consequence of photoinhibition of the PS II donor side, but did not show data to support this (see below for a discussion of the involvement of photoinhibition). Using the data they did present, one can calculate a maximum oxygen evolution rate of 192 μmol O_2/mg Chl per h for their PS II preparation before Mn and extrinsic protein removal. Using their values of 25 and 92 μmol of O_2/mg Chl per h for Mn depleted and photoactivated samples, respectively, a maximum of 35% photoactivation can be calculated. This value, however, is probably an overestimate considering that similar starting preparations are now known to evolve oxygen at 400-500 μmol O_2/mg Chl per h under appropriate conditions. They may, in fact, have also photoactivated PS II centers which were inactive in their original preparation. They also gave results indicating a pH maximum for photoactivation between pH 6.2 and 6.5 with a significant decrease for pH greater than 7.0, all similar to the pH profile shown for the stability of intact OEC Mn (Critchley et al., 1982; Homann, 1985). Finally, they mention, but do not pursue, the observation that addition of $CaCl_2$ to the oxygen evolution assay medium gave an increase in rate of as much as 50% when $CaCl_2$ was not present during the photoactivation step (see below for clarification of the role of Ca^{2+}).

The first detailed model of the photoactivation process was proposed by Tamura and Cheniae (1987). They studied the photoligation of Mn^{2+} and photoactivation of oxygen evolution using NH_2OH- and Tris-treated PS II membranes. They concluded that at the optimal pH of 6.5, only light and Mn^{2+} were essential for photoactivation, but addition of Ca^{2+} was required for maximum oxygen evolving activity. They performed a kinetic analysis from which they deduced a rate constraint ($t_{1/2}$~125 ms) and the

involvement of an unstable intermediate (half-life of approximately 1 s). In this study, they showed evidence for photoinhibition by weak light aging of PS II membranes without Mn^{2+} prior to photoactivation (contradicting their previous observations, see above). The effect of weak light aging is to inhibit photoactivation and the photoreduction of DCIP by Mn^{2+} (but not by DPC or TPB) and is not observed if the incubation includes Mn^{2+}. These results indicated photodamage to the Mn^{2+} binding site without loss of primary electron transport through the PS II reaction center. Finally, they proposed the following biochemical features to describe the photoactivation process: 1) Sequential weak binding and photooxidation of 2 Mn^{2+} ions before their ligation to PS II with high affinity is required. 2) Ligation of the first Mn ion promotes the weak binding of the second Mn^{2+}, which occurs via the slow rate-limitting step. 3) Photooxidation of this second Mn^{2+} leads to the ligation of 2 more Mn^{2+} ions during a light-independent reaction. And 4) Mn^{2+} and Ca^{2+} can both interact at the binding sites for either cation in PS II.

The function of Ca^{2+} was studied further and reported by Tamura et al. (1989b). They showed that PS II membranes devoid of Mn required only light and the addition of Mn^{2+} in order to photoligate Mn, but this was not sufficient to reconstitute oxygen evolution. Incubation of these inactive, but Mn-containing, PS II membranes with Ca^{2+} in the dark led to recovery of oxygen evolution (and the release of approximately 1 Mn/PS II, which was presumed to be bound at the Ca-binding site). The ability of divalent cations to reconstitute oxygen evolution after dark incubation with the Mn-religated PS II membranes was as follows: $Ca^{2+} > Sr^{2+} >> Ba^{2+}, Mg^{2+}$. This ordering of cations is similar to the requirement for regaining oxygen evolution in PS II membranes lacking Ca^{2+} and the 17 and 24 kDa extrinsic proteins (Ghanotakis et al., 1984b). They also indicated a maximum yield of photoactivation in the range of 40-50%, a measurement of 1.2-1.6 Ca/200 Chl and a block in the S_2 to S_3 transition for Ca^{2+}-deficient preparations (shown by them using thermoluminescence measurements). Finally, they conclude that: 1) photoligation of Mn^{2+}

does not require Ca^{2+}, 2) this Mn-complex formed during photoligation of Mn^{2+} is inactive in oxygen evolution, and 3) the inactive Mn-complex can be changed to an active complex by incubation in the dark with Ca^{2+}.

In the most comprehensive publication on the mechanism of photoactivation, Miller and Brudvig (1989) described the kinetics and the cofactor requirements in much greater detail than previously available. They studied the reconstitution by "light-dependent photoactivation" of the Mn complex and oxygen evolution in PS II membrane preparations depleted of Mn. They measured the Mn^{2+} and Ca^{2+} dependences of the effective rate constant and yield of photoactivation. They discussed the molecular details of the elementary steps in photoactivation and proposed a revised mechanism for photoactivation, including dissociation constants and binding stoichiometries for Mn^{2+} and Ca^{2+}. Experimentally, they treated PS II membranes with NH_2OH to deplete them of Mn and then photoactivated using the procedures of Tamura and Cheniae (1987). They used various Mn^{2+} and Ca^{2+} concentrations and took samples at different points during the incubation in order to study the cation dependences and kinetics of the process. They reported a strong correlation between rate of oxygen evolution, EPR multiline signal amplitude and Mn content of the membranes. In these data, they presented values of photoactivation yields between 30 and 40% (of the typical control rate of 450 μmol O_2/mg Chl per h). In agreement with Ono and Inoue (1983a) and Tamura and Cheniae (1987), they observed a competition between Mn^{2+} and Ca^{2+} for the Ca^{2+} binding site. But, they also noted a slight competition of Ca^{2+} with Mn^{2+} for the Mn-binding site. They compared their results with the two models available in the literature: 1) The "1 stage model" of Ono and Inoue (1983a), which requires that both Mn^{2+} and Ca^{2+} must be bound in their appropriate sites to allow assembly and photoactivation. And 2) The "2 stage model" of Tamura and Cheniae (1987), which states that PS II can photoligate 4 Mn ions in the absence of Ca^{2+} without reconstituting oxygen evolution and then bind Ca^{2+} in

the dark to regain the ability to evolve oxygen. Results and simulations by Miller and Brudvig (1989) are most consistent with the "2 stage model" of Tamura and Cheniae (1987), where Mn^{2+} is involved in the rate-determining step, but Ca^{2+} stimulates the yield of photoactivation and is not involved in the rate-determining step. Since they observed optimal yields of 40% of control oxygen evolution activity, they proposed that photoactivation must occur in parallel with inactivating photochemical processes (commonly lumped together and called photoinhibition). The authors divided these effects into three possible types of damage to PS II which may limit the yield of photoactivation: 1) damage during isolation and/or NH_2OH-treatment, 2) Photoinhibition, which they defined as light-induced loss of primary electron transport through PS II and 3) Photoinactivation, which they explained as light-induced loss of photoactivation capability without the loss of primary electron transport. They measured or calculated the contribution due to each of these 3 types of damage under conditions that would yield 40% photoactivation of oxygen evolution. Of the total yield possible, they assigned 25% to photoinhibition (as measured by decrease in DPC-stimulated DCIP photoreduction). Using their mathematical model of photoactivation, they calculated that at least 90% of the total PS II centers were competent for photoactivation at the start of the process, and explained that damage during isolation and NH_2OH-treatment must account for maximally 10% of the total. This leaves 25%, which they attributed to the photoinactivation process (see above for data from Tamura and Cheniae, 1987, where weak light aging of PS II membranes without Mn^{2+} prior to photoactivation indicated this type of damage). From their model, they also calculated dissociation constants and binding stoichiometries for the binding of Mn^{2+} and Ca^{2+} to both the Mn- and Ca-binding sites. To the Mn-binding site, one Mn^{2+} binds with K_d= 51 μM or one Ca^{2+} binds with K_d= 70 mM. To the Ca-binding site, one Ca^{2+} binds with K_d= 0.3 mM or one Mn^{2+} binds with K_d= 90 μM. Note that both the binding stoichiometries and dissociation constants differ from the values determined from the components of the high-affinity Mn-binding site as measured by the Mn^{2+}/DPC non-

competitive assay for DCIP photoreduction (see Chapter 8). These differences can be explained by the different experimental conditions used in the two cases. The chemical model which Miller and Brudvig presented can be schematically represented as follows:

1) 1st Mn^{2+} binds ----hv----> Mn^{3+},

2) 2nd Mn^{2+} binds ----hv----> $(Mn^{3+})_2$,

3) 3rd & 4th Mn^{2+} bind ---n(hv)---> $(Mn)_4$, ligated but inactive,

4) Ca^{2+} binds --------> $(Mn)_4$ active in O_2 evolution.

This is a simplification, showing only the steps leading to active OEC formation, of the more correct scheme which would express the binding of every cation as a different equilibrium. In this model, the "2 stages" are 1) photoligation of Mn^{2+} requiring light and Mn^{2+} (steps 1-3), and 2) binding of Ca^{2+} which is required for expression of oxygen evolution (step 4). Considering the evidence for an unstable intermediate (Tamura and Cheniae, 1987), Miller and Brudvig concluded that one Mn^{2+} ion is bound and photooxidized in the rate-determining step of photoactivation and that it corresponds to the second Mn^{2+} bound (step 2 above).

This chapter describes experiments based on modifications of the Mn photoactivation protocol first applied to PS II-enriched membrane preparations by Tamura and Cheniae (1986), as discussed above. The procedure involves incubation of Mn-depleted (Tris- or hydroxylamine-treated) PS II membranes under low light (approximately 1 W/m^2 at the sample) in the presence of $MnCl_2$ and $CaCl_2$ with DCIP as the electron acceptor at room temperature for 30-45 min. In the report of Tamura and Cheniae (1986), with 33 kDa protein added for the oxygen evolution assay, this treatment yielded an increase of oxygen evolution rates of 25% for Tris-treated PS II membranes, 35% for Tris-treated PS II membranes photoactivated in the presence of 33 kDa protein and apparently

50-60% for NH_2OH-treated PS II membranes (Tamura and Cheniae, 1987). Other groups have reported photoactivation yields of 10-25% oxygen evolution activity starting with NH_2OH-treated PS II membranes. After optimizing the photoactivation procedure, Miller and Brudvig (1989) reported 40% as being consistently their maximum yield of oxygen evolution.

As done in the experimental series to examine antibody effects on oxygen evolution (Chapter 5), a variety of PS II membrane preparations have again been used. Preparations that lack all of the extrinsic polypeptides, thereby increasing the chances of antibody effects while simultaneously accepting a decrease in yield of photoactivation, were examined first. Then, the yield of photoactivation was maximized by removing less of the extrinsic proteins. The first preparation used, Tris-treated PS II membranes, lack all three extrinsic proteins (17, 24 and 33 kDa) and have lost all of the OEC Mn. The other preparation used, NH_2OH-treated PS II membranes, lack two extrinsic proteins (17 and 24 kDa) and the OEC Mn, but retain the majority of the 33 kDa extrinsic protein. For both preparations, the maximum reconstitution of oxygen evolution occurred with 1 mM $MnCl_2$, 50 mM $CaCl_2$ and the presence of 33 kDa protein. This required addition of purified 33 kDa protein in the case of Tris-treated PS II membranes (Tamura and Cheniae, 1987), although a small rate (20% maximum) of oxygen evolution is expected in the presence of 200 mM Cl^- and 10 mM Ca^{2+} without adding the 33 kDa protein (Miyao et al., 1987). Experiments using both of these preparations with preincubation of the PS II membranes with antibody will be explained in this chapter. For Tris-treated PS II membranes, the antibody incubation was followed by photoactivation in the presence or absence of added 33 kDa protein. Then, the oxygen evolution rate was measured with or without the addition of purified 33 kDa protein. For NH_2OH-treated PS II membranes, the antibody incubation was followed by photoactivation and then measurement of the oxygen evolution rate. The data from maximizing the yield of photoactivation while studying the antibody effects is consistent

with the two reports (Miller and Brudvig, 1989; Tamura et al., 1989b) published after these experiments were done. Additionally, there were some effects of preincubation with anti-D1-a on the yield of photoactivation. There was little or no effect indicated by preliminary results of preincubations with the other two antibodies, anti-D1-b and anti-D2-a.

Procedures

PS II membrane preparation

PS II membrane fragments were prepared from spinach leaves essentially as described by Berthold, et al. (1981), but including modifications from Ford and Evans (1983), Rutherford et al. (1984) and Dr. J.-L. Zimmermann (Service Biophysique, CEN-Saclay, France). The details of this preparation are presented in Chapter 4.

Tris treatment of PS II membranes

After thawing, spinach PS II membranes were depleted of Mn and all 3 extrinsic proteins by Tris-treatment as described by Tamura and Cheniae (1987). After centrifugation (30,000 x g, 10 min), the membranes were resuspended at 500 μg Chl/ml in 0.8 M Tris-HCl pH 8.4, 0.4 M sucrose. The incubation was carried out for 40 min under room lights at 4°C with occasional mixing. The membranes were then collected by centrifugation (30,000 x g, 10 min), washed twice in SMN Buffer and resuspended in the same buffer. This procedure differs from the Tris treatments described in Chapters 4 and 7.

NH_2OH treatment of PS II membranes

After thawing, spinach PS II membranes were diluted to 500 μg Chl/ml with SMN Buffer containing hydroxylamine (at 5 mM final concentration). The membranes were

treated for 1 h at 4°C in the dark with occasional mixing as described by Tamura and Cheniae (1987). The membranes were then collected by centrifugation (30,000 x g, 10 min) and washed twice in SMN Buffer (at approx 500 μg Chl/ml) before resuspension in the same buffer. PS II membranes lose OEC Mn and the 17 and 24 kDa proteins, but retain the 33 kDa extrinsic protein, after this treatment, which is harsher than the hydroxylamine treatment described in Chapter 6.

Isolation of 33 kDa protein

The 33 kDa protein was isolated as described in Chapter 5. The protein was stored frozen in SMN Buffer at -70°C.

Photoactivation

The procedures used here are modifications of the protocol for Mn photoactivation described by Tamura and Cheniae (1987). Mn-depleted (Tris- or hydroxylamine-treated) PS II membrane preparations were pelleted (30,000 x g, 10 min) and resuspended to 1 mg Chl/ml with 2x SMNC Buffer (40 mM MES-NaOH pH 6.5, 0.8 M sucrose, 30 mM NaCl, 10 mM $MgCl_2$). To portions of these samples, an equal volume of antibody or pre-immune serum was added (1 μl of serum per mg of Chl). When testing different amounts of added serum, the serum was diluted with PBS before addition of an equal volume to the PS II membranes. These PS II membrane/antibody mixtures were incubated for 1 to 4 h in darkness at 4°C with occasional mixing. This mixture was then transferred to wells on a polystyrene cell culture plate (or petri dishes) containing an equal volume of 2x freshly made photoactivation buffer (2 mM $MnCl_2$, 100 mM $CaCl_2$ and 200 μM DCIP in SMN Buffer). The PS II membrane concentration at this point was 250 μg Chl/ml. The PS II membranes were then photoactivated by incubation under low light (fluorescent lamps, approximately 1 W/m^2 at the sample) at room temperature (21-23°C) for 40 min. The samples were gently swirled every 5 min to ensure mixing. After the photoactivation, the

samples were transferred to darkness and kept on ice until measurement of oxygen evolution activity. Addition of purified 33 kDa protein in SMN Buffer was at different points through the procedure and included a 30 min incubation in darkness at 4°C before continuation with the next step of the procedure. The controls for photoactivation were treated identically to the antibody samples except for addition of PBS instead of serum during the 1-4 h incubation.

Oxygen evolution assays

Each assay used 25 μg of Chl per sample and was run as previously described (Chapter 5). Preparations lacking the 33 kDa extrinsic protein were assayed with or without an additional incubation on ice with 35 μg of purified 33 kDa protein for 30 min to 1 h before the assay.

Results and Discussion

This chapter focuses on experiments aimed at characterizing possible antibody effects on PS II reaction centers by studying the Mn photoactivation protocol first applied to PS II-enriched membrane preparations by Tamura and Cheniae (1986). In Table 7-1, data from a representative preliminary experiment using Tris-treated PS II membranes without antibody incubation are presented. Next, in Tables 7-2 through 7-7, results from experiments using Tris-treated and hydroxylamine-treated PS II membranes to characterize the effects of anti-D1-a on the photoactivation process are given. Finally, in Tables 7-8 and 7-9, the results of a few preliminary experiments using Tris-treated and hydroxylamine-treated PS II membranes to study the effects of the other antibodies, anti-D1-b and anti-D2-a, on the photoactivation process are given.

The goal of the experiment whose results are presented in Table 7-1 was to reproduce the published experiments of Tamura and Cheniae (1987) using Tris-treated PS II membranes. The Tris-treated PS II membranes were photoactivated with or without the 33 kDa extrinsic protein and the rate of oxygen evolution for each of these was then measured with or without the 33 kDa protein. Tris treatment removes all three (17, 24 and 33 kDa) extrinsic polypeptides along with the active Mn, so addition of a slight molar excess of purified 33 kDa protein and incubation on ice for 30-60 min was required for those samples which were to be photoactivated or assayed in the presence of 33 kDa protein. All other samples were incubated under similar conditions with the addition of SMN Buffer to compensate for dilution. The amount of 33 kDa protein required was described in Chapter 5, where purified 33 kDa protein was used to reconstitute the oxygen evolution of $CaCl_2$-treated PS II membranes (which retain the active Mn but lack the three extrinsic proteins). Also, two illumination conditions which differed by a factor of 4-5 in light intensity (high light of 1 W/m^2 at the sample, which is approximately equal to the intensity described by Tamura and Cheniae, 1987) were used to examine the effects of light intensity on the photoactivation process.

The results shown in Table 7-1 give relative increases in oxygen evolution due to photoactivation for different samples which are comparable to those reported by Tamura and Cheniae (1987). The percentages for these samples which contain the 33 kDa protein during assay for oxygen evolution are approximately 1/3 to 1/2 of the percentages calculated from their reported oxygen evolution rates, but the increases relative to control samples are in closer agreement. The main differences appear in the samples for which these results show very low oxygen evolution. These samples can be divided into two groups. One group contains samples which were Tris-treated but received no illumination (first column of Table 7-1, but not including the untreated control). Tamura and Cheniae (1987) reported approximately 5% oxygen evolution for similarly treated samples. This

Table 7-1

Preliminary experiment of photoactivation of Tris-treated PS II membranes without antibody incubation. The photoactivation procedure used was similar to that described by Tamura and Cheniae (1987). The Tris-treated PS II membranes were photoactivated for 45 min (denoted as hv in the table) after an incubation with or without purified 33 kDa extrinsic protein. The rate of oxygen evolution (denoted as O_2 in the table) for each of these samples was then measured after an incubation with or without with purified 33 kDa protein. The "low" and "high" light illuminations were both near the illumination intensity used by Tamura and Cheniae (1987).

	Illumination		
Sample Type	None	Low	High
Control, untreated	555 (100%)		
Control, no illumination	~0 (~0%)		
hv without 33; O_2 without 33	~0 (~0%)	~0 (~0%)	~0 (~0%)
hv without 33; O_2 with 33	~0 (~0%)	33 (6%)	63 (11%)
hv with 33; O_2 with same 33	~0 (~0%)	81 (15%)	93 (17%)

may be due to more complete removal of the active Mn or of the 33 kDa protein here than in their samples. The other group contains Tris-treated samples which were both photoactivated and assayed for oxygen evolution without addition of 33 kDa protein (third row of Table 7-1). Tamura and Cheniae (1987) reported as high as 25% oxygen evolution for similarly photoactivated and assayed samples. Their results can only be interpreted as residual 33 kDa protein in their preparations, as shown by only a 5% increase in the oxygen evolution obtained by the addition of 33 kDa protein after photoactivation but before the assay of oxygen evolution for their samples. These results are more consistent with the more recent data of Miller and Brudvig (1989) which showed a requirement for addition of purified 33 kDa protein in order to measure appreciable oxygen evolution rates from Tris-treated PS II membranes photoactivated in the presence of $MnCl_2$ and $CaCl_2$. Finally, the two illuminations conditions which were used differed by a factor of 4-5 in light intensity, but gave relatively small differences in yield, indicating that the photoactivation process is not very sensitive to the exact light intensity in this weak light domain.

Table 7-2 shows the results of the first experiment addressing whether there were any effects of preincubation with anti-D1-a on the ability to photoactivate Tris-treated PS II membranes. Also, two illumination conditions which differed by a factor of 4-5 in light intensity (low light was 1 W/m^2 at the sample) were again used to confirm the insensitivity to these changes in light intensity of the photoactivation process. The yields of oxygen evolution after photoactivation were similar to those of the previous experiment (Table 7-1). Again, these results are more consistent with those of Miller and Brudvig (1989) than Tamura and Cheniae (1987) in that photoactivation occurs without the 33 kDa protein and is detected only if oxygen evolution is measured with added 33 kDa protein. As summarized in Table 7-2, each of the samples preincubated with 1 μl of anti-D1-a serum per mg of Chl shows slightly less yield of photoactivation than the corresponding sample

Table 7-2

Photoactivation of Tris-treated PS II membranes following preincubations with anti-D1-a or pre-immune serum. After incubations with anti-D1-a or pre-immune serum, the Tris-treated PS II membranes were photoactivated (hv) with different light intensities for 45 min after an incubation with or without purified 33 kDa extrinsic protein. The rate of oxygen evolution (O_2) for each of these samples was then measured after an incubation with or without with purified 33 kDa protein.

	Preincubation		
Sample Type	No Preinc.	Anti-D1-a	Non-Immune
Control, untreated	555 (100%)		
Control, no illumination	~0 (~0%)		
hv without 33; O_2 with 33			
low light		76 (14%)	95 (17%)
hi light		81 (15%)	92 (17%)
hv with 33; O_2 with same 33			
low light		92 (17%)	111 (20%)
hi light		84 (15%)	95 (17%)

preincubated with 1 μl of pre-immune serum per mg of Chl. The differences are on the order of 2-3% of the maximal photoactivation yield (which was assumed to be the rate of oxygen evolution prior to Tris treatment, as before). These differences represent a 12-20% change of the rate of oxygen evolution for the anti-D1-a samples relative to the pre-immune samples. Finally, the light intensity again does not significantly alter the results, so illumination with 1 W/m^2 at the sample was used for the rest of the experiments.

The data presented in Table 7-3 is from an experiment to duplicate the results in Table 7-2 using illumination of 1 W/m^2 and to expand upon them. To confirm results indicating that no oxygen evolution is observed unless the 33 kDa protein is added at some point prior to assay for oxygen evolution, this protein was again omitted for one series of samples. This observation was confirmed, as shown by the lack of photoactivation for all samples whose results are on the third, forth and fifth rows of Table 7-3. These results are again consistent with those reported by Miller and Brudvig (1989) while they contradict the earlier data of Tamura and Cheniae (1987). In order to quantitate the effect of anti-D1-a seen previously, the amount of serum used was as before for a given sample (1 μl of serum per mg of Chl) and, additionally, it was increased by a factor of 10 for a matching sample (10 μl of serum per mg of Chl). The results (Table 7-3) are approximately consistent with those of the previous experiment for the same amount of added serum. For the samples in which the amount of serum was increased 10-fold, an increase in the difference between the immune and pre-immune samples was expected. Surprisingly, the yield of photoactivation decreased for all samples in which the serum was increased. This effect was further investigated using hydroxylamine-treated PS II membrane preparations and the results are presented in the following tables.

As described thus far, Tris-treated PS II membranes gave little or no photoactivation unless the 33 kDa protein was added before the measurement of oxygen

Table 7-3

Photoactivation of Tris-treated PS II membranes following preincubations with different amounts of anti-D1-a or pre-immune serum. After incubations with anti-D1-a or pre-immune serum, the Tris-treated PS II membranes were photoactivated (hv) by illumination at 1 W/m^2 for 45 min after an incubation with or without purified 33 kDa extrinsic protein. The rate of oxygen evolution (O_2) for each of these samples was then measured after an incubation with or without with purified 33 kDa protein.

	Preincubation		
Sample Type	No Preinc.	Anti-D1-a	Non-Immune
Control, untreated	555 (100%)		
Control, no illumination	~0 (~0%)		
hv without 33; O_2 without 33	~0 (~0%)		
and 1x serum		~0 (~0%)	~0 (~0%)
and 10x serum		~0 (~0%)	~0 (~0%)
hv without 33; O_2 with 33	40 (7%)		
and 1x serum		49 (9%)	61 (11%)
and 10x serum		~0 (~0%)	~0 (~0%)
hv with 33; O_2 with same 33	81 (15%)		
and 1x serum		76 (14%)	88 (16%)
and 10x serum		~0 (~0%)	~0 (~0%)

evolution. Additionally, when the 33 kDa protein was added, Tris-treated PS II membranes gave generally low photoactivation yields (usually 15-20%) and small differences for samples preincubated with immune serum relative to pre-immune serum. The results were quite similar whether the 33 kDa protein was added before or after photoactivation, as long as it was added before the measurement of oxygen evolution. For these reasons, there was no advantage in using Tris-treated PS II membranes and, a series of experiments was performed using hydroxylamine-treated PS II membranes. Hydroxylamine treatment removes the active OEC Mn and most of the 17 and 24 kDa proteins while retaining the 33 kDa protein. These preparations give higher yields of photoactivation, reportedly up to 60% (Tamura and Cheniae, 1987). Miller and Brudvig (1989) discussed their consistently attaining photoactivation yields of 40% for this type of sample.

The results of the first photoactivation experiment using hydroxylamine-treated PS II membranes are presented in Table 7-4. Again, the treatment of these samples removed all of their oxygen-evolving activity if no photoactivating illumination was performed. For photoactivations, two different illuminations were used as in Table 7-2, with the low light being 1 W/m^2 at the sample. The amount of added serum was as before (1 µl of serum per mg of Chl), and increased by a factor of 5 for a second sample of each treatment. Table 7-4 shows results which indicate that the samples preincubated with 1 µl of serum gave good photoactivation, with yields in the range of 45-52%. These samples showed a difference of 5-6% for the preincubation with immune vs pre-immune serum. Also, there is apparently little effect of light intensity on the yield of photoactivation, as was the case with Tris-treated PS II membranes. The 5-fold increase in serum gave large decreases in photoactivation for the samples incubated with both immune and pre-immune serum, as was seen for the 10-fold increase in serum used with the Tris-treated PS II membranes in Table 7-3.

Table 7-4

Photoactivation of hydroxylamine-treated PS II membranes following preincubations with different amounts of anti-D1-a or pre-immune serum. After incubations with anti-D1-a or pre-immune serum, the hydroxylamine-treated PS II membranes were photoactivated (hv) with different light intensities for 45 min.

	Preincubation		
Sample Type	No Preinc.	Anti-D1-a	Non-Immune
Control, untreated	585 (100%)		
Control, no illumination	~0 (~0%)		
High hv	214 (37%)		
High hv, 1x serum		262 (45%)	295 (50%)
High hv, 5x serum		77 (13%)	90 (15%)
Low hv	217 (37%)		
Low hv, 1x serum		269 (46%)	302 (52%)
Low hv, 5x serum		81 (14%)	92 (16%)

The goals of the next experiment were to reproduce the previous results and test the yield of photoactivation for the same hydroxylamine-treated PS II membrane preparation used in the previous experiment (Table 7-4) after a 24 h frozen storage at -80°C. The results presented in Table 7-5 indicate that the yields of oxygen evolution for individual samples were diminished by approximately 10% relative to those shown in Table 7-4. For this reason, further experiments utilized freshly prepared hydroxylamine-treated PS II membrane preparations from frozen PS II membrane aliquots. The sample preincubated with anti-D1-a (1 μl of serum per mg of Chl) still shows 5% less yield of oxygen evolution relative to the sample preincubated with pre-immune serum. The samples with 5-fold increase in serum again gave large decreases in photoactivation for the samples incubated with both immune and pre-immune serum, as was seen in the previous experiment.

The next experiment was intended to test a smaller range of serum to Chl ratios in order to see if there was a correlation between the amount of serum added and the yield of oxygen evolution following photoactivation. The results are shown in Table 7-6 for a series of added serum amounts representing 1/2, 1, 2 and 4 times the reference ratio added in previous experiments (1 μl of serum per mg of Chl). This experiment used freshly prepared hydroxylamine-treated PS II membrane preparations from frozen PS II membrane aliquots. However, the yields are all relatively low compared to the results in Table 7-4. These results are among those which show the inconsistency of the photoactivation procedure as described earlier and was also presented by Miller and Brudvig (1989). There is still a difference between the samples preincubated with anti-D1-a and those preincubated with pre-immune serum. The yield of oxygen evolution following photoactivation decreases with increasing amount of added serum for each pair of samples as had been previously observed. Surprisingly, the difference between samples preincubated with anti-D1-a and those preincubated with pre-immune serum is greatest for the smallest amount of

Table 7-5

Photoactivation of hydroxylamine-treated PS II membranes following preincubations with different amounts of anti-D1-a or pre-immune serum. After incubations with anti-D1-a or pre-immune serum, the hydroxylamine-treated PS II membranes were photoactivated (hv) by illumination at 1 W/m^2 for 45 min.

	Preincubation		
Sample Type	No Preinc.	Anti-D1-a	Non-Immune
Control, untreated	585 (100%)		
Control, no illumination	~0 (~0%)		
Photoactivated	154 (26%)		
Photoactivated, 1x serum		207 (35%)	235 (40%)
Photoactivated, 5x serum		63 (11%)	69 (12%)

Table 7-6

Photoactivation of hydroxylamine-treated PS II membranes following preincubations with different amounts of anti-D1-a or pre-immune serum. After incubations with anti-D1-a or pre-immune serum, the hydroxylamine-treated PS II membranes were photoactivated (hv) by illumination at 1 W/m^2 for 45 min.

	Preincubation		
Sample Type	No Preinc.	Anti-D1-a	Non-Immune
Control, untreated	585 (100%)		
Control, no illumination	~0 (~0%)		
Photoactivated	188 (32%)		
Photoactivated, 1/2 x serum		135 (23%)	184 (31%)
Photoactivated, 1 x serum		118 (20%)	157 (27%)
Photoactivated, 2 x serum		86 (15%)	118 (20%)
Photoactivated, 4 x serum		25 (4%)	50 (9%)

serum and decreases as the amount of serum is increased. This may indicate effects of the added serum on these samples whose explanations are not as straight forward as expected.

The results shown in Table 7-7 are of a time course of illumination performed in order to see if the anti-D1-a effect had any dependance on the length of illumination. The illumination intensity was maintained constant at approximately 1 W/m^2. Again, somewhat low overall yields of photoactivation were obtained for these samples. The progression of yield with time was different for the samples preincubated with immune serum than for the other two sample types. For samples with no preincubation, the yields reach a maximum at 30 min and then decrease slightly with longer illuminations. The yields of samples preincubated with pre-immune serum also reach a maximum at 30 min and then plateau off or decrease slightly with longer illuminations. The yields of samples preincubated with anti-D1-a serum, however, continue to increase all of the way out to the last time point, 60 min of illumination. The differences between immune and pre-immune samples also reach a maximum at 30 min and then decrease with longer illuminations. The differences at 30 and 45 min are similar to those previously observed for 45 min illuminations. These results indicate somewhat different effects of the lengths of illumination for the different sample types. The different time dependences may be explained by competing equilibria for the binding of Mn and antibody to sites important for the photoactivation process. Alternatively, there may be antibody protection against reaction center damage as was seen for oxygen evolution after prolonged incubations of $CaCl_2$-treated PS II membranes (Chapter 5).

Thus far, experiments focussing on the effects of anti-D1-a on the photoactivation process have been described. Table 7-8 presents preliminary data for the same process using preincubations of NH_2OH-treated PS II membranes with the other two antibodies, anti-D1-b and anti-D2-a. The different samples of each antibody were from three rabbits

Table 7-7

Photoactivation time course of illumination of hydroxylamine-treated PS II membranes following preincubations with a constant amount of anti-D1-a or pre-immune serum. After incubations with anti-D1-a or pre-immune serum, the hydroxylamine-treated PS II membranes were photoactivated (hv) by illumination at 1 W/m^2 for 0, 15, 30, 45 or 60 min.

	Preincubation		
Sample Type	No Preinc.	Anti-D1-a	Non-Immune
Control, untreated	585 (100%)		
Control, no illumination	16 (??%)		
Photoactivated, 0 min	~0 (?%)	~0 (?%)	~0 (?%)
Photoactivated, 15 min	100 (17%)	99 (17%)	123 (21%)
Photoactivated, 30 min	134 (23%)	145 (25%)	182 (31%)
Photoactivated, 45 min	122 (21%)	160 (27%)	181 (31%)
Photoactivated, 60 min	112 (19%)	164 (28%)	178 (30%)

Table 7-8

Photoactivation of hydroxylamine-treated PS II membranes following preincubations with anti-D1-b, anti-D2-a or pre-immune serum. After the incubations with anti-D1-b, anti-D2-a or pre-immune serum, the hydroxylamine-treated PS II membranes were photoactivated (hv) by illumination at 1 W/m^2 for 45 min.

	Preincubation		
Sample Type	No Preinc.	Anti-serum	Non-Immune
Control, untreated	585 (100%)		
Control, no illumination	29 (5%)		
Photoactivated	128 (22%)		
Photoactivated, Anti-D1-b		121 (21%)	69 (12%)
Photoactivated, Anti-D1-b		103 (18%)	100 (17%)
Photoactivated, Anti-D1-b		142 (24%)	126 (22%)
Photoactivated, Anti-D2-a		137 (23%)	110 (19%)
Photoactivated, Anti-D2-a		125 (21%)	101 (17%)
Photoactivated, Anti-D2-a		132 (23%)	89 (15%)

which were producing antibody against the corresponding protein as screened by western blotting analysis (Chapter 4). The overall yields of oxygen evolution following photoactivation were again fairly low (15-25%) for this type of sample (compare to Table 7-4). Although preliminary, the results seem to all show slightly greater yield for samples which were preincubated with immune sera relative to those samples which were preincubated with pre-immune sera. This is an interesting effect, which is the opposite of that observed when the preincubations used anti-D1-a.

The results presented in Table 7-9 are from another preliminary experiment using anti-D1-b and anti-D2-a preincubations of Tris-treated PS II membranes. The purpose of this experiment was to determine if the increase in photoactivation yield seen in the previous experiment was due to a functional replacement of the 33 kDa extrinsic protein by the binding of antibody. The results indicate that there is no such effect, as seen by the lack of photoactivation in samples treated with antibody without additional 33 kDa protein for the assay of oxygen evolution. When purified 33 kDa protein was added prior to assay for oxygen evolution, reasonable yields were obtained (compare to Table 7-2). Again, the yields for samples which were preincubated with immune sera were slightly higher than those for samples which were preincubated with pre-immune sera. This slight variation was not further investigated.

In summary, the experiments described in this chapter were aimed at characterizing possible antibody effects on PS II reaction centers by studying the Mn photoactivation protocol. As described in several publications (best explained by Miller and Brudvig, 1989), the photoactivation procedure is not easily reproducible. The results vary from one experiment to the next and the yields of oxygen evolution depend on factors not fully characterized. However, the results in this chapter indicate that the first antibody produced, anti-D1-a, may inhibit the photoactivation process. Small decreases in yield of oxygen

Table 7-9

Photoactivation of Tris-treated PS II membranes following preincubations with anti-D1-b, anti-D2-a or pre-immune serum. After the incubations with anti-D1-b, anti-D2-a or pre-immune serum, the Tris-treated PS II membranes were photoactivated (hv) by illumination at 1 W/m^2 for 45 min after an incubation with or without purified 33 kDa extrinsic protein. The rate of oxygen evolution (O_2) for each of these samples was then measured after an incubation with or without with purified 33 kDa protein.

	Preincubation		
Sample Type	No Preinc.	Anti-serum	Non-Immune
Control, untreated	555 (100%)		
Control, no illumination	~0 (~0%)		
hv without 33; O_2 without 33	~0 (~0%)		
Anti-D1-b		~0 (~0%)	~0 (~0%)
Anti-D1-b		~0 (~0%)	~0 (~0%)
Anti-D1-b		~0 (~0%)	~0 (~0%)
Anti-D2-a		~0 (~0%)	~0 (~0%)
Anti-D2-a		~0 (~0%)	~0 (~0%)
Anti-D2-a		~0 (~0%)	~0 (~0%)
hv without 33; O_2 with 33	85 (15%)		
Anti-D1-b		79 (14%)	56 (10%)
Anti-D1-b		67 (12%)	65 (12%)
Anti-D1-b		93 (17%)	82 (15%)
Anti-D2-a		89 (16%)	73 (13%)
Anti-D2-a		81 (15%)	65 (12%)
Anti-D2-a		86 (15%)	57 (10%)

evolution due to incubation with anti-D1-a before photoactivation were observed when using Tris-treated PS II membranes. Somewhat greater decreases in yield were observed with hydroxylamine-treated PS II membranes. The effect was influenced by the amount of added antiserum and the duration of illumination. Results for preincubation with the other two antibodies, anti-D1-b and anti-D2-a, are preliminary, but seem to indicate little or no effect on the yields of oxygen evolution after photoactivation.

8. ASSAY OF HIGH-AFFINITY Mn-BINDING SITES

Introduction

In this chapter, experiments that examine antibody effects on the high-affinity Mn-binding sites of PS II are presented. The antibodies used were those previously described which were raised against the peptides corresponding to two overlapping segments of the carboxyl end of the D1 protein and one antibody against the C-terminus of the D2 protein. The Mn^{2+}/DPC competition for DCIP photoreduction assay was developed by Hsu et al. (1987) and subsequently used by the groups of Seibert (at SERI, in Colorado) and Inoue (at RIKEN, in Japan). A summary of each major contribution, along with the relevant conclusions and the remaining questions, are presented in order to explain this complicated assay and shed some light on the advances it has provided to the knowledge of Mn-binding in PS II.

Hsu et al. (1987) examined the effect of exogenous electron donors on the oxidizing side of PS II by measuring light-induced electron transport through PS II. The electron transport was followed by monitoring the exogenous electron acceptor DCIP whose 590 nm absorption is quenched upon reduction by PS II. The initial slope of the DCIP quenching reaction was used to calculate the rate of electron transport through the photosystem. For intact PS II, where endogenous Mn is still bound, H_2O acts as the ultimate electron donor by way of the Mn cluster of the OEC. After removal of Mn by Tris or hydroxylamine treatment, exogenous electron donors must be added in order to observe electron transport. Two such donors are Mn^{2+} (at mM concentrations) and DPC (at μM concentrations). Hsu et al. (1987) observed that when they used DPC as the donor to Tris-treated PS II particles, Mn^{2+} at 0.1-10 μM acts as an inhibitor of DPC photooxidation.

They studied this competition between Mn^{2+} and DPC in detail and suggested that the "highly specific Mn(II) binding site on the oxidizing side of Photosystem II... is the site for the endogenous Mn in the O_2-evolving complex of PS II." (Hsu et al. 1987). They based this conclusion on the following observations: 1) the presence of endogenous Mn blocks DPC donation to PS II, 2) Mn removal by Tris treatment stimulates electron transport with DPC as donor, 3) Mn^{2+} in low concentrations acts as a competitive inhibitor of DPC electron donation (but, see discussion of Preston and Seibert, 1991a, below), 4) Mn^{2+} binds to a site with high specificity and dissociation constant of about 0.15 μM, 5) Mn binding decreases with increasing ionic strength, indicating an electrostatic interaction, 6) the affinity of Mn binding also depends on the anions present with an ordering of effectiveness resembling the requirement for reactivation of oxygen evolution from Cl^--depleted PS II (Critchley et al., 1982) and 7) the binding affinity of Mn^{2+} decreased as the pH was shifted from 6.1 to 7.7, consistent with the behavior of endogenous Mn which is destabilized at high pH and the observation that OH^- reversibly inhibits oxygen evolution competitively with Cl^- (Critchley et al., 1982; Homann, 1985).

The model proposed by Hsu et al. (1987), competitive Mn^{2+} inhibition of DPC-supported DCIP photoreduction at the same binding site for Mn^{2+} and DPC, and their conclusion that the highly specific Mn-binding site could correspond to the site for active OEC Mn on the intrinsic membrane proteins of PS II seem reasonable. The experimental evidence, however, is only circumstantial, although consistent, with their assertions. One of the main criticisms lies in the single Mn site postulated (along with one dissociation constant) while it is accepted that the active OEC contains four Mn per reaction center (reviewed by Amesz, 1983; Dismukes, 1986). Another question left unanswered was why the maximum inhibition by Mn^{2+} of DPC electron donation was only 50-70%. Given that DPC does not alter the DCIP photoreduction rate measured when the OEC is intact (H_2O donates electrons through the endogenous Mn) one would expect Mn^{2+} to reach 100%

inhibition. As mentioned before, Mn^{2+} can also donate electrons to PS II (at approximately half the DPC rate) although at high concentrations compared to the μM levels where inhibition of DPC donation is observed. Also, side reactions, including direct redox reactions between Mn^{2+}, DPC, DCIP and their corresponding oxidized or reduced species, could also be influencing the observed changes in rates. Finally, Hoganson et al. (1989) reported measurements of rates of Y_Z^+ reduction where Mn^{2+} binding appeared to be weaker at pH 6 than at pH 7.5, in contrast to the results of Hsu et al. (1987) described above.

Preston and Seibert (1991a; 1991b) have recently addressed many of the problems explained above by investigating the mechanism of Mn^{2+} inhibition of DPC-supported DCIP photoreduction further and proposing a more complete model of the interactions. The interaction between Mn^{2+} and DPC appeared to have different mechanisms at different DPC concentration ranges. At the "high" concentration used for Mn^{2+}/DPC competition assays, the mechanism was shown to be non-competitive, consistent with their results which had indicated different binding sites for Mn^{2+} and DPC (Preston and Seibert, 1991a). They also proposed a different mechanism in the "low DPC concentration range" where the electron donation from the two species seemed to be additive. Incorporating the evidence of electron donation by DPC to two different sites, probably Y_Z and Y_D (Blubaugh and Cheniae, 1990; Tamura et al., 1990), they proposed that Mn blocks access by DPC to only one of these, probably Y_Z. The second site of DPC electron donation was not well characterized and may also involve direct donation to P680 or donation to P680 through Cyt *b*-559. Also, they combined calculations with experimental results and explained why they believe that the side reactions explained above do not influence the initial rate of DCIP photoreduction measured in this assay. Finally, the photoactivation of Mn depleted preparations was proposed to require several sequential binding and oxidation steps (Tamura and Cheniae, 1987) and has been recently shown to require the binding of

only one Mn^{2+} and its oxidation to Mn^{3+} before the second Mn^{2+} ion can bind and be oxidized, which then allows the last two Mn^{2+} ions to bind (Miller and Brudvig, 1990). The Mn^{2+} competition of DPC photooxidation is proposed by Preston and Seibert (1991b) to measure four different "Mn-binding sites" (these may provide four ligands to anywhere from one to four Mn ions). In the same report, they provide measurements of Mn content which show 1.0 Mn bound per reaction center (photoactivation conditions) and 3.2 Mn bound per reaction center (Mn^{2+}/DPC assay conditions). This result is most consistent with the assignment of four high-affinity Mn-binding sites being measured by the Mn^{2+}/DPC assay and explains the difference in pH dependence reported by Hoganson et al. (1989), under whose photoactivation conditions only one Mn^{2+} is expected to bind.

Tamura et al. (1989a) showed the connections between photoligation of Mn as described in Chapter 7, chemical modification by DEPC, the involvement of histidine residues on the D1 protein (and possibly the D2 protein) and the Mn^{2+}/DPC competition assay developed by Hsu et al. (1987). They described the following results: 1) oxygen evolution activity of PS II membranes was not changed by DEPC treatment, but the capability to photoligate Mn to NH_2OH-treated PS II membranes (as measured by Mn quantitation) was lost after incubation with DEPC, 2) photoreduction of DCIP with either DPC or Mn^{2+} as the electron donor was reduced, but at a much slower rate than the loss of photoactivation activity, 3) the specific modification of histidine residues by DEPC was shown by the pH dependence with pK_a of 6.9 and the NH_2OH reversibility of the DEPC effect on photoactivation, 4) previously photoligated Mn inhibited the modification by DEPC, 5) treatment with DEPC greatly decreased Mn-binding affinity as shown by the Mn^{2+}/DPC photooxidation assay and also decreased the rate of photoactivation and 6) many PS II proteins were radioactively labeled by [^{14}C]-DEPC, but labeling of the D1 protein and the D1/D2 protein dimer were suppressed by photoligated Mn (involvement of the D2 protein was not confirmed due to heavy labeling in the corresponding region of the

gel). Of main importance to this section are the demonstration that DEPC modification alters the amount of Mn^{2+} inhibition of DPC electron donation as measured by DCIP photoreduction, that modification by DEPC is specific for histidine residues and labels the D1 protein (and possibly the D2 protein) and that DEPC treatment prevents the photoligation of Mn. Also, the authors speculated that possible residues involved in the DEPC modification (and, therefore, also Mn-binding) include: His-190 and/or His-337 on at least the D1 protein. They cannot, however, exclude His-92 and His-332 of the D1 protein as possible Mn ligands for which the symmetrical amino acids on the D2 protein are not histidines.

Seibert et al. (1989) proposed that the high-affinity Mn-binding site measured by the Mn^{2+} inhibition of DPC-stimulated DCIP photoreduction described by Hsu et al. (1987) can be divided into at least two different components. They showed that PS II-enriched membranes from the LF-1 mutant of *Scenedesmus obliquus* apparently contain half of the Mn-binding site measured for WT *Scenedesmus* preparations. Using DEPC (the histidine chemical modifier described above) they showed that half of the Mn-binding site of WT *Scenedesmus* (or spinach or wheat) preparations is blocked after modification. This component is not available in the LF-1 *Scenedesmus* preparation, as indicated by no change in Mn^{2+} inhibition after DEPC modification. They also showed that LF-1 membranes cannot be photoactivated, consistent with the requirement of the full high-affinity Mn-binding site for photoactivation described by Tamura et al. (1989b). Another important result was the demonstration that the full high-affinity Mn-binding site is present in the isolated reaction centers complex (D1/D2/Cyt *b*-559/4.2 kDa proteins), limiting the possible proteins which might provide these ligands to Mn. Finally, they too speculated on the possible residues responsible for the observed DEPC modification. They considered His-332 and His-337 of the D1 protein to be the primary candidates based on the proposed steric hindrance of this component of the Mn-binding site in the LF-1 mutant. They could

not eliminate His-92 of the D1 protein or possible involvement of the D2 protein, on which they proposed His-190 could also be considered.

Preston and Seibert (1989) regenerated the blocked component of the high-affinity Mn-binding site of membranes (but not thylakoids) from the LF-1 mutant of *Scenedesmus obliquus* by mild protease treatment with papain, subtilisin or carboxypeptidase A. They performed DEPC modification of the protease-treated LF-1 membranes for which they observed the same results as with WT *Scenedesmus* or spinach and concluded the native site had become accessible. Finally, they were unsuccessful in photoactivating the protease-treated membranes, indicating that the product was still unable to perform this function, probably because the protease cleavages were not identical to the processing which occurs upon insertion of the D1 protein into the thylakoid membrane. This observation is consistent with the indication that the -COOH group of Ala-344 of the C-terminus of the processed D1 protein provides a ligand to OEC Mn (B. Diner, Du Pont, Wilmington, DE, unpublished results), but it would be a ligand not detected by the Mn^{2+}/DPC assay.

In a preliminary report, Preston and Seibert (1990) proposed that the high-affinity Mn-binding site consists of four separately identifiable components, "corresponding to the four Mn required for functional O_2 evolution." They based this conclusion on studies using combinations of proteases and amino acid chemical modifiers to alter the amount of Mn^{2+} inhibition of DPC-stimulated DCIP photoreduction in the assay described by Hsu et al. (1987). The results of protease and amino acid chemical modifier studies, along with studies of the mechanism of the Mn^{2+}/DPC assay discussed above, were explored further by Preston and Seibert (1991a, 1991b). In Preston and Seibert (1991a), they used EDC (a carboxyl group modifier) and found that it blocks all of the high-affinity Mn-binding site available in the LF-1 mutant of *Scenedesmus obliquus* and half of the Mn site in spinach or WT *Scenedesmus*, the half insensitive to DEPC (the histidine modifier previously used).

Again, $MnCl_2$ (2 mM) provides complete protection from EDC modification, while six other divalent ions were ineffective. They also showed the EDC and DEPC effects to be mutually exclusive and specific to the lumenal side of the thylakoid membrane. An important result was that the removal of the two more loosely bound of the four OEC Mn by aging $CaCl_2$-treated membranes in low NaCl buffer (Ono and Inoue, 1985; Cole et al., 1987; Seibert et al., 1988) uncovers the EDC-sensitive half of the Mn site and not the DEPC-sensitive half of the site. This result is strong evidence that the Mn^{2+}/DPC assay is detecting ligands which correlate to at least two functional Mn and, possibly, all four.

In their most recent publication, Preston and Seibert (1991b) combined the amino acid chemical modifiers described above with protease treatments in order to better define the high-affinity Mn-binding site using the DPC/Mn^{2+} non-competitive inhibition assay for DCIP photoreduction (Preston and Seibert, 1991a). In Table 8-1, a summary of their results, which they used as proof in dividing the site into four independent components, is presented. Basically, their data indicate that the DEPC-sensitive and EDC-sensitive halves of the high-affinity site can each be divided into two components which demonstrate differential sensitivity to the proteases used (see Table 8-2 for interpretation of their results). The two DEPC-sensitive components (histidine residues) are most exposed to proteases, one of them removable by three of the enzymes used, and both accessible in the presence of the extrinsic polypeptides. The two EDC-sensitive components (carboxyl-containing residues) are more protected, neither of them being accessible when the 33 kDa protein is present, and one becoming available to one of the enzymes upon its removal while the other was not sensitive to any of the proteases used. They proposed the following as likely residues for the location of the DEPC-sensitive components of the high-affinity site: His-92, His-332 and His-337 on the D1 protein along with His-62, His-88 and His-337 on the D2 protein. The strongest possibilities for residues of the EDC-sensitive components are given as any carboxyl-containing residue on the C-terminal ends

Table 8-1

Combination of treatments with amino acid chemical modifiers and proteases in order to define the high-affinity Mn-binding site using the Mn^{2+}/DPC competition assay for DCIP photoreduction (Preston and Seibert, 1991a, 1991b and unpublished results). For a single sample, the rate of DCIP photoreduction in the presence of 10 μM $MnCl_2$ divided by the rate in the absence of $MnCl_2$ gives a fractional rate of DCIP photoreduction. As this number increases, the number of components of the Mn-binding site available to Mn^{2+} decreases. Loss of 0, 1, 2, 3 or 4 components would ideally correspond to fractional rates of 0.50, 0.625, 0.75, 0.875 and 1.00, respectively. Comparing data from simultaneous treatments (with amino acid chemical modifiers and proteases) against data from separate treatments allows for the identification of the amino acids involved (see Table 8-2).

Enzyme	Enz. only	Enzyme +DEPC	Enzyme +EDC
none	0.50	0.75	0.75
Carboxypeptidase A	0.63	0.75	0.87
Subtilisin	0.62	0.75	
CPase A + Subtilisin	0.76		
Trypsin (Tris-PS II)	0.77		0.87
Trypsin (NH_2OH-PS II)	0.63	0.75	
Staph. aureus V8 protease	0.63		0.88
CPase A + CPase B	0.75	0.75	

Table 8-2

Interpretation of data presented in Table 8-1. Comparing data from simultaneous treatments (with amino acid chemical modifiers and proteases) against data from separate treatments allows for the identification of the amino acids involved. Different protease or amino acid chemical modifier treatments affect various combinations of histidine and/or carboxyl-containing (Glu or Asp) residues. The high-affinity Mn-binding site as measured by the Mn^{2+}/DPC non-competitive assay can be divided in this way into four discrete components (Preston and Seibert, 1991b).

Enzyme or chem. modifier	Missing # of Components	Type of Residue
none	0	
DEPC	2	His, His
EDC	2	COOH, COOH
Carboxypeptidase A	1	His
Subtilisin	1	His
CPase A + Subtilisin	2	His, His
Trypsin (Tris-PS II)	2	His, COOH
Trypsin (NH_2OH-PS II)	1	His
Staph. aureus V8 protease	1	COOH
CPase A + CPase B	2	His, His

of the D1 and D2 proteins. Of all these, they proposed only His-337 of the D1 protein as being a prime candidate for a ligand of the Mn-binding site. Although they proposed the four components located by the Mn^{2+}/DPC assay to be sites involved in photoligation of Mn during photoactivation and/or binding the functional OEC Mn, they also provided some alternative explanations. These explanations include the possibility that protease and chemical modifier action at sites other than those directly ligating Mn could induce conformational changes and allosteric effects which could be mistaken as direct ligands to Mn. Also, they pointed out that the Mn^{2+}/DPC components may, in fact, be any of two to four terminal ligands to each of the four Mn and that there is no certainty as to the actual number of Mn detected (any number from one to four being possible).

Recently, Seibert has investigated the components of the high-affinity Mn-binding site using the DPC/Mn^{2+} non-competitive inhibition assay for DCIP photoreduction (Preston and Seibert, 1991a) on membrane preparations from site-specific mutants of amino acids on the D1 and D2 proteins provided to him by other investigators. One of these mutants in which His-337 of the D2 protein was replaced by tyrosine, has been characterized as still containing all four components of the Mn-binding site, but with an interesting decrease in affinity for the binding of Mn^{2+} (M. Seibert, SERI, Golden, CO, personal communication). This could be explained as a removal of a strong ligand to Mn (His) and its replacement with a residue acting as a ligand, but more weakly (Tyr). In this case, one ligand to Mn has been changed but Mn^{2+} is still able to bind, in contrast with amino acid chemical modification and protease treatment which seem to "remove" components of the Mn site as measured by a decrease in Mn^{2+} inhibition of DPC electron donation to PS II. The residue changed in the mutant, His-337 of the D2 protein, is also one of two possible histidine residues involved as a DEPC-sensitive component as shown by other recent experiments (M. Seibert, personal communication). The second histidine residue was removed by treatment with both carboxypeptidase A (which cleaves C-terminal

amino acids, stops at Arg residues and, by itself, removes only one histidine component) and carboxypeptidase B (which digests away C-terminal Arg residues, allowing CPase A to continue digesting past Arg residues). The combination of these two proteases removes a second DEPC-sensitive component of the Mn-binding site, being either His-337 of the D2 protein or His-332 of the D1 protein.

In summary, this is a complex assay, and as has been described above, there are many models and possible explanations consistent with the experimental data. The simplest model (M. Seibert, personal communication), however, which is consistent with all of the current data, is useful as a starting point for further predictions and experiments. The high-affinity Mn-binding site as measured by the Mn^{2+}/DPC non-competitive assay can be divided into four discrete components (Preston and Seibert, 1991b). Probably only one of these components corresponds to the first Mn-binding site detected during photoactivation (see Chapter 7). Of these four components, two are histidine and the other two carboxyl-containing (Glu or Asp) residues. These amino acid residues are proposed to be four (of 12-16 total) terminal ligands to one, two, three or four Mn ions functional in the OEC of PS II. Each of these four components has the same binding affinity (K_D of 0.3-0.4 μM) and, modification or removal of any number of components does not alter the binding affinity of the remaining components (M. Seibert, personal communication). If one modifies or removes one ligand to a specific Mn, a decrease in affinity would be expected for binding of Mn to any other of its terminal ligands (as was observed with the mutant in which His-337 of the D2 protein was replaced by tyrosine, see above) because binding affinity is an additive phenomenon. This information from binding affinities, in combination with Mn quantitation studies and the appearance of two components upon aging and loss of two Mn, is most consistent with the explanation of the four components as ligands to four separate Mn ions.

In this chapter, the use of antibodies raised against the peptides corresponding to the two overlapping segments of the carboxyl end of the D1 protein and one against the C-terminus of the D2 protein to test whether there is any effect of these antibodies on the four components of the high-affinity Mn-binding site as measured by the Mn^{2+}/DPC non-competitive assay (Preston and Seibert, 1991b) are explained. The experiments described in this chapter were done in collaboration with Christopher Preston and Michael Seibert of the Photoconversion Research Branch, Solar Energy Research Institute, Golden, CO and have been submitted for publication (Dalmasso et al., 1992). Only one of the three antibodies produced (anti-D1-a) had any effect on the Mn-binding site, an effect consistent with the rendering of one of the four components of the Mn-binding site inaccessible to Mn^{2+}. This component was shown to be one of the two DEPC-sensitive (histidine) residues. The other two antibodies (anti-D1-b and anti-D2-a) and pre-immune serum from all three rabbits had no effect on the assay. These results, in combination with western blotting analysis (Chapter 4) and solution binding assays (Chapter 6), decrease the likelihood of the corresponding regions of peptides D1-b and D2-a as involved in Mn ligation and are most consistent with the proposal that His-337 on the D1 protein is a ligand in one of the high-affinity Mn-binding sites of PS II as described by Preston and Seibert (1991b).

Procedures

PS II membrane preparation

PS II membrane fragments were prepared from spinach leaves essentially as described by Berthold, et al. (1981), but including modifications from Ford and Evans (1983), Rutherford et al. (1984) and Dr. J.-L. Zimmermann (Service Biophysique, CEN-Saclay, France). The details of this preparation are presented in Chapter 4.

Tris treatment of PS II membranes

Spinach PS II membranes were Mn-depleted by Tris-treatment as described in Chapter 4. This treatment, which is harsher than that presented in Chapter 7, was shown to be occasionally necessary for complete removal of Mn from spinach PS II membranes as measured by the Mn^{2+}/DPC assay (Preston and Seibert, 1991a).

Antibody incubations

PS II membranes were incubated with antibody or with the appropriate pre-immune serum on ice at about 1 mg Chl/ml for 4 h. To a sample of 300 µg Chl, 100 µl of either Buffer A, antibody or pre-immune serum was added. Samples were assayed for DPC-supported DCIP photoreduction immediately upon completion of the incubation without removing excess antibody.

DEPC modification

Histidine residues were modified with DEPC as described by Tamura et al. (1989a) prior to exposure to the antibodies. In addition to histidine, DEPC can, under various conditions, also modify cysteine, tyrosine, lysine, serine, arginine and the alpha-amino group of amino acids (Miles, 1977). Tamura et al. (1989a) concluded that under their conditions, which were reproduced here, DEPC specifically modifies histidine residues. They showed this by studying the pH dependence of reaction, chemical reversal using NH_2OH, rates of inactivation and examining the labeling of control extrinsic proteins. Spinach PS II membranes were incubated at 100 µg Chl/ml with 500 µM DEPC (from 100 mM stock dissolved in ethanol) in SMN Buffer (0.4 M sucrose, 50 mM MES-NaOH pH 6.5, 20 mM NaOH) for 60 min at 20°C in the dark. The reaction was stopped by addition of a 5-fold volume of 4°C 10 mM histidine in SMN Buffer and pelleted by centrifugation (30,000 x g, 10 min). The pellet was resuspended in the previous final volume of SMN

Buffer and washed twice. The final pellet was resuspended in 1/10 the original incubation volume of SMN Buffer. Untreated controls were incubated and washed under the same conditions, but without DEPC, in parallel with the treated samples.

High-affinity manganese assays

DPC-stimulated DCIP photoreduction was measured using an Aminco DW2a spectrophotometer in the splitbeam mode as described by Preston and Seibert (1991a). Samples consisted of 5 μg Chl/ml in buffer containing 0.4 M sucrose, 50 mM MES-NaOH (pH 6.5), 20 mM NaCl, 200 μM DPC and 30 μM DCIP and the indicated amounts of $MnCl_2$ added from 100 μM or 5 mM stocks prepared in assay buffer. Continuous, saturating red light was passed through a heat filter (Melles Griot 03MHG007) and a 630 nm cut-off filter (Schott RG630) and focused on the sample cuvette at a 90° angle to the spectrophotometer beam. DCIP reduction was monitored at 600 nm with the photomultiplier protected from the sample illumination light by a 600 nm narrow bandpass filter (Melles Griot 03FIV045). The pathlength was 1 cm and an extinction coefficient of 13 per mM per cm (Armstrong, 1964) was used to calculate the rates of DCIP photoreduction from the initial slope of quenching of absorption after providing light..

Results and Discussion

The high-affinity Mn-binding assay was first published by Hsu et al. (1987) and its Mn^{2+}/DPC non-competitive mechanism was later described by Preston and Seibert (1991a). This assay was used here to determine the effects of the three antibodies to the carboxyl ends of the D1 and D2 proteins (see Chapter 3) on the components of the high-affinity Mn-binding site of PS II. The amino acid chemical modifier DEPC shown by Tamura et al. (1989a) to specifically modify histidine residues was used later in conjunction

with the antibodies in order to define which of the four components of the high-affinity Mn-binding site described by Preston and Seibert (1991b) was altered by interaction with antibody.

Figure 8-1 shows the profile of a typical assay for $MnCl_2$ inhibition of DPC-stimulated DCIP photoreduction using Tris-treated PS II membranes. The PS II membranes for the experiments described in this chapter were Tris-treated as previously described in order to remove all the functional OEC Mn. Along with removal of the intrinsic Mn, the 17, 24 and 33 kDa extrinsic polypeptides of PS II are also removed by Tris treatment. The maximum rates of DCIP photoreduction for these preparations with no added $MnCl_2$ were generally 300-500 μmoles DCIP reduced/mg Chl per h. Under the conditions used in these experiments (0.4 M sucrose, 50 mM MES-NaOH pH 6.5, 20 mM NaCl, 200 μM DPC and 30 μM DCIP), $MnCl_2$ inhibits DPC to DCIP photoreduction by about 50% (usually to within 2%). This corresponds to a fractional rate of 0.50 as explained in Table 8-1. Maximum inhibition is seen between 2 and 5 μM $MnCl_2$ with no further inhibition occurring at higher concentrations of $MnCl_2$ up to 100 μM (at this high $MnCl_2$ concentration, a slight increase in rate is routinely observed, possibly due to electron donation from Mn^{2+}). The average binding affinity of Mn^{2+} to the components of the high-affinity Mn-binding site present in a given assay can be estimated as the $MnCl_2$ concentration required to induce half of the maximum amount of inhibition (Tamura et al., 1989a). In the assay shown in Figure 8-1, the half-inhibition occurs at approximately 0.25 μM $MnCl_2$. This value is consistent with previously published values (estimated from this type of assay) which range from 0.15 μM to 0.40 μM (Hsu et al., 1987; Tamura et al., 1989b; Seibert et al., 1989).

Incubation of PS II membranes with serum containing antibodies to the carboxyl-terminal end of the D1 protein (anti-D1-a) for 4 h resulted in one of the four components of the high-affinity Mn-binding site becoming unavailable for Mn^{2+} binding. This can be

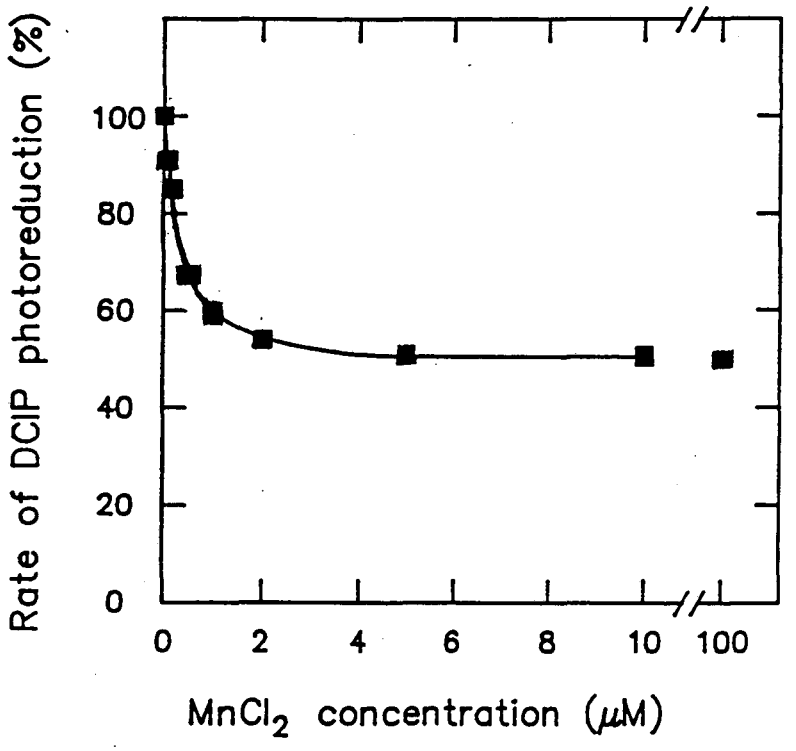

Figure 8-1: Example of Mn^{2+}/DPC assay using Tris-treated PS II membranes

Profile of a typical assay for $MnCl_2$ inhibition of DPC-stimulated DCIP photoreduction using Tris-treated PS II membranes. The rate of DCIP photoreduction at a given $MnCl_2$ concentration relative to the control rate with no $MnCl_2$ is plotted against the $MnCl_2$ concentration. The maximum rates of DCIP photoreduction for these preparations with no added $MnCl_2$ were generally 300-500 μmoles DCIP reduced/mg Chl per h. Maximum inhibition of 50% is seen between 2 and 5 μM $MnCl_2$ with no further inhibition occurring at higher concentrations of $MnCl_2$ up to 100 μM.

seen as a reduction of the maximum $MnCl_2$ inhibition of DPC to DCIP activity from 50% to 37% (Figure 8-2). This can also be expressed as a change in fractional rate from 0.50 to 0.63 as explained in Table 8-1. In contrast, incubation for the same period of time with the pre-immune serum from the same rabbit did not alter the number of binding sites available (a maximum of 50% inhibition is still measured). The maximum inhibition is shown on the right side of this and subsequent figures, divided into a scale of four components, labeled to indicate the number of high-affinity Mn-binding components detectable in the sample as described by Preston and Seibert (1991b). The control PS II membranes used in this experiment had been incubated on ice in Buffer A for 4 h and show the same results as the incubation with pre-immune serum with all four components present. Increasing the incubation time for either the anti-D1-a serum or the pre-immune serum to 16 h did not alter the results (data not shown). Note that the half-inhibition occurs at approximately the same Mn^{2+} concentration for all three treatments, consistent with anti-D1-a affecting one component from each reaction center as opposed to totally inhibiting 1/4 of all the centers.

Incubation of PS II membranes with the other antibodies (anti-D1-b or anti-D2-a), did not affect the number of high-affinity Mn-binding sites present (Figures 8-3 and 8-4). Their pre-immune serums likewise had no-effect. These results were not changed by increasing the incubation time to 16 h (data not shown). Although the actual binding sites for these two antibodies are not well characterized, they have been shown to bind to Tris-treated PS II membranes in solution binding assays (see Chapter 6). Combining the solution binding data with the lack of effect on the Mn^{2+}/DPC assay decreases, but does not eliminate, the likelihood that these regions of the D1 and D2 proteins are involved in providing ligands for high-affinity Mn.

It has been previously suggested that the carboxyl end of the D1 protein contains one of the two DEPC-sensitive components of the high-affinity Mn-binding site that are presumably histidine residues (Preston and Seibert 1991b). To determine whether the

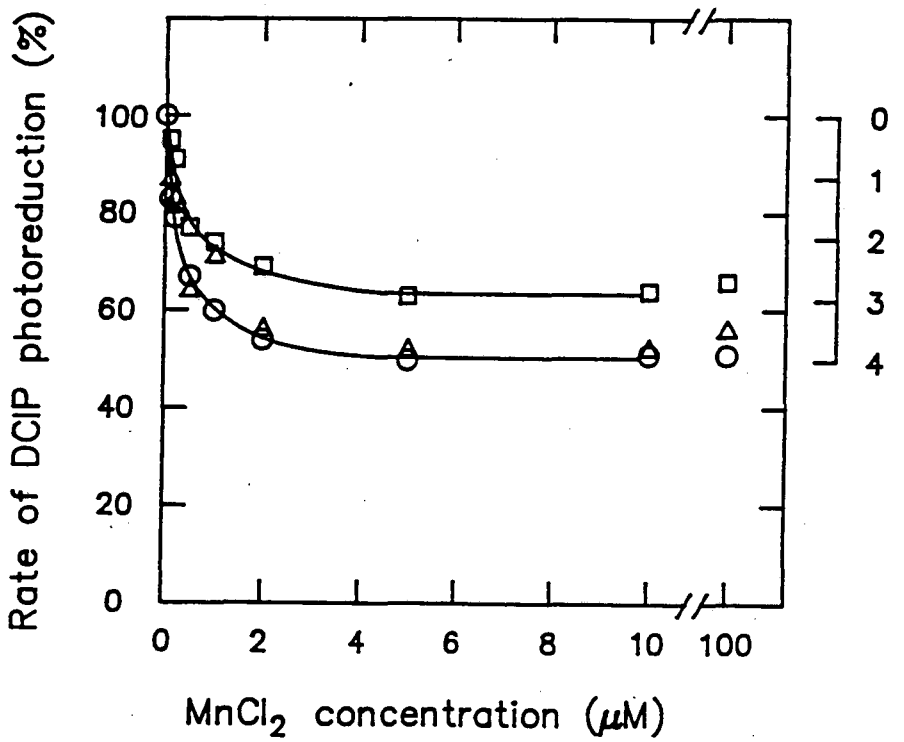

Figure 8-2: Results of Mn^{2+}/DPC assay using Tris-treated PS II membranes and anti-D1-a

Inhibition of one component of the high-affinity Mn-binding site in PS II in the presence of anti-D1-a. Tris-treated PS II membranes were incubated for 4 h with SMN Buffer (O), anti-D1-a (□) or pre-immune serum (Δ). 100% activities were 449, 379 and 451 μmoles DCIP reduced/mg Chl per h for SMN Buffer, anti-D1-a and pre-immune serum treatments, respectively. The maximum inhibition is shown on the right side of this and subsequent figures, divided into a scale of four components, labeled to indicate the number of high-affinity Mn-binding components detectable in the sample as described by Preston and Seibert (1991b).

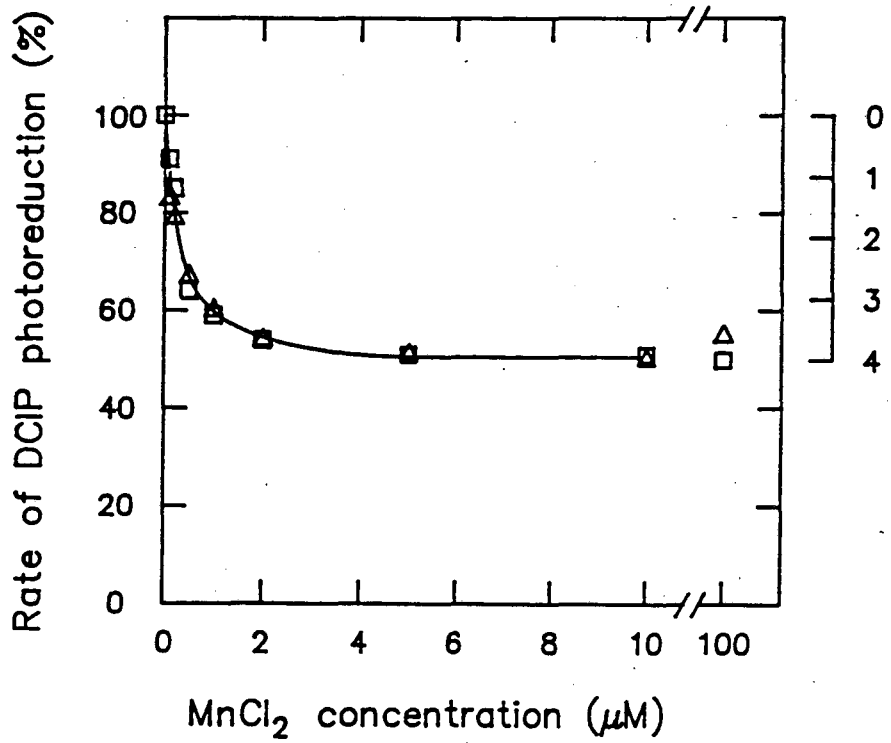

Figure 8-3: Results of Mn^{2+}/DPC assay using Tris-treated PS II membranes and anti-D1-b

Lack of inhibition of the high-affinity Mn-binding site in PS II in the presence of anti-D1-b. Tris-treated PS II membranes were incubated for 4 h with the anti-D1-b (□) or pre-immune serum (Δ). 100% activities were 469 and 538 μmoles DCIP reduced/mg Chl per h for the anti-D1-b and pre-immune serum treatments, respectively. The maximum inhibition is shown on the right side, divided to show the number of high-affinity Mn-binding components detectable in the sample, as described in Figure 8-2.

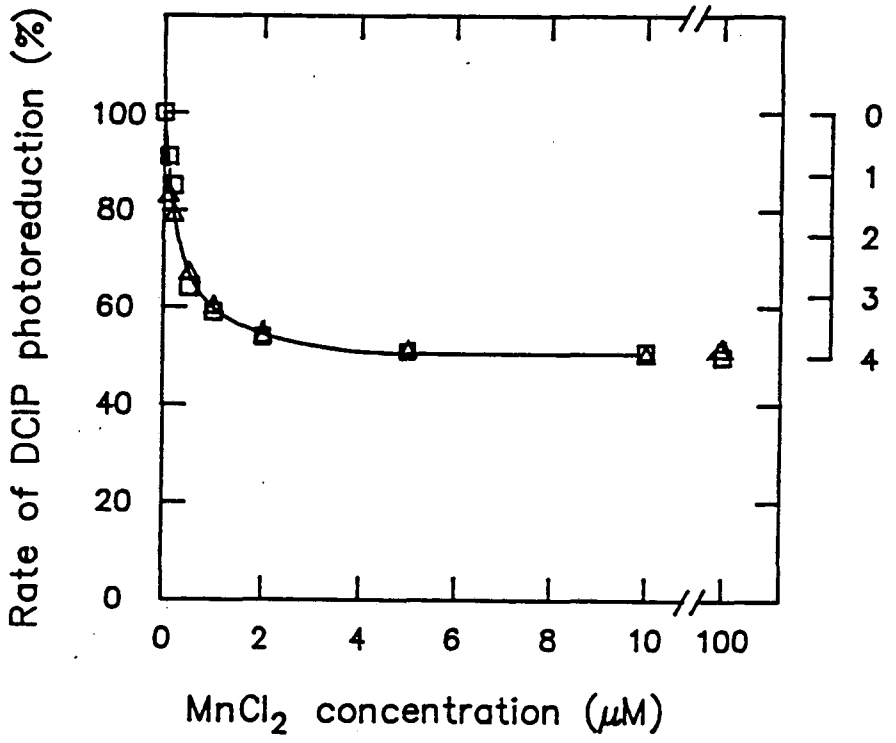

Figure 8-4: Results of Mn^{2+}/DPC assay using Tris-treated PS II membranes and anti-D2-a

Lack of inhibition of the high-affinity Mn-binding site in PS II in the presence of anti-D2-a. Tris-treated PS II membranes were incubated for 4 h with the anti-D2-a (□) or pre-immune serum (Δ). 100% activities were 385 and 416 μmoles DCIP reduced/mg Chl per h for the anti-D2-a and pre-immune serum treatments, respectively. The maximum inhibition is shown on the right side, divided to show the number of high-affinity Mn-binding components detectable in the sample, as described in Figure 8-2.

component of the high-affinity Mn-binding site affected by anti-D1-a was this component, Tris-treated PS II membranes were first modified with DEPC and then incubated with the serum. Modification of PS II membranes with DEPC affected two components as shown by reduction of $MnCl_2$ inhibition of DPC to DCIP activity from 50% to 25% (Figure 8-5). This can also be expressed as a change in fractional rate from 0.50 to 0.75 as explained in Table 8-3 (see Table 8-3 for summary of results). This result contrasts to only one component being affected by anti-D1-a serum as discussed above (in this set of experiments, all control samples were treated as in the DEPC procedures, but in the absence of DEPC, in order to control for any artifacts during the incubations or washes as described in the procedures section). Incubation of DEPC-treated PS II membranes with anti-D1-a serum failed to further decrease the $MnCl_2$ inhibition of DPC to DCIP activity. It has been previously shown that the four components of the high-affinity Mn-binding site affect the Mn-binding assay in a discrete manner (Preston and Seibert 1991b). Therefore, from the results shown in Figure 8-5, one can conclude that the component of the high-affinity Mn-binding site affected by anti-D1-a is one of the two blocked by modification of histidine residues by DEPC (see Table 8-4 for interpretation of these results). These data, in combination with solution binding assay (Chapter 6) and western blotting assay results (Chapter 4), is further evidence that a DEPC-sensitive component of the high-affinity Mn-binding site is located on the carboxyl end of the D1 protein. This histidine would be located on the portion of D1-a which does not overlap with D1-b, making His-337 of the D1 protein a prime candidate for providing a ligand to high-affinity Mn.

In Figure 8-6, a schematic diagram of the reaction center core proteins, D1 and D2, is shown with the results of this chapter graphically depicted and combined with information from western blotting assays (Chapter 4) and solution binding assays (Chapter 6). The topology of the proteins in the membrane was adapted from that proposed by Trebst (1986) and later verified by Sayre et al. (1986), as described earlier. This folding

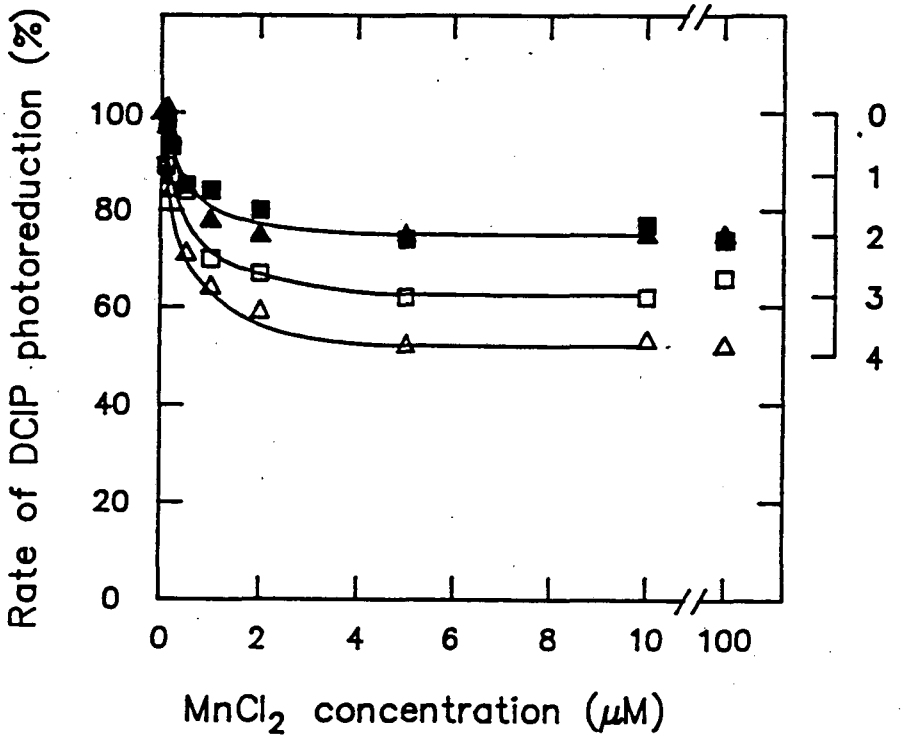

Figure 8-5: Results of Mn^{2+}/DPC assay using Tris-treated PS II membranes, anti-D1-a and DEPC-modification

Anti-D1-a inhibits a DEPC-sensitive, high-affinity Mn-binding site. Tris-treated PS II membranes were incubated for 4 h with anti-D1-a (□, ■) or pre-immune serum (Δ, ▲). Open symbols are control samples and closed symbols are samples modified with 500 μM DEPC prior to incubation with the antibodies. 100% activities were 332, 222, 403 and 216 μmoles DCIP reduced/mg Chl per h for the anti-D1-a, DEPC then anti-D1-a, pre-immune serum and DEPC then pre-immune serum treatments, respectively. The maximum inhibition is shown on the right side, divided to show the number of high-affinity Mn-binding components detectable in the sample, as described in Figure 8-2.

Table 8-3

Use of the Mn^{2+}/DPC competition assay for DCIP photoreduction and a combination of treatments with anti-D1-a, anti-D1-b or anti-D2-a sera and DEPC. Complete Mn^{2+}/DPC competition assays are shown in Figures 8-2 through 8-5. For a single sample, the rate of DCIP photoreduction in the presence of 10 μM $MnCl_2$ divided by the rate in the absence of $MnCl_2$ gives a fractional rate of DCIP photoreduction. As this number increases, the number of components of the Mn-binding site available to Mn^{2+} decreases. Loss of 0, 1, 2, 3 or 4 components would ideally correspond to fractional rates of 0.50, 0.625, 0.75, 0.875 and 1.00, respectively. Comparing data from simultaneous treatments (with antisera and DEPC) against data from separate treatments allows for the identification of the amino acids involved (see Table 8-4).

Spinach PS II + Antibody	No chemical treatment	+ DEPC
None*	0.50	0.75
anti-D1-a	0.63	0.75
anti-D1-b	0.50	
anti-D2-a	0.50	

*Approximately the same for all corresponding control incubations (with pre-immune serum or Buffer A)

Table 8-4

Interpretation of data presented in Table 8-3. Comparing data from simultaneous treatment (with antisera and DEPC) against data from separate treatments allows for the identification of the amino acids involved. Modification of PS II membranes with DEPC affects two histidine components as shown by a change in fractional rates of $MnCl_2$ inhibition of DPC to DCIP activity from 0.50 to 0.75. This result contrasts to only one component being affected by anti-D1-a serum as shown by a change in fractional rates from 0.50 to 0.63. Incubation of DEPC-treated PS II membranes with anti-D1-a serum failed to further decrease the $MnCl_2$ inhibition of DPC to DCIP activity. Therefore it can be concluded that the component of the high-affinity Mn-binding site affected by anti-D1-a is one of the two blocked by modification of histidine residues by DEPC.

Preparation and Treatment	Missing # of Components	Type of Residue
Tris-PS II	0	none
+ DEPC	2	His, His
+ anti-D1-a	1	His*
+ anti-D1-a and DEPC	2	His, His

*Concluded from sequential treatment with both DEPC and anti-D1-a giving the same result as treatment with DEPC alone.

Figure 8-6: Diagram of D1 and D2 showing results of Mn^{2+}/DPC assay combined with previous results

Diagrammatic representation of the five transmembrane helix models showing the results of this chapter combined with information from western blotting assays (Chapter 4) and solution binding assays (Chapter 6). The topology of the proteins in the membrane was adapted from that proposed by Trebst (1986) and later verified by Sayre et al. (1986), as explained earlier. As described in Figure 2-5, only lumenal histidine and carboxyl-containing amino acids (aspartic and glutamic acids) are shown, with the position number of histidines labeled explicitly. The two regions corresponding to the D1-b and D2-a peptides appear to not contain any of the components of the high-affinity Mn-binding site and are therefore shaded. The region of the D1-a peptide which does not overlap with the D1-b peptide contains one of the four components detected by the Mn^{2+} competition for DPC-stimulated DCIP photoreduction assay and is circled.

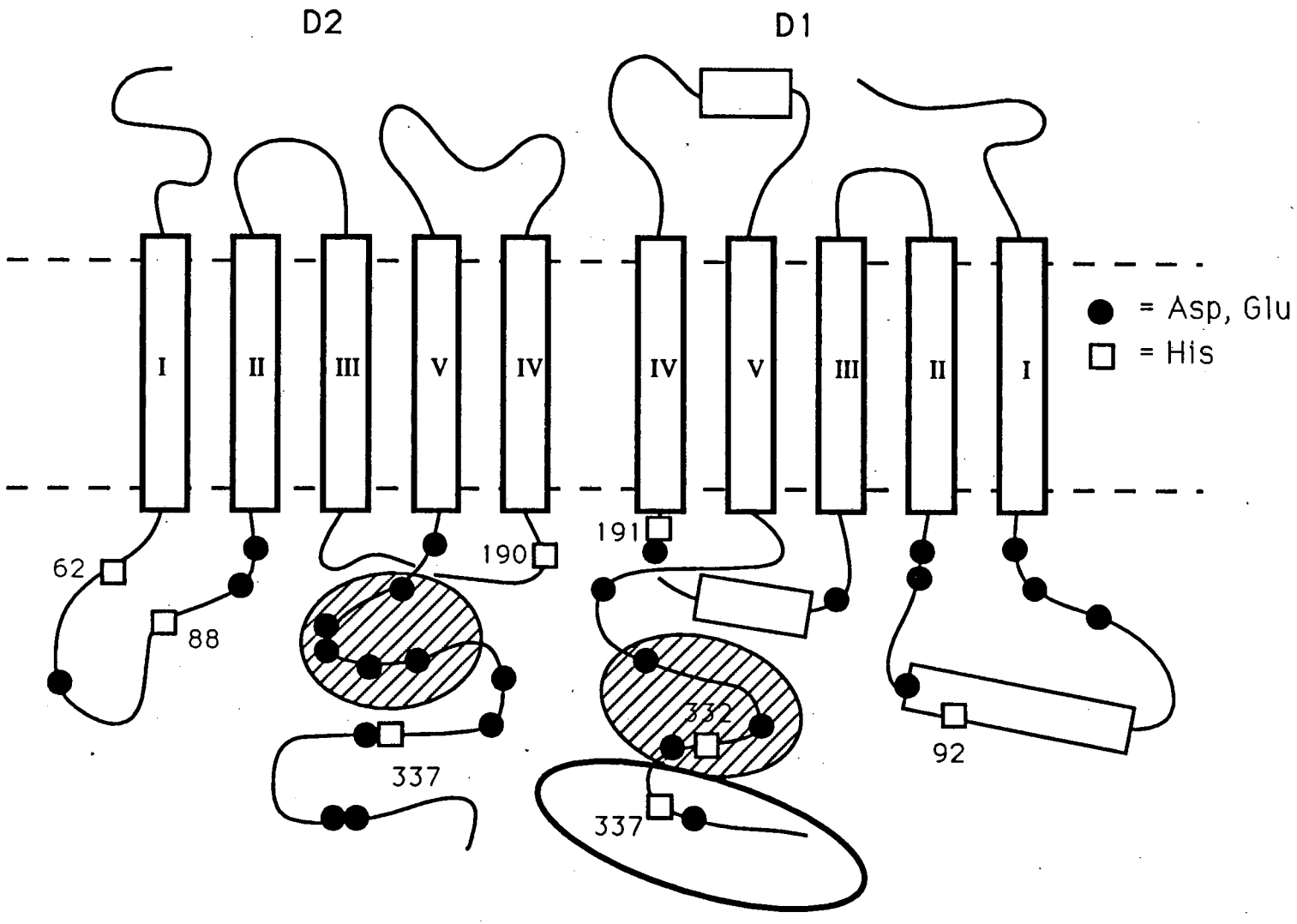
D2
D1
I
II
III
V
IV
IV
V
III
II
I
= Asp, Glu
= His
62
88
190
191
337
332
337
92

model is described in more detail in the first 2 chapters. To summarize, the two regions corresponding to the D1-b and D2-a peptides appear to not contain any of the components of the high-affinity Mn-binding site detected by the assay of Mn^{2+} competition for DPC-stimulated DCIP photoreduction and are therefore shaded in Figure 8-6. The region of the D1-a peptide which does not overlap with the D1-b peptide contains one of the four components detected by the Mn^{2+} competition for DPC-stimulated DCIP photoreduction assay and is circled in Figure 8-6. Because of the results of the study which combined incubation with anti-D1-a and modification with DEPC, it is quite probable that His-337 of the D1 protein provides the Mn ligand which is detected by the Mn^{2+}/DPC competition assay.

Appendix 1: List of Abbreviations

ATP	adenosine triphosphate
BCIP	5-bromo-4-chloro-3-indolyl phosphate
BSA	bovine serum albumin
Chl	chlorophyll
CPase A	carboxypeptidase A
CPase B	carboxypeptidase B
Cyt	cytochrome
D	Tyr-160 of the D2 protein (D^+ is the source of EPR signal II)
D1	32 kDa (herbicide-binding) PS II reaction center protein
D2	34 kDa PS II reaction center protein
DCBQ	2,6-dichloro-*p*-benzoquinone
DCIP	2,6-dichlorophenol indophenol
DEPC	diethylpyrocarbonate
DMSO	dimethyl sulfoxide
DPC	diphenylcarbazide
DTT	dithiothreitol
EDTA	ethylenediaminetetraacetic acid
ELISA	enzyme-linked immuno-sorbent assay
EPR	electron paramagnetic resonance

ESEEM	electron spin echo envelope modulation
EXAFS	extended X-ray absorption fine structure
FAB	fast atom bombardment
Fab	binding fragment of IgG
Fc	constant fragment of IgG
Hepes	4-(2-hydroxyethyl)-1-piperazineethanesulfonic acid
HPLC	high performance liquid chromatography
kDa	kilodaltons
MES	4-morpholineethanesulfonic acid
$NADP^+$	nicotinamide-adenine dinucleotide phosphate, oxidized form
NADPH	nicotinamide-adenine dinucleotide phosphate, reduced form
NBT	nitroblue tetrazolium
OEC	oxygen-evolving complex
P680	PS II reaction center chlorophyll *a* complex (primary electron donor in PS II)
PAGE	polyacrylamide gel electrphoresis
PBS	phosphate buffered saline
PPD	purified protein derivative of tuberculin bacillus
PS I	photosystem I
PS II	photosystem II
SDS	sodium dodecyl sulfate

SMN	0.4 M sucrose, 20 mM MES-NaOH pH 6.5, 15 mM NaCl, 10 mM $MgCl_2$
SMNC	0.4 M sucrose, 50 mM MES-NaOH pH 6.5, 50 mM NaCl, 50 mM $CaCl_2$
TFA	trifluoroacetic acid
TPB	tetraphenylboron
Tris	tris(hydroxymethyl)aminomethane
Tween-20	polyoxyethylenesorbitan monolaurate
XANES	X-ray absorption near-edge structure
XAS	X-ray absorption spectroscopy
Y_D	Tyr-160 of the D2 protein (same as D)
Y_Z	Tyr-161 of the D1 protein (same as Z)
Z	Tyr-161 of the D1 protein (intermediate electron donor between the OEC Mn and P680)

Appendix 2: List of Amino Acid 3 and 1 Letter Codes

Alanine	Ala	A
Arginine	Arg	R
Asparagine	Asn	N
Aspartic acid	Asp	D
Cysteine	Cys	C
Glutamine	Gln	Q
Glutamic acid	Glu	E
Glycine	Gly	G
Histidine	His	H
Isoleucine	Ile	I
Leucine	Leu	L
Lysine	Lys	K
Methionine	Met	M
Phenylalanine	Phe	F
Proline	Pro	P
Serine	Ser	S
Threonine	Thr	T
Tryptophan	Trp	W
Tyrosine	Tyr	Y
Valine	Val	V

Appendix 3: List of Figures

		page
Fig. 1-1:	Photosynthetic Z-scheme	3
Fig. 1-2:	Schematic of PS II proteins	7
Fig. 1-3:	S-state scheme	15
Fig. 2-1:	Folding pattern of the D1 and D2 proteins	34
Fig. 2-2:	Sequence comparison of D1 to L subunit	36
Fig. 2-3:	Sequence comparison of D2 to M subunit	38
Fig. 2-4:	Diagram of D1 and D2 with all possible Mn ligands labeled	42
Fig. 2-5:	Diagram of D1 and D2 showing regions to be synthesized	45
Fig. 2-6:	Sequences of peptides synthesized	50
Fig. 2-7:	Diagram of D1 and D2 showing synthesized peptide regions	52
Fig. 2-8:	Possible peptide fragmentation patterns	62
Fig. 4-1:	PAGE of various PS II preparations	74
Fig. 4-2:	Western blot of gel in Fig. 4-1 using anti-D1-a	80
Fig. 4-3:	Darker exposure of western blot of gel in Fig. 4-1 using anti-D1-a	82
Fig. 4-4:	PAGE examples of the best resolution for the D1 and D2 proteins	86

Fig. 4-5:	Western blots using enzymatic detection	90
Fig. 4-6:	Western blots of PS II and carboxypeptidase A-treated PS II preparations	93
Fig. 8-1:	Example of Mn^{2+}/DPC assay using Tris-treated PS II membranes	164
Fig. 8-2:	Results of Mn^{2+}/DPC assay using Tris-treated PS II membranes and anti-D1-a	166
Fig. 8-3:	Results of Mn^{2+}/DPC assay using Tris-treated PS II membranes and anti-D1-b	167
Fig. 8-4:	Results of Mn^{2+}/DPC assay using Tris-treated PS II membranes and anti-D2-a	168
Fig. 8-5:	Results of Mn^{2+}/DPC assay using Tris-treated PS II membranes, anti-D1-a and DEPC-modification	170
Fig. 8-6:	Diagram of D1 and D2 showing results of Mn^{2+}/DPC assay combined with previous results	173

REFERENCES

Åkerlund, H.-E., Jansson, C. and Andersson, B. (1982) *Biochim. Biophys. Acta* 681, 1-10.

Alt, J., Morris, J., Westhoff, P. and Herrmann, R. (1984) *Curr. Genet.* 8, 597-606.

Amesz, J. (1983) *Biochim. Biophys. Acta* 726, 1-12.

Armstrong, J. McD. (1964) *Biochim. Biophys. Acta* 86, 194-197.

Arnon, D. I. (1949) *Plant Physiol.* 24, 1-15.

Babcock, G. T. (1987) in *New Comprehensive Biochemistry, Vol. 15, Photosynthesis* (Amesz, J., ed.) pp. 125-158, Elsevier, Amsterdam.

Berthold, D. A., Babcock, G. T. and Yocum, C. F. (1981) *FEBS Lett.* 134, 231-234.

Blankenship, R. E., Babcock, G. T. and Sauer, K. (1975) *Biochim. Biophys. Acta* 387, 165-175.

Blankenship, R. E. and Prince, R. C. (1985) *Trends Biol. Sci.* 10, 383.

Blubaugh, D. J. and Cheniae, G. (1990) *Biochemistry* 29, 5109-5118.

Brudvig, G. W., Beck, W. F. and de Paula, J. C. (1989) *Annu. Rev. Biophys. Biophys. Chem* 18, 25-46.

Chapman, D. J., Gounaris, K. and Barber, J. (1988) *Biochim. Biophys. Acta* 933, 423-431.

Critchley, C., Baianu, I. C., Govindjee and Gutowsky, H. S. (1982) *Biochim. Biophys. Acta* 682, 436-445.

Cole, J. L., Yachandra, V. K., McDermott, A. E., Guiles, R. D., Britt, R. D., Dexheimer, S. L., Sauer, K. and Klein, M. P. (1987) *Biochemistry* 26, 5967-5973.

Cooper, S. R., Dismukes, G. C., Klein, M. P. and Calvin, M. C. (1978) *J. Amer. Chem. Soc.* 100, 7248-7252.

Dalmasso, E. A., Preston, C., Sauer, K., Hearst, J. E. and Seibert, M., (1992) *Biochim. Biophys. Acta* (submitted).

Debus, R. J., Barry, B. A., Babcock, G. T. and McIntosh, L. (1988a) *Proc. Natl. Acad. Sci. USA* 85, 427-430.

Debus, R. J., Barry, B. A., Sithole, I., Babcock, G. T. and McIntosh, L. (1988b) *Biochemistry* 27, 9071-9074.

Deisenhofer, J., Epp, O., Miki, K., Huber, R. and Michel, H. (1984) *J. Biol. Chem.* 259, 3900-3908.

Deisenhofer, J., Epp, O., Miki, K., Huber, R. and Michel, H. (1985) *J. Mol. Biol.* 180, 385-398.

Dekker, J. P., van Gorkom, H. J., Brok, M. and Ouwehand, L. (1984) *Biochim. Biophys. Acta* 764, 301-309.

DeRose, V. J. (1990) *Ph.D Thesis, Lawrence Berkeley Laboratory, University of California, Berkeley*, Lawrence Berkeley Laboratory Report LBL-30077.

DeRose, V. J., Yachandra, V. K., McDermott, A. E., Britt, R. D., Sauer, K. and Klein, M. P. (1991) *Biochemistry* 30, 1335-1341.

Diner, B. A., Ries, D. F., Cohen, B. N. and Metz, J. G. (1988) *Nature* 318, 618-624.

Dismukes, G. C. (1986) *Photochem. Photobiol.* 43, 99-115.

Dismukes, G. C. (1988) *Chemica Scripta* 28A, 99-104.

Dismukes, G. C. and Siderer, Y. (1981) *Proc. Natl. Acad. Sci. USA* 78, 274-278.

Edelman, M. and Reisfeld, A. (1978) in *Chloroplast Development* (Akoyunoglou, G. and Argyroudi-Akoyunoglou, J. H., eds.) pp. 641-652, Elsevier Biomedical Press, Amsterdam.

Erickson, J. M., Rahire, M., Malnoë, P., Girard-Bascou, J., Pierre, Y., Bennoun, P. and Rochaix, J.-D. (1986) *EMBO J.* 5, 1745-1754.

Evelo, R. G., Styring, S., Rutherford, A. W. and Hoff. A. J. (1989) *Biochim. Biophys. Acta* 973, 428-442.

Ford, R. C. and Evans, M. C. W. (1983) *FEBS Lett.* 160, 159-164.

Frank, H. A., Hansson, Ö. and Mathis, P. (1989) *Photosynth. Res.* 20, 279-289.

Fukuhara, Y., Ise, Y. and Kakinuma, K. (1988) *FEBS Lett.* 229, 150-156.

Ghanotakis, D. F., Babcock, G. T. and Yocum, C. F. (1984a) *Biochim. Biophys. Acta* 765, 388-398.

Ghanotakis, D. F., Babcock, G. T. and Yocum, C. F. (1984b) *FEBS Lett.* 167, 127-130.

Ghanotakis, D. F., de Paula, J. C., Demetriou, D. M., Bowlby, N. R., Petersen, J., Babcock, G. T. and Yocum, C. F. (1989) *Biochim. Biophys. Acta* 974, 44-53.

Gingrich, J. C., Buzby, J. S., Stirewalt, V. L. and Bryant, D. A. (1988) *Photosynth. Res.* 16, 83-99.

Gingrich, J. C., Gasparich, G. E., Sauer, K. and Bryant, D. A. (1990) *Photosynth. Res.* 24, 137-150.

Goodin, D. B., Yachandra, V. K., Britt, R. D., Sauer, K. and Klein, M. P. (1984) *Biochim. Biophys. Acta* 767, 209-216.

Greenberg, B. M., Gaba, V., Mattoo, A. K. and Edelman, M. (1987) *EMBO J.* 6, 2865-2869.

Guengerich, F. P., Wang, P. and Mason, P. S. (1981) *Biochemistry* 20, 2379-2385.

Guiles, R. D., Yachandra, V. K., McDermott, A. E., Cole, J. L., Dexheimer, S. L., Britt, R. D., Sauer, K. and Klein, M. P. (1990a) *Biochemistry* 29, 486-496.

Guiles, R. D., Zimmermann, J.-L., McDermott, A. E., Yachandra, V. K., Cole, J. L., Dexheimer, S. L., Britt, R. D., Weighardt, K., Bossek, U., Sauer, K. and Klein, M. P. (1990b) *Biochemistry* 29, 471-485.

Hansson, Ö., Andréasson, L.-E. and Vänngård, T. (1986) *FEBS Lett.* 195, 151-154.

Hearst, J. E. (1986) in *Encyclopedia of Plant Physiology, New Series, Vol. 19, Photosynthesis II* (Staehlin, L. A. and Arntzen, C. J., eds.) pp. 382-389, Springer-Verlag, Berlin.

Hearst, J. E. and Sauer, K. (1983) in *Proc. 6th Int. Congr. Photosynthesis, Vol. II,* (Sybesma, C., ed.) pp. 355-359, S. Nijhoff/Junk, The Hague.

Hearst, J. E. and Sauer, K. (1984) Z. *Naturforsch.* 39C, 421-424.

Hoganson, C. W. and Babcock, G. T. (1988) *Biochemistry* 27, 5848-5855.

Hoganson, C. W. and Babcock, G. T. (1989) *Biochemistry* 28, 1448-1454.

Hoganson, C. W., Ghanotakis, D. F., Babcock, G. T. and Yocum, C. F. (1989) *Photosynth. Res.* 22, 285-293.

Holschuh, K., Bottomley, W. and Whitfeld, P. R. (1984) Nucl. Acids Res. 12, 8819-8834.

Homann, P. H. (1985) *Biochim. Biophys. Acta* 809, 311-319.

Hsu, B-D., Lee, J-Y. and Pan, R-L. (1987) *Biochim. Biophys. Acta* 890, 89-96.

Hundal, T., Virgin, I, Styring, S. and Andersson, B. (1990) *Biochim. Biophys. Acta* 1017, 235-241.

Ikeuchi, M. and Inoue, Y. (1987) *FEBS Lett.* 210, 71-76.

Ikeuchi, M. and Inoue, Y. (1988) *FEBS Lett.* 241, 99-104.

Ikeuchi, M., Koike, H. and Inoue, Y. (1988) *Biochim. Biophys. Acta* 932, 160-169.

Innes, J. B. and Brudvig, G. W. (1989) *Biochemistry* 28, 1116-1125.

Joliot, P., Barbieri, G. and Chabaud, R. (1969) *Photochem. Photobiol.* 10, 309-329.

Kent, S. and Clark-Lewis, I. (1985) in *Synthetic Peptides in Biology and Medicine* (Alitalo, K., Partanen, P. and Vaheri, A. eds.) Elsevier, Amsterdam.

Kim, D. H., Britt, R. D., Klein, M. P. and Sauer, K. (1990) *J. Amer. Chem. Soc.* 112, 9389-9391.

Kok, B., Forbush, B. and McGloin, M. (1970) *Photochem. Photobiol.* 11, 457-476.

Kuwabara, T. and Murata, N. (1982) *Plant Cell Physiol.* 23, 533-539.

Lachmann, P. J., Strangeways, L., Vyakarnam, A. and Evan, G. (1986) in *Synthetic Peptides as Antigens* (Ciba Foundation Symposium 119) pp. 25-57, Wiley, Chichester.

Laemmli, U. K. (1970) *Nature (Lond.)* 227, 680-685.

Ljungberg, U., Åkerlund, H.-E. and Andersson, B. (1986) *Eur. J. Biochem.* 158, 477-482.

Marder, J. B., Goloubinoff, P. and Edelman, M. (1984) *J. Biol. Chem.* 259, 3900-3908.

Mattoo, A. K., Hoffman-Falk, H., Marder, J. B. and Edelman, M. (1984) *Proc. Natl. Acad. Sci. USA* 81, 1380-1384.

Merrifield, R. B. (1963) *J. Amer. Chem. Soc.* 85, 2149.

Metz, J. G. and Bishop, N. I. (1980) *Biochem. Biophys. Res. Commun.* 94, 560-566.

Metz, J. G., Wong, J. and Bishop, N. I. (1980) *FEBS Lett.* 114, 61-66.

Metz, J. G., Bricker, T. M. and Seibert, M. (1985) *FEBS Lett.* 185, 191-196.

Metz, J. G., Pakrasi, H. B., Seibert, M. and Arntzen, C. J. (1986) *FEBS Lett.* 205, 269-274.

Michel, H. and Deisenhofer, J. (1986) in *Encyclopedia of Plant Physiology, New Series, Vol. 19, Photosynthesis II* (Staehlin, L. A. and Arntzen, C. J., eds.) pp. 371-381, Springer-Verlag, Berlin.

Michel, H. and Deisenhofer, J. (1988) *Biochemistry* 27, 1-7.

Miles, E. W. (1977) *Methods Enzymol.* 47, 431-442.

Miller, A.-F. and Brudvig, G. W. (1989) *Biochemistry* 28, 8181-8190.

Miller, A.-F. and Brudvig, G. W. (1990) *Biochemistry* 29, 1385-1392.

Mimuro, M., Yamazaki, I., Itoh, S., Tamai, N. and Satoh, K. (1988) *Biochim. Biophys. Acta* 933, 478-486.

Miyao, M., Murata, N., Lavorel, J., Maison-Peteri, B., Boussac, A. and Etienne, A.-L. (1987) *Biochim. Biophys. Acta* 890, 151-159.

Miyao, M. and Murata, N. (1984) *FEBS Lett.* 170, 350-354.

Miyao, M. and Murata, N. (1985) *FEBS Lett.* 180, 303-308.

Murata, N. et al. (1984) *Biochim. Biophys. Acta* 765, 363-369.

Nakatani, H. Y., Ke, B., Dolan, E. and Arntzen, C. J. (1984) *Biochim. Biophys. Acta* 765, 347-352.

Nanba, O. and Satoh, K. (1987) *Proc. Natl. Acad. Sci. USA* 84, 109-112.

Newell, W. R., van Amerongen, H., van Grondelle, R., Aalberts, J. W., Drake, A. F., Udvarhelyi, P. and Barber, J. (1988) *FEBS Lett.* 228, 162-166.

Nisimoto, Y., Yamashita, J. and Horio, T. (1973) *J. Biochem.* 73, 515-521.

Ohad, I., Kyle, D. J. and Hirshberg, J. (1985) *Embo J.* 4, 1655-1659

Ohba, M., Sato, R., Yoshida, Y., Bieglmayer, C. and Ruis, H. (1979) *Biochim. Biophys. Acta* 572, 352-362.

Ono, T.-A. and Inoue, Y. (1983a) *Biochim. Biophys. Acta* 723, 191-201.

Ono, T.-A. and Inoue, Y. (1983b) *FEBS Lett.* 164, 255-260.

Ono, T.-A. and Inoue, Y. (1985) *Biochim. Biophys. Acta* 806, 331-340.

Pecoraro, V. L. (1988) *Photochem. Photobiol.* 48, 249-264.

Pickering, M. V. and Newton, P. (1990) *LC-GC* 8, 778-781.

Preston, C. and Seibert, M. (1989) *Photosynth. Res.* 22, 101-113.

Preston, C. and Seibert, M. (1990) in *Current Research in Photosynthesis, Vol. 1* (Baltscheffsky, M., ed.) pp. 925-928, Kluwer Academic Publishers, Dordrecht.

Preston, C. and Seibert, M. (1991a) *Biochemistry* 30, 9615-9624.

Preston, C. and Seibert, M. (1991b) *Biochemistry* 30, 9625-9633.

Rao, J. K. M., Hargrove, P. A. and Argos, P. (1983) *FEBS Lett.* 156, 165-169.

Rasmussen, O. F., Bookjans, G., Stummann, B. M. and Henningsen, K. W. (1984) *Plant Mol. Biol.* 3, 191-199.

Reichlin, M. (1980) *Methods Enzymol.* 70, 159-165.

Renger, G. and Weiss, W. (1986) *Biochim. Biophys. Acta* 850, 184-196.

Rivier, J., McClintock, R., Galyean, R. and Anderson, H. (1984) *J. Chrom.* 288, 303-328.

Rochaix, J.-D., Dron, M., Rahire, M. and Malnoë, P. (1984) *Plant Mol. Biol.* 3. 363-370.

Rogers, S., Wells, R. and Rechsteiner, M. (1986) *Science* 234, 364-368.

Rutherford, A. W., Seibert, M. and Metz, J. G. (1988) *Biochim. Biophys. Acta* 932, 171-176.

Rutherford, A. W., Zimmerman, J. L. and Mathis, P. (1984) *FEBS Lett.* 165, 156-162.

Sauer, K., Yachandra, V. K., Britt, R. D. and Klein, M. P. (1991) in Manganese Redox Enzymes (Pecoraro, V. L., ed.), VCH Publishers, New York (in press).

Saygin, O. and Witt, H. T. (1987) *Biochim. Biophys. Acta* 893, 452-469.

Sayre, R. T., Andersson, B. and Bogorad, L. (1986) *Cell* 47, 601-608.

Seibert, M., DeWit, M. and Staehlin, L. A. (1987) *J. Cell Biol.* 105, 2257-2265.

Seibert, M., Cotton, T. M. and Metz, J. G. (1988) *Biochim. Biophys. Acta* 934, 235-246.

Seibert, M., Tamura, N. and Inoue, Y. (1989) *Biochim. Biophys. Acta* 974, 185-191.

Sigel, M. B., Sinha, Y. N. and VanderLaan, W. P. (1983) *Methods Enzymol.* 93, 3-12.

Silverthorne, J. and Ellis, R. J. (1980) *Biochim. Biophys. Acta* 607, 319-330.

Sivaraja, M. and Dismukes, G. C. (1988) *Biochemistry* 27, 3467-3475.

Styring, S. A. and Rutherford, A. W. (1988) *Biochemistry* 27, 4915-4923.

Takahashi, Y. and Satoh, K. (1989) *Biochim. Biophys. Acta* 973, 138-146.

Takahashi, M., Shiraishi, T. and Asada, K. (1988) *FEBS Lett.* 240, 6-8.

Takayama, H., Iwaki, S., Tamoto, K. and Koyama, J. (1984) *Biochim. Biophys. Acta* 799, 151-157.

Tam, J. P., Heath, W. F. and Merrifield, R. B. (1983) *J. Amer. Chem. Soc.* 105, 6442-6455.

Tamura, N. and Cheniae, G. (1985) *Biochim. Biophys. Acta* 809, 245-259.

Tamura, N. and Cheniae, G. (1986) *FEBS Lett.* 200, 231-236.

Tamura, N. and Cheniae, G. (1987) *Biochim. Biophys. Acta* 890, 179-194.

Tamura, N., Ikeuchi, M. and Inoue, Y. (1989a) *Biochim. Biophys. Acta* 973, 281-289.

Tamura, N., Inoue, Y. and Cheniae, G. (1989b) *Biochim. Biophys. Acta* 976, 173-181.

Tamura, N., Inoue, H. and Inoue, Y. (1990) *Plant Cell Physiol.* 31, 469-477.

Taylor, M. A., Nixon, P. A., Todd, C. M., Barber, J. and Bowyer, J. R. (1988) *FEBS Lett.* 235, 109-116.

Telfer, A., Barber, J. and Evans, M. C. W. (1988) *FEBS Lett.* 232, 209-213.

Tetenkin, V. L., Gulyaev, B. A., Seibert, M. and Rubin, A. B. (1989) *FEBS Lett.* 250, 459-463.

Towbin, H., Staehelin, T and Cordon, J. (1979) *Proc. Natl. Acad. Sci. USA* 76, 4350-4353.

Trebst, A. (1986) *Z. Naturforsch.* 41C, 240-245.

Virgin, I, Styring, S. and Andersson, B. (1988) *FEBS Lett.* 233, 408-412.

Webber A. N., Packham, L., Chapman, D. J., Barber, J. and Gray, J. C. (1989) *FEBS Lett.* 242, 259-262.

Yachandra, V. K., Guiles, R. D., McDermott, A. E., Britt, R. D., Dexheimer, S. L., Sauer, K. and Klein, M. P. (1986) *Biochim. Biophys. Acta* 850, 324-332.

Yachandra, V. K., Guiles, R. D., McDermott, A. E., Cole, J. L., Britt, R. D., Dexheimer, S. L., Sauer, K. and Klein, M. P. (1987) *Biochemistry* 26, 5974-5981.

Yamashita, T., Tsuji, J. and Tomita, G. (1971) *Plant Cell Physiol.* 12, 117-126.

Yocum, C. F., Yerkes, C. T., Blankenship, R. E., Sharp, R. R. and Babcock, G. T. (1981) *Proc. Natl. Acad. Sci. USA* 78, 7507-7511.

Youvan D. C., Bylina, E. J., Alberti, M., Begusch, H. and Hearst, J. E. (1984) *Cell* 37, 949-957.

Zurawski, G., Bohnert, H., Whitfeld, P. and Bottomley, W. (1982) *Proc. Natl. Acad. Sci. USA* 79, 7699-7703.

LAWRENCE BERKELEY LABORATORY
TECHNICAL INFORMATION DEPARTMENT
1 CYCLOTRON ROAD
BERKELEY, CALIFORNIA 94720